Design and Evaluation of a Pneumatic Caisson Shaft Alternative for a Proposed Subterranean Library at MIT

by

Jon Brian Isaacson

B.Sc. Geological Engineering 1998
B.Sc. Economics 2000
M.Sc. Geological Engineering 2000
University of Missouri-Rolla

Submitted to the Department of Civil and Environmental Engineering
in Partial Fulfillment of the Requirement for the Degree of

MASTER OF ENGINEERING
in Civil and Environmental Engineering
AT THE
MASSACHUSETTS INSTITUTE OF TECHNOLOGY

JUNE 2001

Signature of Author_____
Department of Civil and Environmental Engineering
May 11, 2001

Certified by_____
Herbert H. Einstein, Ph.D.
Professor, Department of Civil and Environmental Engineering
Thesis Supervisor

Accepted by_____
Oral Buyukozturk, Ph.D.
Chairman, Departmental Committee on Graduate Studies

Design and Evaluation of a Pneumatic Caisson Shaft Alternative for a Proposed Subterranean Library at MIT

by

Jon Brian Isaacson

Submitted to the Department of Civil and Environmental Engineering
on May 11, 2001 in Partial Fulfillment of the
Requirement for the Degree of Master of Engineering in
Civil and Environmental Engineering.

Abstract

A deep egress shaft was designed for a proposed subterranean library under McDermott Court on the Massachusetts Institute of Technology Campus. The proposed shaft design utilized secant piles to construct the shaft before excavation. Detailed geotechnical parameters were calculated to refine the secant pile design.

This thesis discusses an alternative design consisting of a prefabricated, segmental caisson with an pneumatically supported excavation face. Geotechnical aspects and structural calculations were conducted to design a pneumatic caisson capable of maintaining stability at the base of the excavation while in the soft soils beneath the site. Caisson launch and ballasting issues were addressed during the design of the pneumatic method. The pneumatic chamber pressure could not counter full hydrostatic conditions over the entire depth of the opening. The construction sequence for the caisson was also designed according to site geotechnical parameters.

A comparison and evaluation between the proposed and alternate methods determined that the pneumatic method was less likely to cause local settlement and groundwater level fluctuations. Structural stability was more reliable for the pneumatic method due to its precast nature. Basal stability of the excavation was better due to the capability of problem and misalignment identification and mitigation by workers at the face. Federal regulations prohibited the pneumatic pressure from countering full hydrostatic conditions in the glacial till. Cost issues were the major drawback of the pneumatic method due to labor costs and low productivity. Mechanization at the face and remote operation could lower costs for the caisson method, which otherwise appears to be the better construction methodology. The stability analysis suggests that deep excavations are possible in the Boston Area using pneumatic methods and it is suggested that it be examined for the sinking of the large diameter library structure itself.

Thesis Supervisor: Herbert H. Einstein, Ph.D.
Professor, Department of Civil and Environmental Engineering

Acknowledgements

I would like to take this opportunity to express my heartfelt thanks to those of you who have helped me to fulfill a childhood dream. My father, Jack, who selflessly provided a wonderful life for his children, if I'm half the father you are I'll never go wrong. My sister, Jenna, whose talented eye can find the beauty in anyone and display it for all to see, I'm very proud of you. My Lady, Molly, who knows me better than I know myself, thank you for your incredible patience and sacrifice while I chased my dream. I shall never forget it, I promise. My grandparents, Schildknechts and Isaacson, never failing to encourage me to pursue my dreams. Thank you for all of your hard work and sacrifice, which has helped make my future so bright. My extended Rolla family, the Albertson Clan, your support has been incredible and unforgettable. My Princess, who's pant I have missed for many months. My late mother, Marcia, and late mentor, Paul, who both have taught me that every day is precious, that we know not what tomorrow brings, and that we should be thankful for every second of life that fate grants us. It is up to us to make the best of those moments, and to fill them with happiness whenever possible.

Sincere thanks are extended to my advisor, Professor Herbert H. Einstein, for the opportunity to learn under his tutelage, you're the reason I came to MIT. I thank you for your patience. Special thanks to the M.Eng. Library Group (Rehkopf et al) without whom the subject of this thesis would have been entirely different. I also wish to extend my gratitude to the Civil and Environmental Engineering Department here at MIT for its financial support during this program. Without exception, I would like to thank every teacher and professor whom I have the privilege of learning under during the course of my life. You have all helped to pave the road I now travel. I appreciate the difficult work that you do, and none of you are unimportant.

Thanks also to every relative and friend that I have, you know who you are. Your support and encouragement has enabled me to move mountains. And finally, my fellow classmates, "M-Engers," the finest bunch I have ever had the privilege of working with on a daily basis. I know one day I will miss this place, the lab I have called home for the past nine months, but it is this family that I will miss most of all. May all of you fulfill your dreams and live incredible lives. We made it, together, and ohmyliver!

Table of Contents

List of Figures

List of Tables

1 Introduction

This thesis refers to a library design proposed by graduate students in the 2001 Masters of Engineering Program of the Civil and Environmental Department of the Massachusetts Institute of Technology (MIT). What follows is a brief overview of the rationale for the proposed library as well as the incorporation of a deep egress system into the proposed library design.

1.1 Proposed Underground Library

The MIT library system consists of three main libraries and a network of ten smaller satellite libraries that serve various academic departments on campus. The MIT library system contains some 2.2 million volumes. The number of volumes within campus libraries exceeds current design capacity by 15%. More volumes are kept on campus by employing compact shelving, which facilitates more storage within a given floorplan. The remaining volumes, nearly 25% of the collection, are stored at an off-site storage facility. Retrieving volumes from the off-site storage facility can take upwards of two days. In addition to the storage of the library collections, student seating has also suffered. The library system can only seat 10% of the student body, compared to a widely used design capacity guideline of 25%.

The MIT Department of Civil and Environmental Engineering set forth a design project for a group of Masters of Engineering students in 2000-2001 to propose a solution to the current issues facing the MIT Library System. A solution for the storage and student seating issues was established based upon the requirements of the MIT Library administration. The solution proposed the construction of a new library facility. Since the MIT campus has very limited free space, which is highly valued by the student body, the facility proposed was an underground structure. Two sites were considered for the library; Killian Court and McDermott Court. Killian Court was eliminated due to likely disruption of graduation ceremonies during construction. Thus, the area of McDermott Court was determined to be the site of the library.
Deep excavations on campus have experienced problems supporting lateral earth loads. In order to build confidence and stability into the design of the underground library, the excavation and support structure was designed as a circular diaphragm wall. The circular nature of the structure would take the lateral earth loads in ring compression along the full depth of the excavation, without the use of cross-bracing or tie-back supports. The area of the court, coupled with the

design geometry of the library yielded an underground structure nearly 32,000 ft^2 and 10 stories deep. Egress tunnels would run from the top floor of the library through shallow tunnels to adjacent buildings, minimizing clutter on the surface of McDermott Court. It would be the deepest excavation MIT Campus had ever witnessed, and one of the deepest structures built in the Boston Area. Figure 1-1 shows the footprint of the underground library and the egress tunnels which connect to it within McDermott Court.

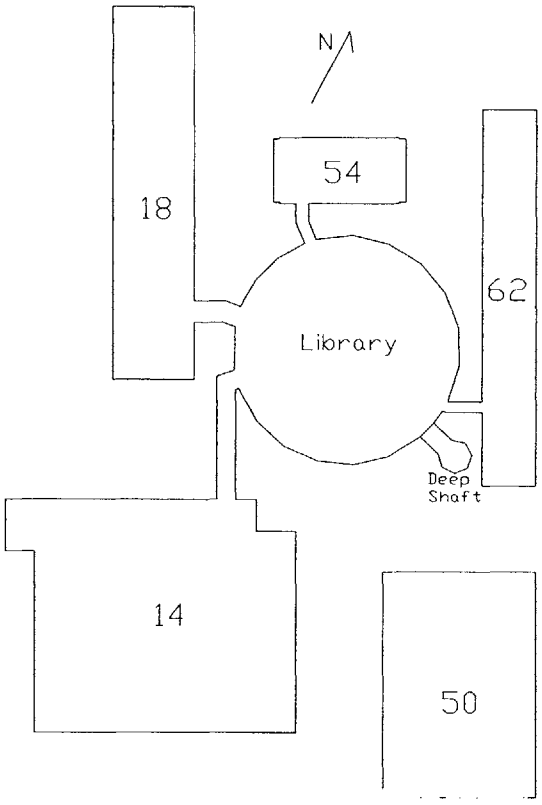

Figure 1-1 Underground library location within McDermott Court (from Rehkopf et al, 2001)

The subsurface conditions beneath McDermott Court exhibit a high ground water level, approximately 8 feet below ground surface, and six soil types underlain by bedrock. Specifically, fill, peat mud, and silty sand form an upper aquifer beneath the court. Below the sand is the Boston Blue Clay, which extends down to a layer of glacial till that overlies the Cambridge Argillite.

1.2 Need for Deep Egress System

The extraordinary depth of the proposed library made emergency egress an issue with regard to a fire within the structure. The four primary entrances for the library connect adjacent buildings to the top floor, therefore making the top floor a critical pathway in the event of a fire. Fire scenarios and emergency exit routes had to be examined to assure that emergency egress from the structure didn't have any fatal flaws.

The layout of the library incorporates a central elliptical skylight that is open from the dome at the top of the library down to the sixth floor. The top floor along this central skylight shaft is the level that serves as the main access into and out of the library via egress tunnels to adjacent campus buildings. Figure 1-2 shows a cross section of the library which shows these features.

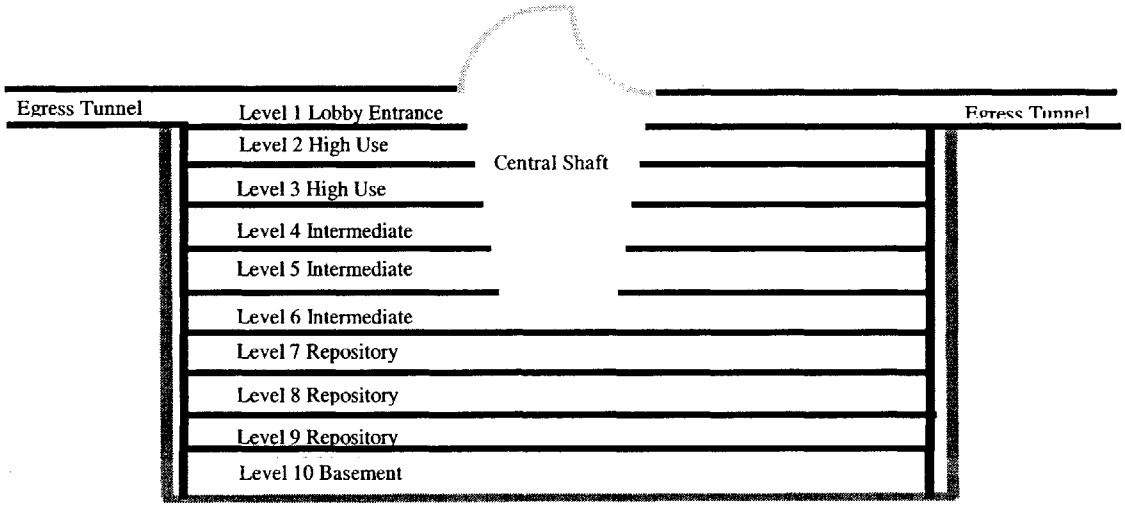

Figure 1-2 . Cross-section of underground library

Multiple fire scenarios were examined to determine the adequacy of the four first floor egress tunnels as structural egresses. It quickly became apparent that a fire that occurred on any floor of the library would obviously separate people in the library into two groups. One group would have access to the first floor via library stairwells and would be able to escape from the fire. The second group was comprised of those on floors beneath the fire. If the fire was close to the stairwells, it could block the route upwards to the first floor and the egress tunnels, thus effectively trapping the second group. The critical case is when there is a fire near the stairwells

and/or egress tunnels on the first floor, which could effectively cut off any or all of the routes of emergency egress for all library occupants.

Mitigation of the critical case of a first floor fire required an alternate route of egress out of the library. This alternate route of escape could not be located on the first floor. Location of the alternate exit on intermediate floors still left a possible second group of library occupants trapped on the floors below the exit if the fire occurred on that particular floor. Location of an alternate emergency egress point on the tenth floor at the base of the library eliminated the trapping of occupants within the library due to egress access. Therefore, an alternate egress tunnel was designed for the tenth floor.

Several approaches were examined to determine the best way to get occupants to the surface from the tenth floor, 125 feet below ground surface. A sloped tunnel was determined to be too costly and the confined site made it an extremely difficult option. The alternative selected is a vertical shaft with stairs that would access the surface next to the library as shown in Figure 1-3. The proposed design of the egress shaft is discussed in Section 4.1. The surface connections for the mechanical and emergency egresses are discussed in Rehkopf et al. (2001) and will not be discussed as part of this thesis.

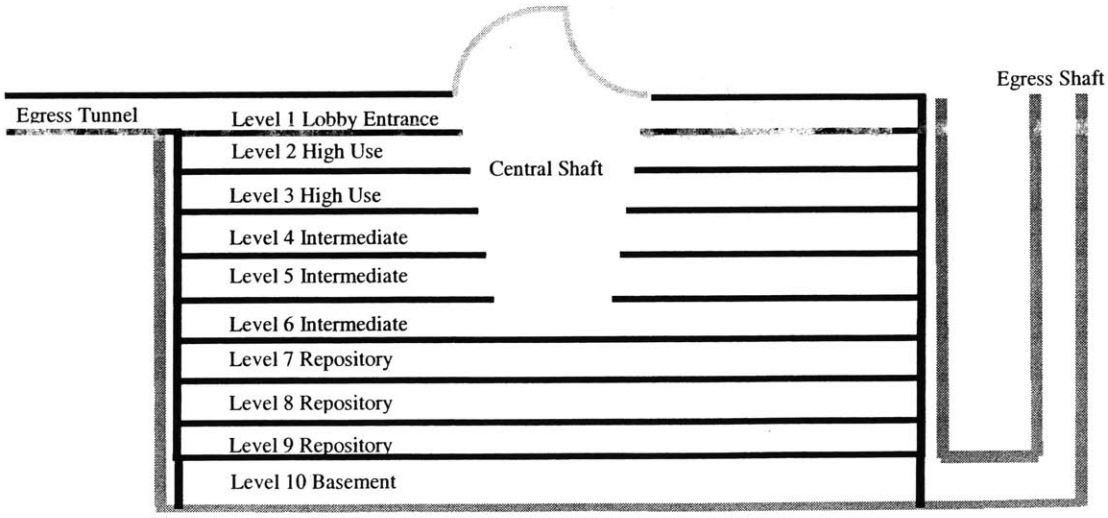

Figure 1-3 . Cross-section of underground library with egress shaft

In order to justify the additional cost of the deep egress system, it was designed as a triple usage feature. In addition to providing a route of emergency egress from the basement of the underground library, it also contains the intake and exhaust ducts for exterior ventilation to the mechanical systems and ductwork on the tenth level. Also, if any large mechanical equipment on the tenth floor needed to be replaced or new equipment installed it might be difficult to move it from the first to the tenth level using the structure's elevators. To solve this problem, the deep egress system was also designed to serve as a shaft for mechanical egress to the tenth level of the library. Also, if the shaft were excavated before the main excavation for the library, it could serve as a test pit, allowing a better understanding of the subsurface conditions of the site and making it possible to modify the design before a problematic situation was actually encountered in library construction.

2 Project Specifications and Requirements

The nature and location of the deep egress system on campus lends itself to a basic set of requirements for its design. Specifically, the triple usage of the shaft provides a rigid set of interior requirements for the design. Other issues requiring address include anticipated earth loads, the factors of safety used in design, and the environmental impacts both during and post-construction.

2.1 Interior Requirements of Shaft Design

The interior requirements of the design of the deep egress system can be broken down into two components; the shaft and the connector tunnel at its base. What follows is a brief description of the internal requirements of the shaft component of this system, shown in Figure 2-1.

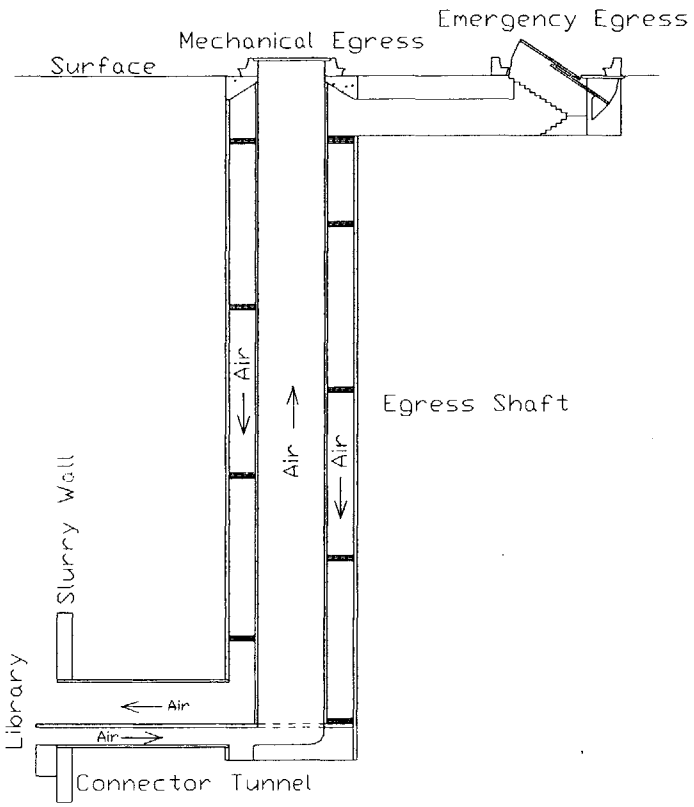

Figure 2-1 Vertical section of proposed shaft/tunnel system (from Rehkopf et al, 2001)

The vertical shaft is designed to provide a route for people, mechanical equipment, and exterior ventilation air from the tenth floor level to the ground surface. The vertical shaft must extend to

a depth of 140 feet below ground surface and have a finished internal diameter of 24 feet. The shaft extends down through saturated soil deposits of fill, peat mud, silty sand, Boston Blue Clay, and is founded in glacial till.

The emergency egress portion, which allows people to exit the library, consists of a spiral stairwell the full vertical length of the shaft. The stairwell is located between an inner wall within the shaft and the interior surface of the permanent liner, which is an annular space 5 feet in width. The stairs within this stairwell take up 6.66 degrees each, yielding 54 steps per revolution. The stair height is the standard of 7 inches, yielding a vertical rise of 31.5 feet per stairwell revolution. The stair surfaces themselves are made of steel grates which permits air to pass through them rather than moving in a spiral fashion up the stairwell. The stairs are secured to the adjacent walls and also bear upon a network of beams between the inner wall and the permanent liner.

The mechanical egress consists of a free and clear vertical shaft that runs the entire depth from the ground surface to the tenth level. The vertical shaft is located within an inner wall with an inner radius of 6.5 feet and a thickness of 0.5 feet, yielding an open shaft 13 feet in diameter. This diameter facilitates the raising and lowering of large mechanical equipment to the tenth floor by a crane on the surface.

The ventilation function of the vertical shaft uses the mechanical and emergency egress portions of the shaft as separate ducts. The steel grating of the stairwell allows vertical movement of air within the shaft annulus. Since it is an emergency egress, it is designed as the fresh air intake duct, allowing those on the stairwell to be free of smoke in the event of a library fire. The open mechanical shaft functions as the exhaust duct for exterior ventilation, as air can freely move up the shaft. Figure 2-2 displays sections of the finished interior requirements of the shaft.

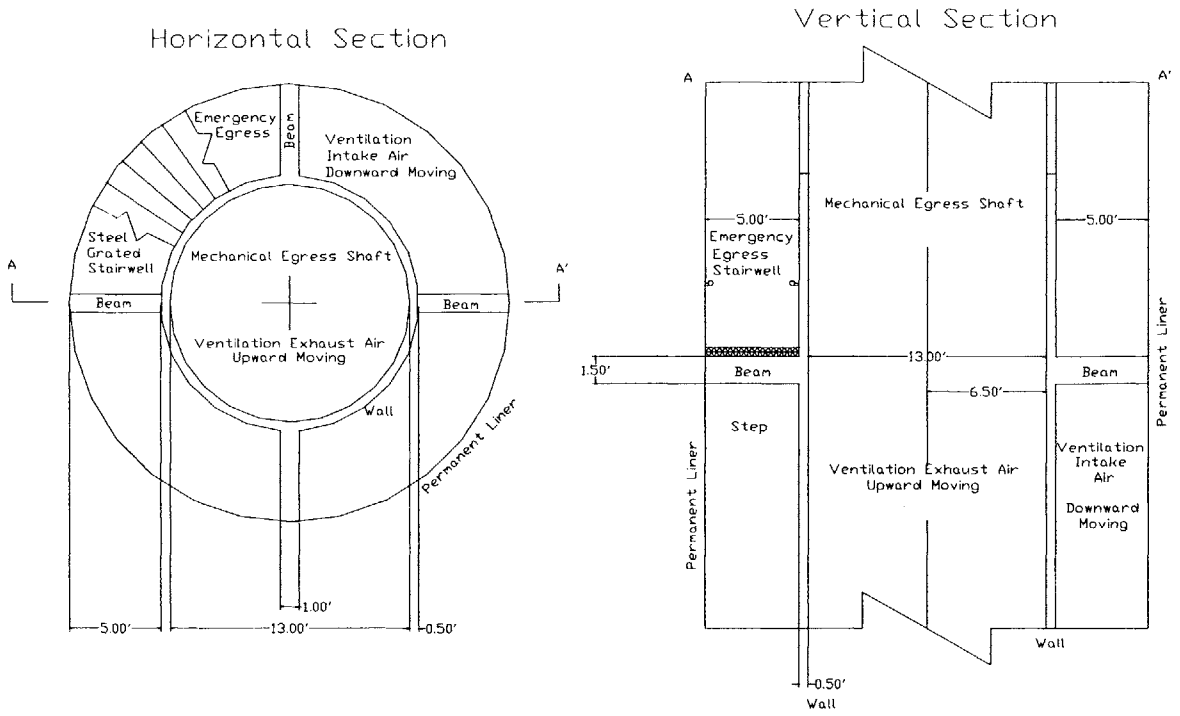

Figure 2-2 Internal design of vertical shaft

2.2 Factors of Safety

The shaft is deep (maximum depth of 140 feet below the ground surface), which makes the factor of safety critical during construction and operation. The shaft must resist the lateral earth pressure imposed on it, as well as the hydrostatic loads at high groundwater levels. This basically means that even temporary supports must employ a factor of safety of 2.0 in order to protect both workers from collapse/entrapment within the excavation and the foundations of adjacent structures from settlements. Furthermore, the proximity of the shaft to adjacent structures further necessitates a higher factor of safety to prevent damage to those structures.

Taking all of these aspects into account, the design of the shaft requires the use of a factor of safety greater than that used in typical mining applications, which are usually between 1.0 and 1.5. The proposed design of the library and shaft/tunnel system proposed by Rehkopf et al. (2001) employs a factor of safety of 2.0 for foundation and earth support structures. The shaft design that it proposes uses this factor of safety for both the temporary and permanent support structures of the shaft.

2.3 Environmental Impacts

The construction of the shaft poses potential environmental impacts to adjacent structures and the library structure itself. The most significant potential impacts include ground movements that affect the structures and the drawdown of groundwater levels proximal to the site. These issues are addressed separately.

2.3.1 Ground Movements

Excavation of the shaft itself presents the possibility of ground movements around the shaft. This can occur if the support of the excavation wall is allowed to move a significant amount, allowing the soil to move laterally, which in turn allows for vertical soil movement to replace the displacing soil. Weaker soil at the base of the excavation, if not properly supported, can also heave vertically into the excavation, causing movement behind the vertical walls to replace the displaced soil.

Since the shaft will be excavated within close proximity of an adjacent structure, the foundation of that structure must be protected from such movements. This can be achieved by either underpinning the structure or by designing the shaft wall with sufficient stiffness so that it does not deflect significantly or fail, which would cause horizontal and subsequent ground movements. The minimization of ground movements under the adjacent structure minimizes the disturbance to its foundation, which could cause cracking or settlement within the building.
The shaft/tunnel system must be designed so that installation of the liners minimizes local ground movements. The liners must also be able to resist the range of loads over the life of the library facility so prevent failure and ground movements in the soil mass around it.

2.3.2 Groundwater Drawdown

Groundwater levels at the site of the proposed library are shallow, approximately 8 feet from ground surface. The organic or peaty silts, sands, and Boston Blue Clay beneath the site would be subject to settlement if the groundwater level was lowered below its current level by either the construction process or by leaks within the shaft after construction.

The lowering of groundwater levels within silt and clay deposits, such as the Boston Blue Clay, causes increased effective stress and leads to settlement. Settlement of the soils around the shaft could affect both the library diaphragm wall and the adjacent surface structure. Thus, the lowering of groundwater levels around the system must be minimized to prevent adverse effects on the adjacent structures due to soil settlement.

The shaft must be designed so that it minimizes groundwater inflows into the excavation both during and after construction. Furthermore, seepage must be minimized to further decrease the chance of lowering groundwater levels. Measures must be in place to replenish the groundwater supply by injection if significant lowering occurs near the shaft/tunnel system.

2.4 Other Requirements

Other requirements of the shaft include the feasibility of the design and construction methods, the amount of time required for construction, and the overall cost of construction.

The design must utilize a previously proven method of construction in order to instill confidence in the project given the past history of deep excavation failures on the MIT Campus. Feasibility of the design and construction method will most likely play a critical role in the selection of the methods employed for shaft construction.

The MIT Campus has few windows of opportunities in which to construct the library and the shaft. The construction process will likely cause some disturbance to the surrounding campus area, which is to be minimized. The disruption imposed on campus will be a direct result of the methods used and also the time involved in construction. The shorter the installation period, the more confined the environmental impacts of construction on campus. Thus, the method employed to install the shaft should be able to do so reliably within the minimum amount of time possible.

Finally, the overall cost of the shaft will be a factor that may ultimately control the selection of a design and construction method. The impact of the additional cost of the shaft on the overall

cost of the underground library will be minimized if the most economic methodology is used for its installation.

3 Geotechnical Analysis

The design of a vertical shaft in soils requires that the nature of stresses and other properties of the adjacent ground be quantified. The original shaft design proposed by Rehkopf et al (2001) was based upon generalized geotechnical parameters. More detailed geotechnical parameters have been assembled based upon soil information, specifically those beneath MIT Campus Area.

3.1 Proposal Parameters

In order to design the support required for the egress shaft system as well as the library support walls, the stresses imposed on each component had to first be calculated. In order to simplify the design, several assumptions about the McDermott Court subsurface geology were made. The major component of design involves the sizing of the shaft wall, referred to as a liner. To design the shaft, the maximum lateral earth pressure (σ_{hmax}) on the liner was calculated, and included both horizontal effective stress and hydrostatic loading. This horizontal pressure was estimated using Equation 1,

$$\sigma_{h_{max}} = \sigma_h' + u = D\left(K_o \gamma_{soil} + \gamma_{water}\right) \qquad (1)$$

where D is the depth below ground surface, K_o is the coefficient of horizontal stress, and γ is the unit weight of soil and water. The equation is based upon the assumption that the groundwater surface is as the ground surface. The simplified and conservative values of γ_{soil} of 125 pcf, depth D of 140 feet below ground surface (the same as the depth of the library slurry wall), and a K_o value of 0.66 were assumed and yielded a σ_{hmax} = 20,286 psf ~ 21,000 psf. This was the lateral pressure used in the design calculations of the proposed secant pile egress shaft.

3.2 Detailed Geotechnical Parameters

A more detailed analysis of geotechnical parameters of site soils was needed to better quantify the design properties and effectively optimize the design of shaft components in contact with ground forces. In order to procure more accurate geotechnical parameters, a more accurate geologic profile of McDermott Court was first required. The soil profile for the shaft site was taken from Boring 1 and 1A of MIT Facilities (1948), which is located within 100 feet of the

proposed shaft centerline. This boring provided soil and groundwater depths down to the Cambridge Argillite, which was also cored. The soils beneath McDermott Court and their depths of occurrence are summarized in Table 3-1.

Soil Type	Top Depth (ft)	Bottom Depth (ft)
Fill	0	11
Organic Silt	11	35.5
Sand	35.5	39.5
Stiff Boston Blue Clay	39.5	49.5
Soft Boston Blue Clay	49.5	117.5
Glacial Till	117.5	142
Cambridge Argillite	142	

Table 3-1 Summary of McDermott Court soil profile (from MIT Facilities, 1948)

Next, unit weights (γ), friction angles (ϕ), undrained strengths (s_U), and over-consolidation ratios (OCR) for the Boston Blue Clay (BBC) and other soils within the soil profile beneath MIT Campus were obtained through personal communications with Professors Charles C. Ladd and Andrew J. Whittle of MIT (2001). The values obtained represent the current state of geotechnical knowledge of campus soils based upon past testing and construction projects. The simplified boring log, soil parameters, and subsequent calculations can be found in Appendix A. Figure 3-1 shows the estimated strengths of the Boston Blue Clay based on information provided by Ladd and Whittle (2001).

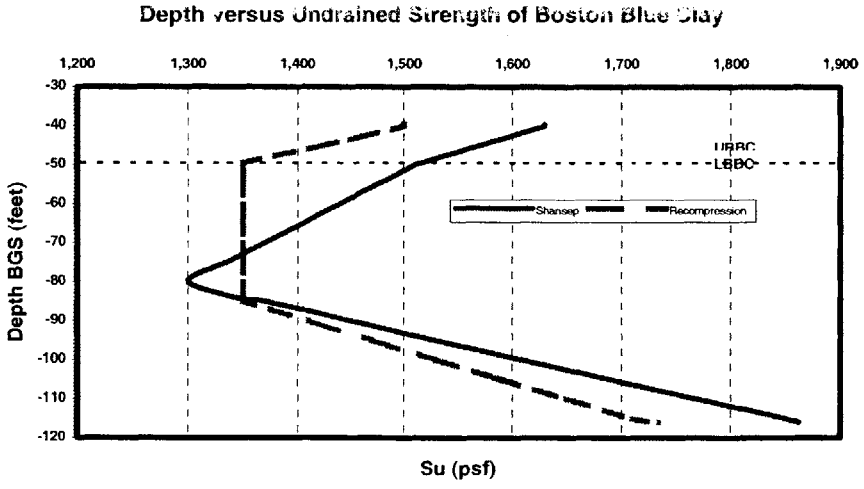

Figure 3-1 Undrained shear strength estimates used for Boston Blue Clay

The coefficient of lateral earth pressure (K_O) was then estimated based upon soil friction angles using the equation proposed by Jaky (1944) shown below.

$$K_o = 1 - \sin\phi \qquad (2)$$

The top of groundwater is located an average of 8 feet below ground surface. This elevation was used, along with soil unit weights and depths, to generate a vertical profile of pore pressures as well as total and effective vertical stresses, shown in Figure 3-2.

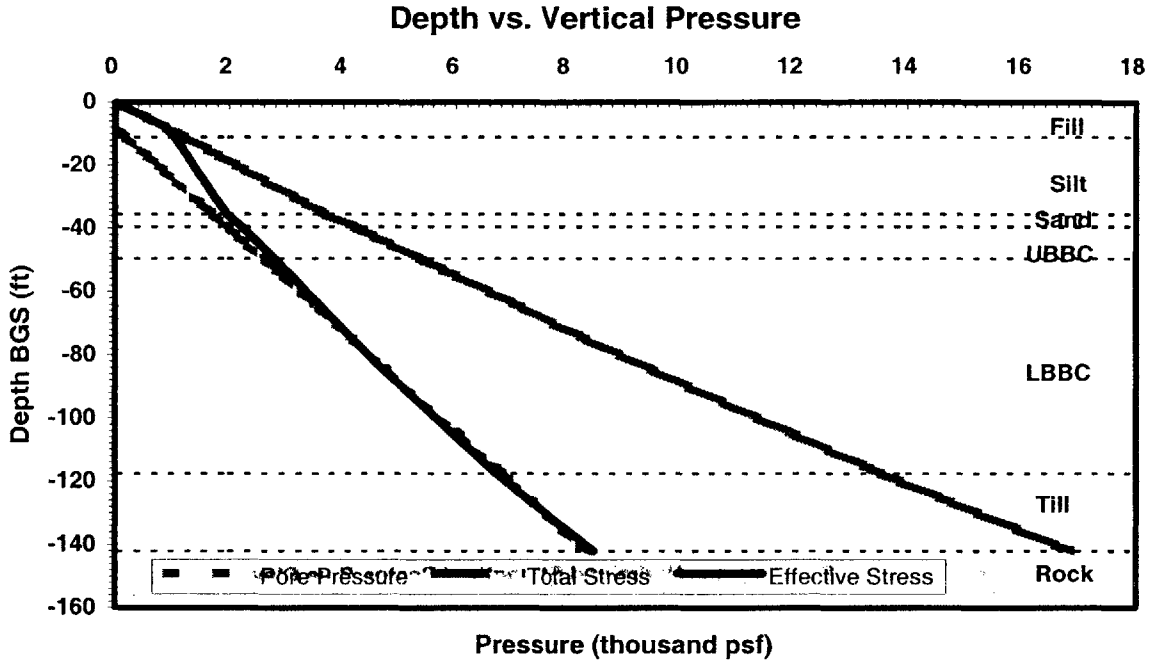

Figure 3-2 Plot of pore pressures and vertical stresses versus depth beneath McDermott Court

The coefficient of lateral earth pressure of each soil was then used to find the horizontal stresses, which are shown in Figure 3-3.

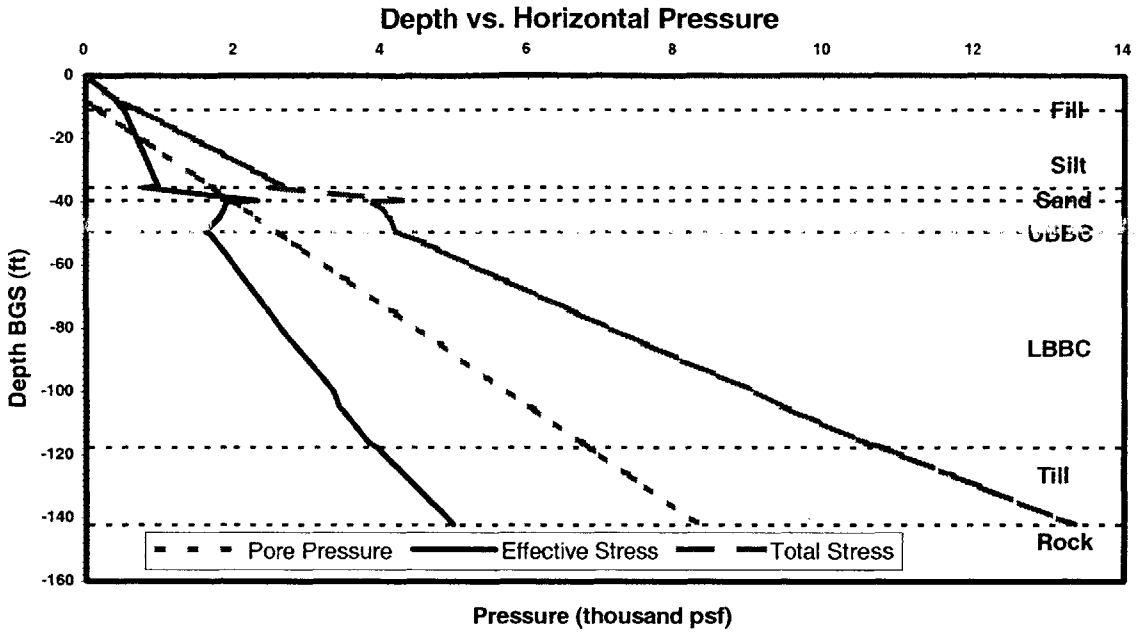

Figure 3-3 Plot of pore pressures and horizontal stresses versus depth beneath McDermott Court

Finally, the coefficient of active earth pressure, K_A, was calculated according to Rankine, shown as Equation 3 below. This coefficient would be needed later to help compute the probable short-term earth pressures and skin friction values for the various soils beneath McDermott Court.

$$K_A = \frac{(1-\sin\phi)}{(1+\sin\phi)} \qquad (3)$$

Using the parameters both given and calculated for campus soils, a more accurate maximum lateral soil pressure upon the shaft wall was found to be 13,333 psf and occurred at the base of the glacial till. Given this new value, it appeared that the proposed value used by Rehkopf et al (2001) was oversimplified and somewhat conservative. Therefore, the proposed value of σ_{hmax} was revised from 21,000 psf to 13,333 psf for the purposes of liner design. Also, notable increases in σ_{ho} were seen in the stiff upper portion of the Boston Blue Clay, which is consistent with this layer's over consolidated nature. All calculations and estimates of geotechnical parameters can be found in Appendix A.

4 Secant Pile Shaft Design

Secant pile design can be considered a pre-construction technique due to the fact that the structure is assembled before it is excavated and put to use. This permits the structure to be put together without the interference of increased loads imposed by the excavation of soil material. The method of design and construction proposed by Rehkopf et al (2001) employs secant piles to form a temporary liner within which a permanent cast in place liner is constructed. This method was proposed for construction of the vertical shaft within the library's deep egress system. Revision of this shaft design utilizes the more detailed geotechnical analysis of ground stresses.

4.1 Proposal Secant Pile Shaft Design

The shaft was designed to resist the lateral earth pressure and hydrostatic load imposed on the circular structure, which was calculated as σ_{hmax} in Section 3.1. Shaft construction was proposed in two steps. The first step involves the installation of a secant pile temporary liner. Once this temporary liner is in place, the center of the shaft can be excavated, the inner shaft foundation can be installed, and then finally a permanent liner can be cast from the bottom up against the inside of the temporary liner.

Secant piles or bored shafts are available in a variety of sizes. The thickness of the permanent liner first had to be calculated in order to find the radius at which the secant piles are to be drilled, which varies dependent upon the diameter of the secant pile itself.

The finished internal radius of the shaft (r_f) is 12 feet. This internal radius ($r_i = r_f$), lateral pressure on the liner ($P=\sigma_{hmax}$), and the desired factor of safety (F) of 2.00 were used to calculate the required thickness of the permanent liner using Equation 4 from Summers (2000).

$$t_{liner} = r_i\left(\sqrt{\frac{\sigma_t}{\sigma_t - 2PF}} - 1\right) \qquad (4)$$ (Lame' Equation from Summers, 2000)

A concrete strength of (σ_t) of 5000 psi (720,000 psf) was used, and the permanent liner thickness (t_p) for the shaft was found to be 0.77 feet. After that thickness was determined, the required

thickness of the temporary liner could then be calculated. The thickness of the liner is a function of the internal radius, requiring that the overlap thicknesses (l) for the temporary liner (t_t=l) to be calculated for each size of secant pile (r_s) available using the radius of pile installation (r_i) in Equation 4. The installation radius (r_i) from the shaft centerline was dependent upon the finished interior radius of the shaft (r_f), the permanent liner thickness (t_p), and the radius of the particular secant pile being examined (r_s), and was calculated using Equation 5. Figure 4-1 illustrates the overlap thickness of a pair of secant piles of radius r_s installed at r_i with a spacing S.

$$r_i = r_f + t_p + r_s \tag{5}$$

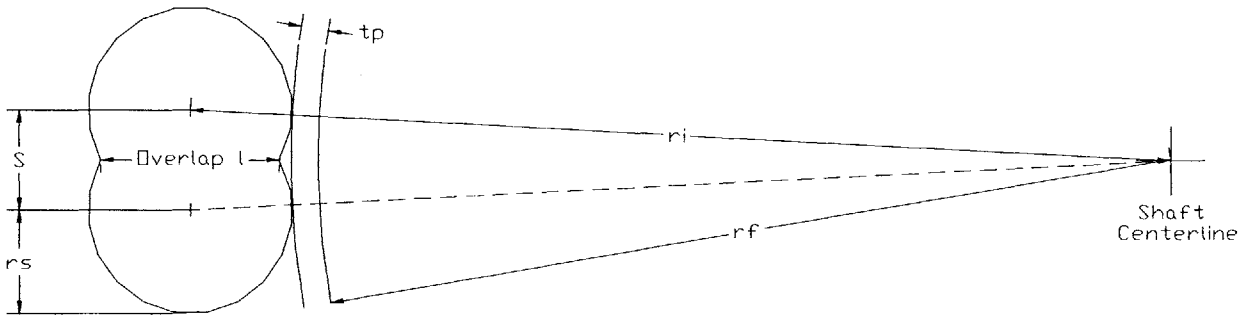

Figure 4-1 Illustration of overlap thickness of secant piles

Next, the spacing (S) was calculated for the different pile sizes (r_s) taking into account drilling deviation (d) to assure that in the worse case scenario the required thickness (or overlap) still occurs at the bottom of the secant piles. The drilling deviation (d) is calculated using Equation 6 and the pile spacing (S) required to reliably achieve the temporary liner thickness (t_t) using Equation 7.

$$d = \%_{deviation} D_{borehole} \tag{6}$$

$$S = 2\sqrt{r_S^{\,2} - \left(\frac{t_t}{2}\right)^2} - d \tag{7}$$

The spacing on the surface is set equal to S. As the depth of drilling increases, the centerline of the base of the hole can deviate from the planned alignment by as much as d. The case that

provides the minimum amount of overlap occurs when adjacent secant piles deviate in opposite directions away from one another by twice the value of d. The maximum amount of overlap occurs when the piles deviate the twice the value of d towards one another. If the pile centerline remains along the planned alignment, the average overlap is obtained. The minimum overlap (l_{min}), average overlap (l_{avg}), and maximum overlap (l_{max}) of the secant piles of each size (r_s) could be calculated using Equation 8, 9, and 10 respectively. The spacing from Equation 7 is set up so that the minimum overlap (l_{min}) was equal to the temporary liner thickness (t_t) for the expected value of deviation (d), which is the critical case for design. Each of these overlaps are illustrated in Figure 4-2.

$$l_{\min} = 2\sqrt{r_s^2 - \left(\frac{S}{2} + d\right)^2} \tag{8}$$

$$l_{avg} = 2\sqrt{r_s^2 - \left(\frac{S}{2}\right)^2} \tag{9}$$

$$l_{\max} = 2\sqrt{r_s^2 - \left(\frac{S}{2} - d\right)^2} \tag{10}$$

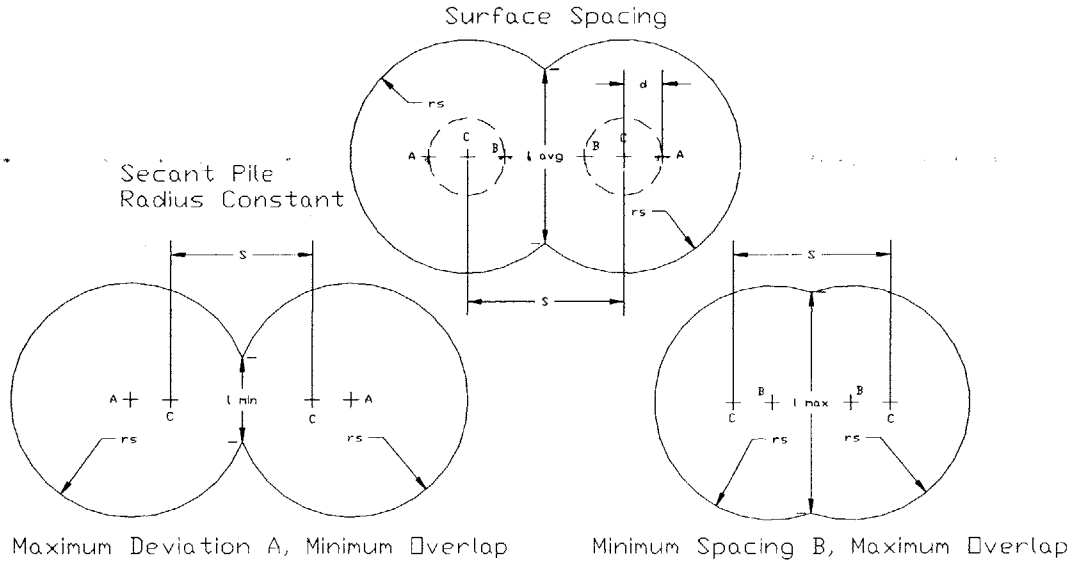

Figure 4-2 Examples of overlap lengths

Finally, the number of secant piles (n) needed to construct the temporary liner depends on the installation radius of the particular size of secant pile (r_i) and its particular spacing (S) and was calculated using Equation 11.

$$n = \frac{2\pi r_i}{S} \tag{11}$$

A spreadsheet was used to calculate the design parameters using the equation above, as well as the most cost effective pile size for the temporary liner, and can be found in Appendix B. The cost analysis revealed that the most efficient design has the parameters Table 4-1 assuming a borehole deviation of 0.5% to a depth of 140 feet below ground surface.

Pile Size (r_s)	Installation Radius (r_i)	Min. Overlap (l_{min})	Pile Spacing (S)	Piles (n)
1.5 ft	14.27 ft	0.913 ft	1.458 ft	62

Table 4-1 Proposed secant pile temporary shaft liner specifications

These parameters were based on the calculated lateral load on the liner ($P=\sigma_{hmax}$), the use of 5000 psi concrete (720,000 psf), and a desired factor of safety (F) of 2.00.

Once all the secant piles are in place, the soil material within the temporary secant pile liner is excavated to the base of the shaft wall. A 2-foot thick mat slab is constructed at the base of the shaft, and slip forms are used to cast a permanent liner against the secant piles from the bottom of the shaft upwards. The permanent liner has an internal radius of 12 feet, a thickness of 0.77 feet, is cast of 5000 psi concrete, and has a factor of safety of 2.00. A cross-section of the vertical shaft is shown in Figure 4-3. After the permanent liner is in place, the internal finishing, which includes the interior shaft wall, cross beams, and stairwell is installed.

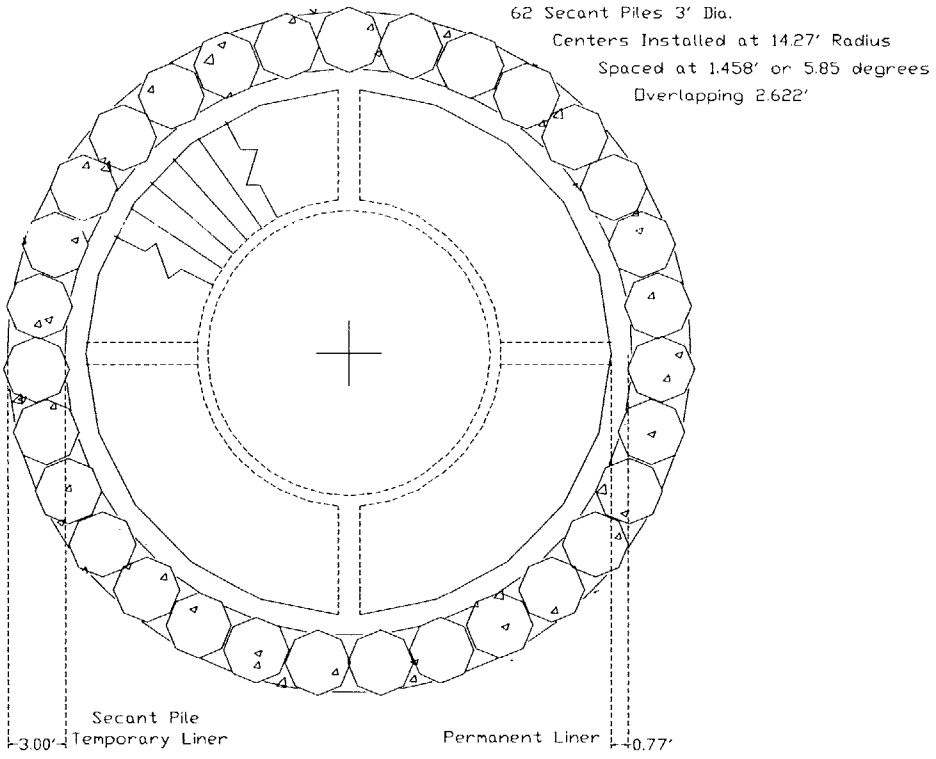

Figure 4-3 Vertical section of proposed secant pile shaft

4.2 Revised Secant Pile Shaft Design

A more detailed analysis of soil properties and stress profiles, discussed in Section 3.2, shows a significant reduction in the σ_{hmax} value assumed during the shaft design of Rehkopf et al (2001). Utilizing the same calculations, a σ_{hmax} value equal to 13,333 psf was used to design the thickness of the permanent liner as well as the secant pile spacing and overlap. These revised calculations can be found in Appendix C.

The outcome of the revision in the maximum horizontal stress value was the optimization of the design to fit the ground conditions of McDermott Court. The revised design parameters are summarized in Table 4-2.

Pile Size (r_s)	Installation Radius (r_i)	Min. Overlap (l_{min})	Pile Spacing (S)	Piles (n)
1.5 ft	13.97 ft	0.548 ft	1.550 ft	57

Table 4-2 Revised secant pile temporary shaft liner specifications

The result of the revised horizontal stress profile was a reduction in the thickness of the permanent liner from 0.77 feet to 0.47 feet, as well as a reduction in the installation radius, minimum overlap, and number of piles required. Pile spacing was also increased. Thus the more detailed analysis of the ground stress conditions of McDermott Court shows that the proposed shaft design by Rehkopf et al (2001) was conservative. Figure 4-4 shows the revised number of secant piles and thinner permanent liner.

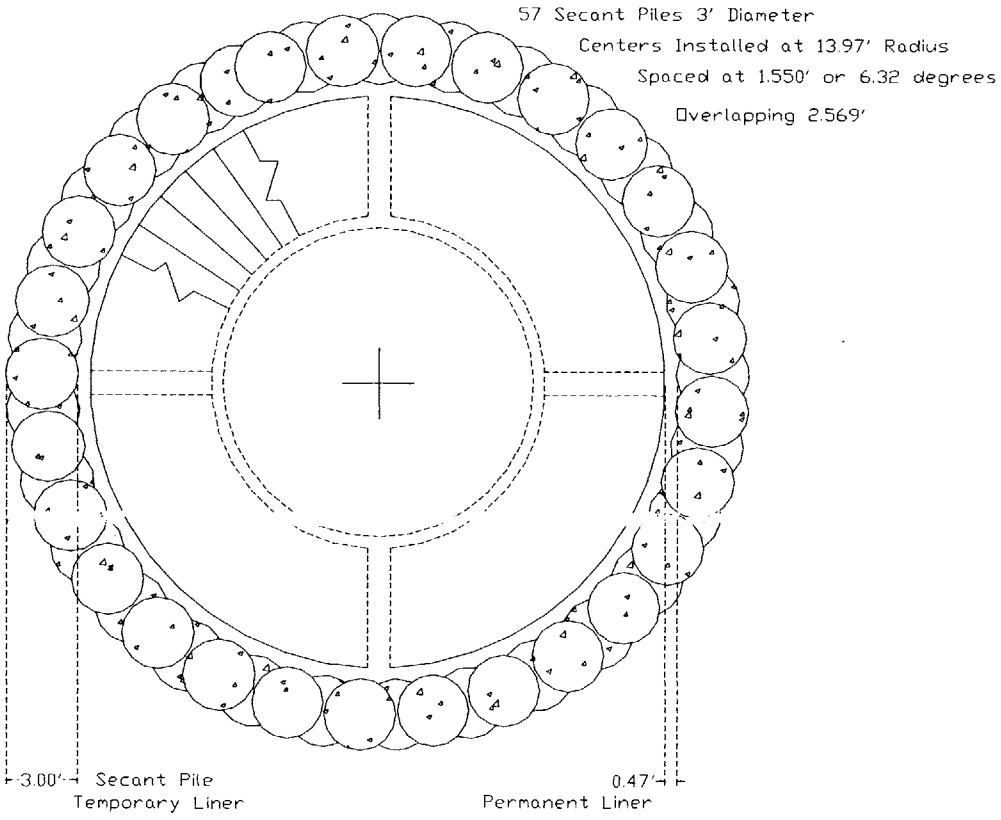

Figure 4-4 Vertical section of revised secant pile shaft

5 Pneumatic Caisson Design and Construction Alternative

The proposed construction method, discussed previously, employs secant piles and is considered an example of pre-constructing the shaft before it is excavated. This method of construction relies upon observation at the surface to understand problems that cannot be seen first hand. Workers installing the piles are unable to verify their exact location or overlap except at the surface, or that the pile quality is not degraded by soil sloughing into the hole when the casing is pulled until the excavation process exposes these flaws. The proposed alternative method was designed to provide far better quality assurance regarding the shaft support structure.

The alternative design and construction method proposed involves the sinking of a prefabricated, segmental structure , shown in Figure 5-15, by means of excavating beneath its foundation. Once the bottom edge of the structure is below groundwater levels and within weak soils, air pressure is applied to the working face to increase basal stability and stop groundwater inflow. This is design methodology is known as a pneumatic caisson. An overview of this method as well as the specific design and construction details for the library shaft are discussed within this chapter.

5.1 Pneumatic Caisson Method

Pneumatic caissons use pressurized air to provide face support during their sinking operations. Specifically, the air pressure in the excavation chamber is designed to minimize groundwater inflow during shaft sinking, thereby allowing workers to excavate at the face while in the dry. Figure 5-1 shows a typical section of a pneumatic caisson.

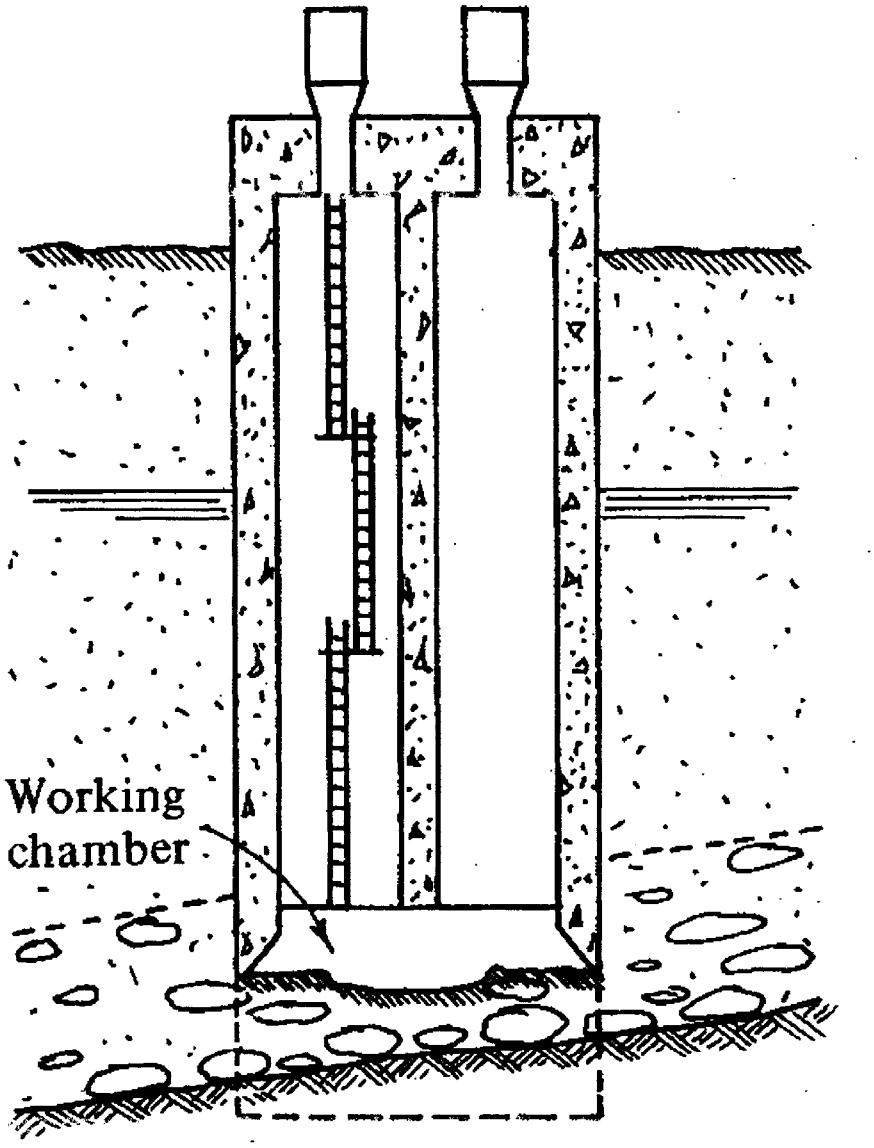

Figure 5-1 Typical section of a land pneumatic caisson (from Swatek, 1975)

Pneumatic caissons were first employed during the construction of the Pedee Bridge in 1852. Their use became widespread in the last century, and was most notably used in the construction of the foundations for the Brooklyn Bridge in New York. The use of the method suffered a serious decline due to the inflation of wages and shorter working hours imposed after World War II (Swatek, 1975). Workers were unable to spend much time excavating at the face due to the need for decompression, and the method suffered from decreased worker productivity as a result. A cross section of the Brooklyn Caisson from Shapiro (1983) is shown in Figure 5-2.

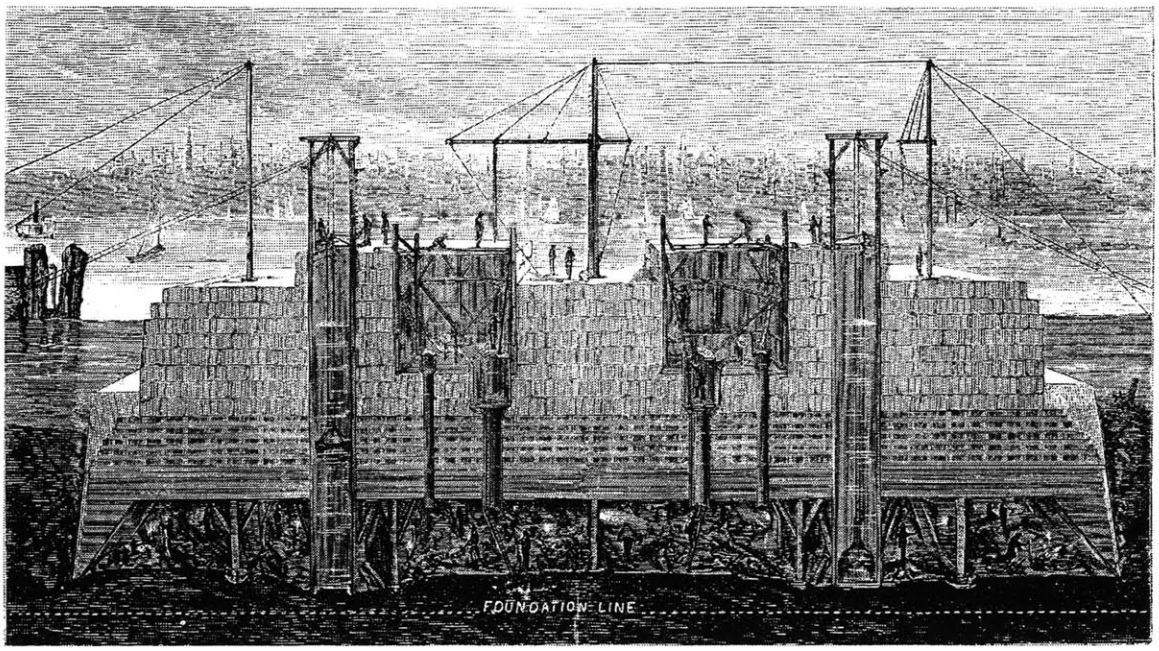

Figure 5-2 Cross section of the Brooklyn Caisson (from Shapiro, 1983)

The caisson is placed directly on the site surface and excavation is conducted within an airtight chamber, which is pressurized. The floor of this chamber is the soil that is being excavated. The caisson walls are made stiff to support the excavation. The excavation proceeds downward by removing soils beneath the walls and caisson supports. As the caisson moves downward, chamber pressures are increased to match or exceed the hydrostatic pressure outside the caisson walls. Robinson (1964) lists obstructions, such as boulders, and resistant stratum as impediments to caisson driving. These obstructions are more easily mitigated and/or removed with actual workers at the face, as opposed to excavation in a slurry caisson. He goes on to state that with the use of pneumatic pressure caissons provide additional support for the excavation face and significantly reduce inflows of groundwater. Material and workers are moved in and out of the chamber through airlocks, which allow the chamber pressure to be maintained. The walls of the caisson slip against the sides of the excavation, creating drag induced by skin friction. Ballast can be added to overcome this resistance to downward movement. Upon achieving the final grade of the excavation, the chamber is backfilled with concrete.

The ultimate depth of excavation possible with pneumatic caissons is limited by the fact that federal regulations prohibit workers from being subjected to chamber pressures greater than

50psi. Therefore, chamber pressures will no longer be fully able to combat groundwater inflows beyond a depth of 115 feet below the groundwater surface without the application of groundwater pumping near the excavation.

5.2 Geotechnical Analysis of Design

The successful installation of pneumatic caissons requires a thorough understanding of ground stresses, the stability of the base or excavation face of the caisson, the frictional resistance of the soil against the sinking process, and the ground settlements adjacent to the caisson. Ground stresses have previously been discussed in Section 3.2. Analysis was conducted to quantify each aspect of geotechnical design, and is discussed in the following sections.

5.2.1 Basal Stability

Basal stability of the caisson is the critical issue concerning the feasibility of a mechanically-assisted excavation of an open face in soft cohesive soils. The weight of the overlying soils exerts a downward force outside the caisson wall. Soft clays will be prone to rotational undrained shear failure if the vertical stress outside the opening is not significantly countered by sufficient undrained shear strength. Figure 5-3 displays the rotational undrained shear failure possible into the open face of the caisson.

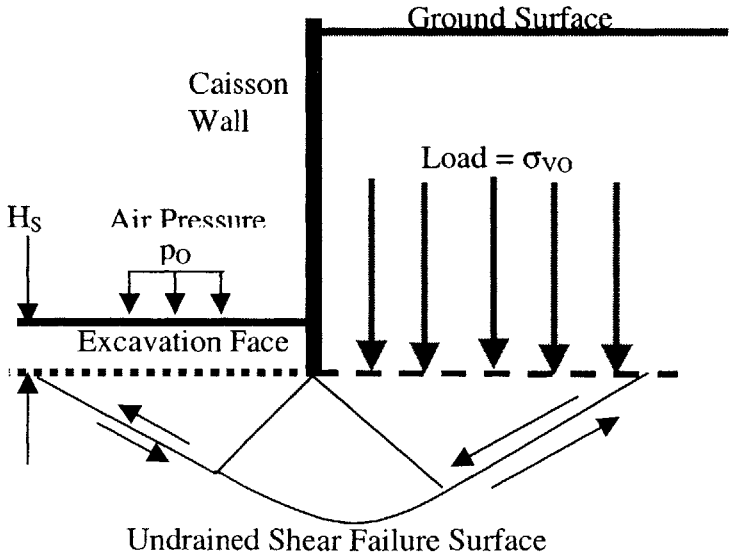

Figure 5-3 Shear failure into pneumatic chamber

Bjerrum and Eide (1956) propose analyzing such situations at the base of an excavation in cohesive soils by treating it as a reverse bearing capacity problem. The equation they propose for computing the factor of safety (FS) of the excavation face involves the undrained bearing capacity equation of Skempton (1951), and is shown below.

$$q_{ULT} = N_C s_U + p_O \qquad (12) \text{ (from Skempton, 1951)}$$

$$FS = \frac{q_{ULT}}{\sigma_{VO}} = \frac{N_C s_U + p_O}{\sigma_{VO}} \qquad (13) \text{ (from Bjerrum and Eide, 1956)}$$

In this case, p_O is the pneumatic chamber pressure applied to the face. This equation was modified to include the affects of the depth of soil embedment (H_S) of the caisson wall on basal stability. Equation 14 is the result of the incorporation of this variable into Equation 13.

$$FS = \frac{N_C s_U + p_O + H_S \gamma}{\sigma_{VO}} \qquad (14) \text{ (modified from Bjerrum and Eide, 1956)}$$

Basal stability was calculated in the same manner for cohesionless soils utilizing a modified version of Terzaghi's (1943) bearing capacity equation using N constants from Vesic (1973) and plugging the resulting q_{ULT} value into Equation 13 shown previously. A value of 1 foot was assumed for B in Equation 15.

$$q_{ULT} = (H_S \gamma + p_O) N_q + \frac{1}{2} \gamma B N_\gamma \qquad (15) \text{ (modified from Terzaghi, 1943)}$$

The basal stability of the excavation at incremental depths in cohesive soils within the site geologic profile were also evaluated employing Peck's (1969) stability factor, N_t, which is computed using the equation below.

$$N_t = \frac{\sigma_{VO} - p_O}{S_U} \qquad (16) \text{ (from Peck, 1969)}$$

Both the Shansep and Recompression triaxial undrained shear strength values were examined for cohesive soils within the soil profile of McDermott Court. Separate analyses of these two different strengths were conducted to look for differences in stability.

First, the ultimate bearing capacity (q_{ULT}) was calculated for depths within the soil profile using Equations 12 and 15. Then the basal stability (FS) of the cohesive soils was calculated using Equation 13 disregarding chamber pressure. This fits the conditions of open face excavation without pneumatic pressure where the face is at the same elevation as the base of the caisson wall. For this case, both the organic silt and the normally consolidated Boston Blue Clay possessed computed factors of safety less than unity.

Then the factors of safety were recomputed utilizing the added support provided by the allowed range of pneumatic air pressures (p_O) and depth of embedment (H_S). The minimum value of the design pneumatic chamber pressure (p_D) was set equal to hydrostatic pressure (u), and the maximum was constrained to 50 psi following federal regulations. Because the excavation face is a temporary feature, a minimum required factor of safety was set at 1.25. The cohesive soil stabilization pressure (p_C) was then back calculated using Equation 14 at various elevations to obtain this value of stability. The design pneumatic chamber pressure (p_D) for each elevation of the excavation face was then taken as the higher value of either the required cohesive soil stabilization pressure (p_C) or hydrostatic (u) pressure. The effect of embedment depth (H_S) upon basal stability was found to be negligible. The design pressure (p_D) is therefore based on the safest assumption that H_S is equal to zero. The resulting factors of safety, FS', calculated in Appendix D for the organic silt and the soft clay, all exceeded the minimum factor of safety with the application of air pressure and an embedment depth of zero. An example of these calculated values is shown in Table 5-1.

Elevation (ft)	q_{ULT} (psf)	FS	p_D (psf)	u (psf)	p_D (psf)	FS'	N_t
-11	1550	1.27	-0.2	1.3	1.3	1.55	4.13
-15	1550	0.96	3.3	3.0	3.3	1.33	4.58
-17	1550	0.85	5.0	3.9	5.0	1.32	4.38
-20	1550	0.73	7.6	5.2	7.6	1.31	4.08

Table 5-1 Example calculation using Shansep s_U sequence for stability analysis (from Appendix D)

The results of the basal stability analysis (N_t) using Equation 16, found in Appendix D, confirms that the soft soils, both the organic silt and the soft, normally consolidated Boston Blue Clay, present the critical cases regarding excavation face stability during caisson sinking. Thus the critical cases of basal stability, open face excavation in the cohesive soils beneath McDermott Court, could be safely mitigated through proper application of chamber air pressures, which provide additional stability.

The required cohesive soil pressure for stabilization within the shallow organic silt deposit controlled the design pressure. Here, hydrostatic pressures were below those required for silt stability, and so the design pressure becomes those that are required to stabilize the excavation face. When the sand layer is reached, the maximum air pressure required for stability decreased dramatically, and thus the design pressure line returns to the hydrostatic pressure. This decrease in pressure also lengthens the time workers can spend at the face. The pressures required to achieve stability within the deeper Boston Blue Clay were always less than the hydrostatic pressure. Thus the design pressure mirrors the hydrostatic line until the maximum pneumatic pressure of 50 psi is reached, at which time it is held constant for the rest of the sinking operation. During this last part of the sinking operation, when pneumatic pressures are below hydrostatic levels, groundwater inflows will occur unless the soils surrounding the excavation are depressurized by groundwater withdrawal. This withdrawal would last until the base slab sealed the bottom of the excavation chamber at the end of the drive. The resulting design pneumatic chamber air pressures as they relate to caisson depth are summarized in Figure 5-4.

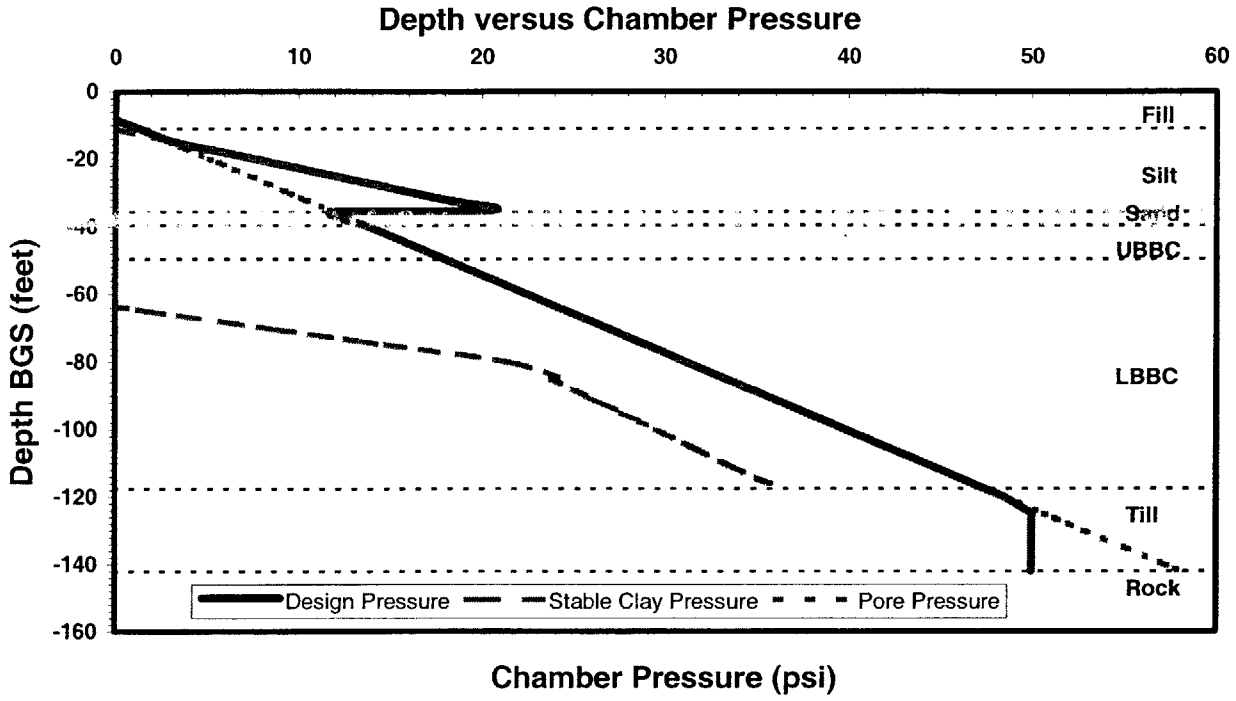

Figure 5-4 Pressure requirements for stability and caisson design

The end result of the analysis was to confirm that the application of air pressures to the excavation face within the federally regulated range could achieve a stable face and prevent inward movement and subsequent bearing capacity failure into the pneumatic chamber, which could induce large settlements at the surface and for adjacent structures.

To verify that the stability analysis was correct, the calculated Peck (1969) stability factors (N_t), shown in Table 5-1 above and calculated in Appendix D, were correlated with his descriptions of excavation conditions. The resulting stability factors indicated that conditions of small to moderate amounts of creep would occur at the excavation face, but no serious instability or failure was predicted.

Therefore, the methods of both Peck (1969) and Bjerrum and Eide (1956) indicate that with the proper design chamber pressures applied to the excavation face, which are within the federal limits, basal stability is achievable with a minimum factor of safety of 1.25.

5.2.2 Soil Skin Friction

The caisson is designed to move downward during the installation, facilitated by the removal of material at its base, subjecting the sides of the caisson to contact with the soil and subsequent drag on the caisson induced by soil skin friction. It is important to accurately estimate the values of friction between each type of soil and the caisson wall, so that the total force needed to overcome this friction can be included in the design. It is important to note that skin friction values will vary over time as horizontal effective stresses increase to a maximum value equal to the in-situ horizontal stress (σ_{ho}).

Different methods were used to calculate the skin friction values for cohesive (f_c) and cohesionless (f_s) soils. Also, the friction values for each soil were estimated both for short and long-term cases.

Short-term unit skin frictions for cohesive soils (silt and BBC) were calculated as clay friction on piles. Values of α provided by Dennis and Olson (1983) and Shansep undrained shear strengths (s_U) were used in the following equation to estimate short-term clay skin friction between the caisson and cohesionless soils beneath McDermott Court.

$$F_{LOW-COH} = \alpha s_U \qquad (17) \text{ (from Dennis and Olson, 1983)}$$

Long-term cohesive unit skin frictions were estimated as the Shansep undrained shear strength ($F_{HIGH-COH}=s_U$) of the soil, which is the maximum shear resistance the soil could provide. Over time as the caisson is sinking through the soft soils, it is probable that this value will come to emulate the remolded undrained shear strength because the cohesive soils adjacent to the caisson will continue to be sheared past their peak strength values, significantly altering or destroying the structure of the soil, which contributes some of its strength.

Short-term and long-term unit skin frictions between the caisson wall and cohesionless soils (fill, sand, till) were calculated utilizing values for interface friction angles (ϕ_M) between formed concrete and various soil types specified in Department of the Navy (1982). Short-term friction was calculated utilizing the Rankine active earth pressure coefficient (K_A) from Equation 3 in

Section 3.2 to calculate the horizontal effective stress (σ'_{ho}) at the interface. The unit skin frictions were then calculated using this active horizontal pressure with the equation below.

$$F_{LOW-COHL} = K_A \sigma'_{VO} \tan \phi_M \qquad (18)$$

The long-term cohesionless unit skin frictions were calculated at the full in-situ horizontal effective stress (σ'_{ho}) using the interface friction angles (ϕ_M) and the coefficient of lateral earth pressure (K_O) from Equation 2 in Section 3.2 in the following equation.

$$F_{HIGH-COHL} = K_O \sigma'_{VO} \tan \phi_M \qquad (19)$$

Short and long-term unit skin friction values were calculated using Equations 17 through 19 within respective columns in Appendix E. Table 5-2 summarizes the range of unit skin friction values calculated for each soil within the profile.

Soil Type (F in psf)	Min. F_{LOW}	Max. F_{LOW}	Min. F_{HIGH}	Max. F_{HIGH}
Fill	51	91	79	140
Organic Silt	145	145	250	250
Sand	216	216	346	346
Stiff Boston Blue Clay	722	749	1570	1630
Soft Boston Blue Clay	832	1582	1300	1862
Glacial Till	418	529	1430	1809

Table 5-2 Summary of calculated unit skin friction values (from calculations in Appendix E)

A table of skin friction values by soil type is given in Swatek (1975) as a means of estimating caisson skin friction during sinking operations. Robinson (1964) also provides a summary of lateral friction by soil type for caissons. Except for the soft soil values, Robinson and Swatek's values appear to be conservative compared to the calculated values for the pneumatic caisson shown in Table 5-2. Calculated short and long-term soil skin friction values are shown in Figure 5-5. The calculated low unit skin frictions (F_{LOW}) by soil type are compared to those of Swatek (1975) and Robinson (1964) in Table 5-3.

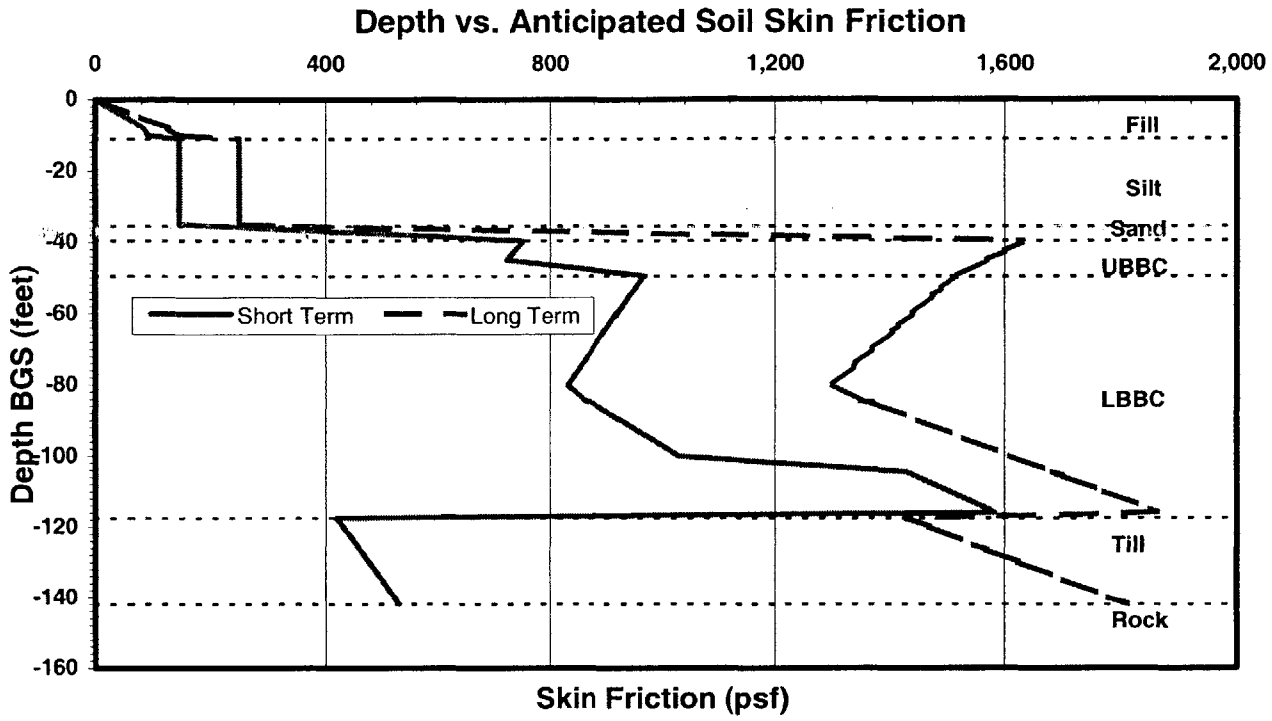

Figure 5-5 Variation of unit skin friction with depth below McDermott Court

Soil Type	Swatek (1975) psf	Robinson (1964) psf	Calculated psf
Soft Clay	150	125	1210
Stiff Clay	1000	1050	740
Dense Sand	700	600	220

Table 5-3 Comparison of low skin friction values

Coller et al (2001) advocate that the injection of bentonite slurry as a lubricant behind the cutting edge of jacked pipe can reduce skin friction in sands up to 50%. Cases where high skin frictions had to be overcome involved the over-injection of the bentonite lubricant, which caused a rapid decrease in skin friction. Over-injection occurs when more slurry is injected than the annular volume between the wall and soil, which forces the soil away from the wall. This method is not advisable in the soft Boston Blue Clay deposit, as voids may be formed within the soil mass adjacent to the caisson, creating a pocket into which soil may flow, inducing surface settlements. The injection of bentonite is recommended for cohesionless layers and will be discussed further in Section 5.3.3.

5.2.3 Simple Settlement

A simple calculation of the maximum possible settlement was made for the caisson sinking operation. Various widths of open space are left behind the cutting edge between the caisson wall and the exterior soil. Assuming that the soil suffers no volumetric strain, the soil around the shaft will eventually sink and fill in the annular space next to the caisson. The maximum settlement (ρ_{MAX}) in this case assuming no soil volumetric strain follows the equation below,

$$\rho_{MAX} = \frac{H_C \pi \left(r_i^2 - (r_c - t)^2 \right)}{\pi \left(r_i^2 - r_c^2 \right)} \qquad (20)$$

where H_C is the height of the caisson, r_i is the radius of influence being examined, r_c is the outer caisson radius, and t is the width of the annular space between the soil and the caisson wall created by over cutting.

Building 62 is located at an approximate radius of 25 feet from the caisson centerline. The depth of the caisson is 142 feet, with an outer radius of 13 feet. The simple settlement calculations based on radii of influence of 15, 20, 25, 30, 50, and 100 feet are calculated for over cut thicknesses between ¼ and 1 inch in Appendix G using Equation 20. The probable maximum settlements, ρ_{MAX}, calculated for various thicknesses of over cutting for a radius of influence of 25 feet are given in Table 5-4.

Over Cut Thickness, t (inches)	ρ_{MAX} (inches)
0.25	1.997
0.50	7.891
0.75	11.847
1.00	15.808

Table 5-4 Probable maximum settlements at a r_i of 25 feet as a function of cutting edge thickness

Upon inspection of the resulting probable maximum settlements for the adjacent structure, it was determined that a grouting program would have to be employed to infill the void once the caisson reached final depth. Based upon the settlement values, the design over cut of the caisson and thickness of the resulting annulus was chosen to be 0.25 inches. This space should be

sufficient to provide adequate separation of the wall and the soil and allow a temporary K_A condition to occur during driving. However, the settlements this thickness can induce are still unacceptable. To counter this, bentonite slurry could be injected during caisson sinking to help to reduce the magnitudes of lateral soil movement into the caisson/soil annulus and minimize settlements, while having the added benefit of reducing skin friction along the length of the caisson as advocated by Coller et al (2001). The reduction in skin friction could ultimately reduce the force necessary to drive it to final depth, and thereby reduce the ballast costs during construction. Therefore, the injection of bentonite slurry into the caisson/soil annulus during construction, followed by the grouting of the annulus once construction is complete, is recommended for the library shaft pneumatic caisson alternative.

5.3 Structural Design

Once the geotechnical analysis for the caisson has been completed, design of the caisson structure can take place. The design of the pneumatic caisson follows the methodology proposed by Swatek (1975). Specific aspects of pneumatic caisson design include the structural configuration, wall of the caisson, meeting anticipated thrust requirements, the pressure bulkhead, aspects of assembly, and the airlock systems used to convey workers and material in and out of the excavation chamber.

5.3.1 Structural Configuration

The structural configuration of the caisson must either facilitate or match the interior requirements set forth in Section 2. Upon examination of the finished shaft and its internal wall, it was decided that the stairwell annulus could be used as a ballast chamber to provide additional driving weight if needed. The stairs would be added to the caisson shaft once sinking had been completed. Without the stairs in place, the mechanical egress wall within the caisson could serve as a ballast compartment to satisfy sinking thrust requirements and conform to the internal finished dimensions (see Figures 5-26 and 5-29).

The mechanical egress shaft within the dividing wall, previously shown in Figure 2-2 of Section 2.1, would then temporarily house the airlock systems used to convey workers and material into and out of the pneumatic excavation chamber at the bottom of the caisson below the pressure

bulkhead. The pressure bulkhead would therefore have several round cutouts through its depth. It was recognized that this structural configuration would require a thick reinforced concrete bulkhead to account for the added stress imposed by the cutouts. The cutout locations would also have to be symmetric in plan in order to keep the caisson symmetrically loaded and prevent weight induced wandering during the driving process. The layout of the airlock cutouts within the pneumatic chamber bulkhead is shown in Figure 5-6.

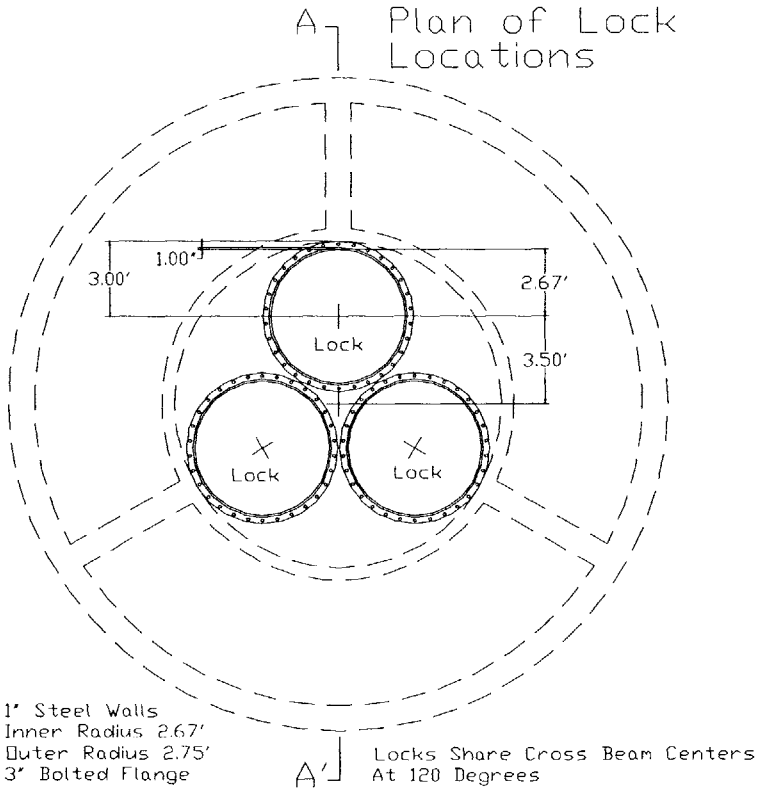

Figure 5-6 Plan of maximum airlock dimensions and cutout locations in pneumatic chamber bulkhead

The large thickness of the bulkhead, coupled with the need for sub-floor connections at the shaft base for ventilation purposes after installation (see Figure 2-1, Section 2.1), led to the conclusion that the top of the bulkhead must be driven 5 feet below the elevation of the library's tenth floor, which is 125 feet BGS.

5.3.2 Caisson Wall

The design of the caisson wall must meet three primary requirements. These three requirements are that the wall must fulfill the function of a shaft liner and resist lateral earth pressures imposed upon it, have enough area to support the maximum driving thrust at its base without failure, and that the leading edge be resistant to abrasion by the soils through which will pass.

First, the outer wall of the caisson must be designed thick enough to resist the probable maximum lateral load imposed upon it. The caisson is also designed to be segmental, significantly reducing the amount of fabrication done on site, and therefore must have enough area to resist the dynamic movement of the caisson through the soil. The segmental structure allows segments to be added quickly without interfering with sinking operations or creating cold joints in the concrete liner that would cause leakage. Proctor and White (1977) state that pressure in squeezing ground, such as soft clay, increases over time and that an estimate of the ultimate clay pressure (p_d) on the liner is given by the equation below.

$$p_d = \gamma z - s_U \qquad (21) \text{ (from Proctor and White, 1977)}$$

They also suggest the equation below to estimate the liner design load in dense sand for a shaft deeper than 5 times its diameter (D).

$$p_d = 0.2\gamma D \qquad (22) \text{ (from Proctor and White, 1977)}$$

Finally, Proctor and White (1977) suggest that the short term horizontal loading on shaft liners in running ground, such as sand, can be calculated utilizing the Rankine active earth pressure coefficient (K_A), previously calculated in Equation 3, using the following equation.

$$\sigma'_{ho} = K_A \gamma z \qquad (23) \text{ (from Proctor and White, 1977)}$$

However, this neglects hydrostatic loading and also, as time passes, the horizontal effective stress, σ'_h, can be expected to return to the original value of σ'_{ho} previously calculated in Section

3.2. When calculated, the long-term horizontal effective stress dominates as the maximum pressure that the liner must resist. Therefore, the in-situ horizontal effective stress, σ'_{ho}, calculated in Section 3.2, was used as the liner design pressure, p_d. Summers (2000) suggests the use of the Lame' equation to design the thickness of the shaft liner in concrete having compressive strength of σ_t, an internal radius of r_i, factor of safety of F, and resisting a pressure P.

$$t = r_i\left(\sqrt{\frac{\sigma_t}{\sigma_t - 2PF}} - 1\right) \qquad \text{(4) (Lame' Equation from Summers, 2000)}$$

The thickness, t, of the caisson wall must also provide enough area to provide the compressive strength needed to resist the maximum weight of the structure in the event that all skin friction is lost between the caisson and the adjacent soil. Therefore, the wall thickness, t, must also satisfy Equation 24 derived below,

$$\frac{LF}{\sigma_t} = A_{wall} = \pi\left((r_i + t)^2 - r_i^2\right)$$

$$t = \sqrt{\frac{L_C F}{\pi\sigma_t} + r_i^2} - r_i \qquad (24)$$

where L_C is the maximum vertical load (caisson live and dead factored loads), F is the factor of safety, σ_t is the concrete compressive strength, A_{wall} is the plan area of the concrete liner, and r_i is the inner radius of the caisson wall.

Due to the dynamic nature of the caisson wall during excavation and driving, a higher factor of safety was desired. Proctor and White (1977) also state that the long-term pressure on shaft liners can become significantly more than anticipated in squeezing cohesive soils, which accurately describes the soft clay, and that further reinforces the need for a higher factor of safety. A preliminary estimate of 1 foot for the thickness of the caisson wall comprised of 5000 psi concrete was used. The compressive loading was determined to be the controlling factor for

the thickness of the caisson wall. Calculations were conducted in Appendix F to determine the maximum factored live and dead loads of the caisson structure, a force found to be 30,614,550 lbs (calculated in p.121 of Appendix F). This is considered the maximum load (L_C) imposed upon the base of the caisson wall if skin friction is neglected. The resulting factor of safety (F) of the 1-foot thick caisson wall using Equation 24 was found to be 1.85. Although this case is unlikely, over injection of lubrication could cause base loads to approach this end loading condition. The maximum lateral loading in the liner (P), calculated in Section 3.2 as 13,333 psf, was calculated using Equation 4 to have a minimum factor of safety (F) of 4.06 for the 1-foot thickness. Therefore, the design of the caisson wall in Appendix F uses a wall thickness, t = 1.000 feet, which adequately satisfies both the end loading and lateral pressure conditions. The calculations to find the caisson wall thickness for design can be found in the spreadsheets included in Appendix F.

The last issue concerning the caisson wall is the design of the leading edge or cutting edge, which will be in direct contact with moving soil under high pressures. Specifically, the glacial till near the base of the planned shaft will present a particularly abrasive layer, which will require some sort of resistant armor to resist erosion of the leading edge.

Swatek (1975) suggests a heavy shoe armored with steel plating for land caissons that will encounter granular, abrasive soils. A typical cross section of a heavy shoe from Swatek is shown in Figure 5-7.

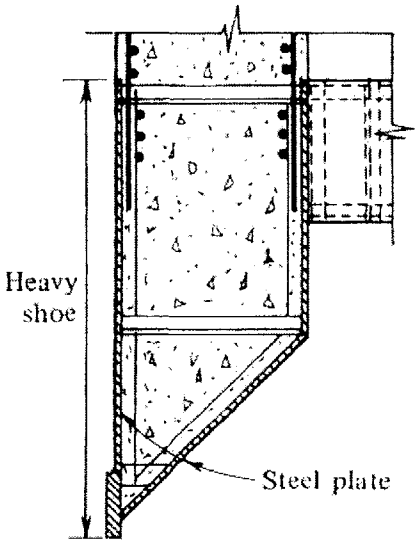

Figure 5-7 Section of heavy shoe for land caisson (from Swatek, 1975)

Robinson (1964) discusses the use of injected water through a system of nozzles behind the cutting edge to reduce lateral friction on the caisson. Megaw and Bartlett (1982) state that bentonite slurry injected around the exterior of the caisson wall has been found an effective lubricant against sometimes-unpredictable skin friction. Bentonite slurry has a higher unit weight, and is therefore better able to hold open any voids between the caisson wall and the adjacent soil until grout can be injected. Also, the cutting edge must also be designed to cut an area slightly larger than the caisson wall above it. This facilitates the introduction of bentonite slurry into this area to reduce skin friction on the caisson walls as advocated by Coller et al (2001) and also prevent excessive lateral soil movements. Therefore, Robinson's (1964) type of injection system will be included in the leading edge design, but bentonite slurry will replace water as the injected fluid. A diagram of the injection nozzle system Robinson proposes is shown in Figure 5-8. A diagram of the designed cutting edge of the caisson is shown in Figure 5-9.

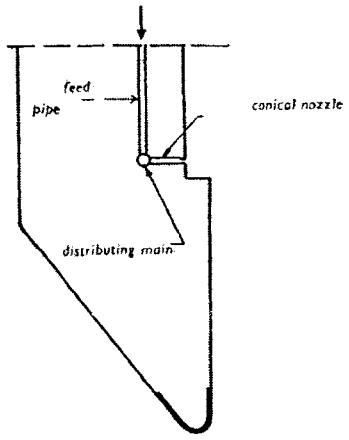

Figure 5-8 Lubricant injection system behind cutting edge (from Robinson, 1964)

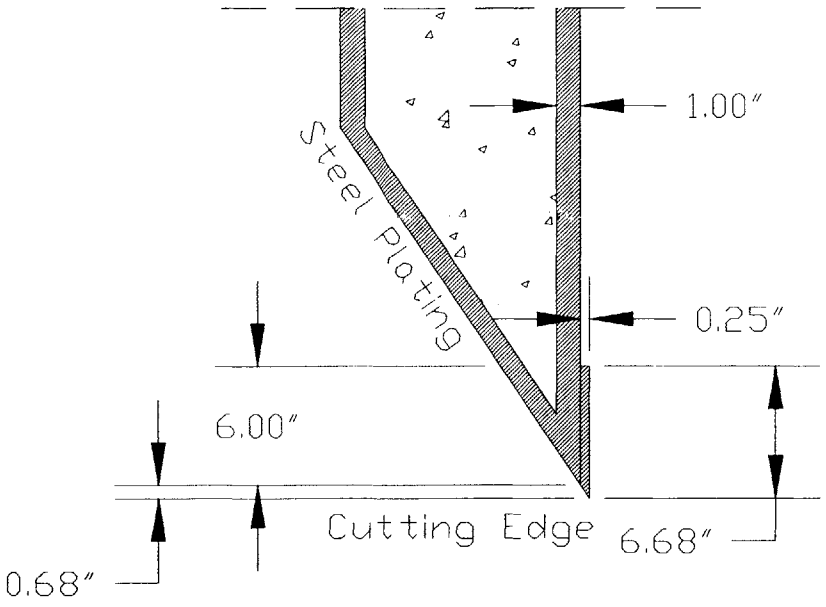

Figure 5-9 Detail of designed cutting edge of pneumatic caisson minus injection system

The caisson wall will consist of precast, steel reinforced concrete segments. A typical steel reinforcement pattern within the wall of a circular caisson is shown in Figure 5-10.

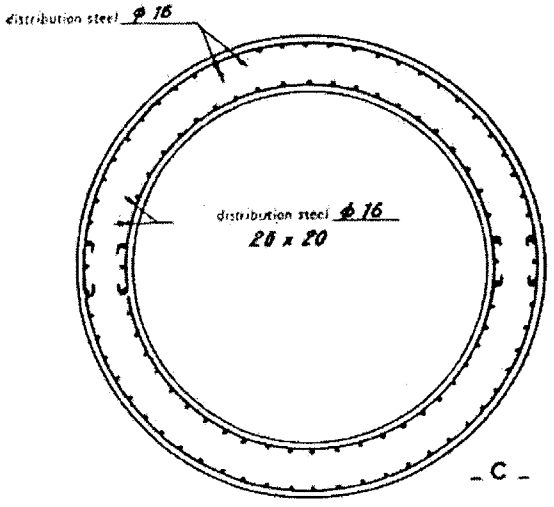

Figure 5-10 Typical reinforcement within circular caisson wall (from Robinson, 1964)

5.3.3 Meeting Anticipated Thrust Requirements

Using the unit skin friction values calculated in Section 5.2.2, multiplied by the outer perimeter of the caisson over a total depth of 142 feet, the cumulative skin friction was calculated over that entire depth within the soil profile. The sums of the skin frictions for the bentonite (TF_{BENT}), short-term (TF_{LOW}), and long-term (TF_{HIGH}) cases were tabulated and can be found within the spreadsheet columns of Appendix E. Bearing capacities were also calculated at various depths along the drive. The bearing capacity of the caisson tip will later be considered in thrust calculations. Both the bearing capacities calculated in Section 5.2.1 and the cumulative skin friction values summarized in Table 5-5 and are plotted in Figure 5-11.

Depth BGS (ft)	End Bearing (psf)	Bentonite TF_{BENT}	Short-term TF_{LOW}	Long-term TF_{HIGH}
0	130,505	32,626	32,626	32,626
20	102,107	640,147	697,918	813,530
40	665,740	1,531,119	1,706,621	2,279,730
60	558,138	3,169,911	3,709,950	5,285,326
80	530,958	4,783,223	5,677,603	8,050,248
100	657,571	6,544,305	7,826,966	11,073,244
120	1,440,744	8,849,994	10,694,154	14,623,679
142	1,654,187	9,438,937	11,723,136	17,777,422

Table 5-5 Summary of end bearing and cumulative friction values (from Appendix E)

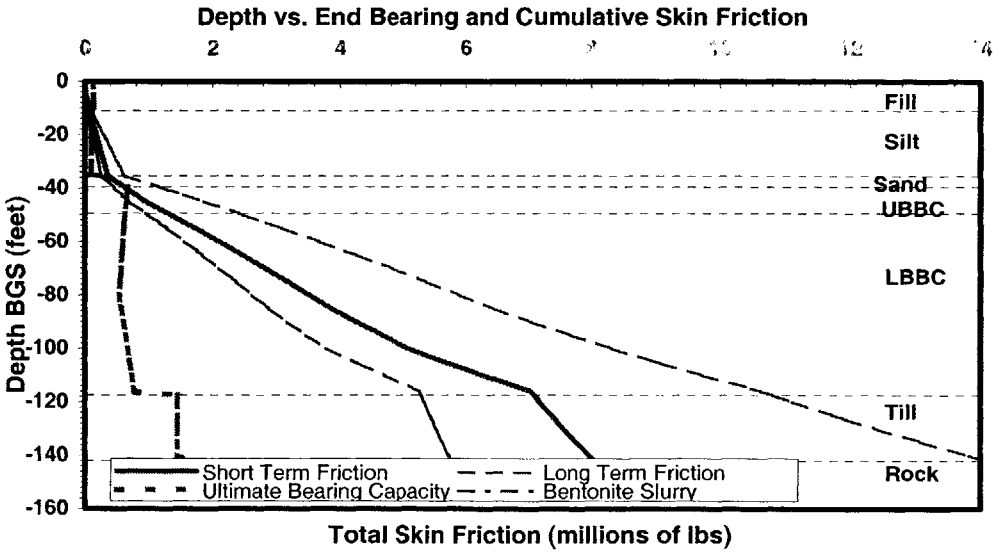

Figure 5-11 Cumulative skin friction on caisson as a function of depth

The bentonite slurry cumulative skin friction (TF_{BENT}) line was calculated as a result of the reduction of the short-term friction using the advocated values from Coller et al. (2001). Assumed skin friction reductions of (R_{COHL}) 50% in cohesionless soils and (R_{COH}) 25% in cohesive soils were used to calculate a best-case skin friction scenario, shown as "bentonite slurry" in Figure 5-11. This is assumed to be the lower limit of cumulative skin friction values.

The cumulative skin friction must be overcome in order for the caisson to sink during excavation at the face. A percentage of 25% of the end bearing value (G) was added as the amount of additional driving force used to promote the downward movement of the caisson beyond the amount of cumulative skin friction and upward pneumatic force at the excavation chamber. This additional force promotes the continual downward movement of the caisson while not introducing excessive loads at the face that could induce failure into the caisson. An assumed percentage of the bearing capacity (G) of 25% assures that bearing failure does not occur, but that a significant amount of thrust still reaches the tip of the caisson to promote downward movement. There is also an upward force from the air pressure in the excavation chamber that acts on the area of the bulkhead that must be overcome. The required driving thrust (TR) for the caisson was calculated as the sum of the cumulative skin friction, 25% of the end bearing (G) of the soil at the cutting edge, and the total of the upward force exerted on the bulkhead by the excavation chamber air pressure used. The resulting required best (TR_{BENT}), worst (TR_{HIGH}) , and anticipated (TR_{LOW}) cases of driving thrusts required over the depth range of the pneumatic caisson are summarized in Table 5-6 and shown in Figure 5-12, resulting in a maximum value of 17.7 million pounds. The calculations for end bearing and cumulative skin friction can be found in the spreadsheets of Appendix E.

Depth BGS (ft)	Bentonite TR_{BENT} (lbs)	Rankine Active TR_{LOW} (lbs)	K_O Condition TR_{HIGH} (lbs)
0	32,626	32,626	32,626
20	640,147	697,918	813,530
40	1,531,119	1,706,621	2,279,730
60	3,169,911	3,709,950	5,285,326
80	4,783,223	5,677,603	8,050,248
100	6,544,305	7,826,966	11,073,244
120	8,849,994	10,694,154	14,623,679
142	9,438,937	11,723,136	17,777,422

Table 5-6 Summary of calculated driving thrusts of library pneumatic caisson (from Appendix E)

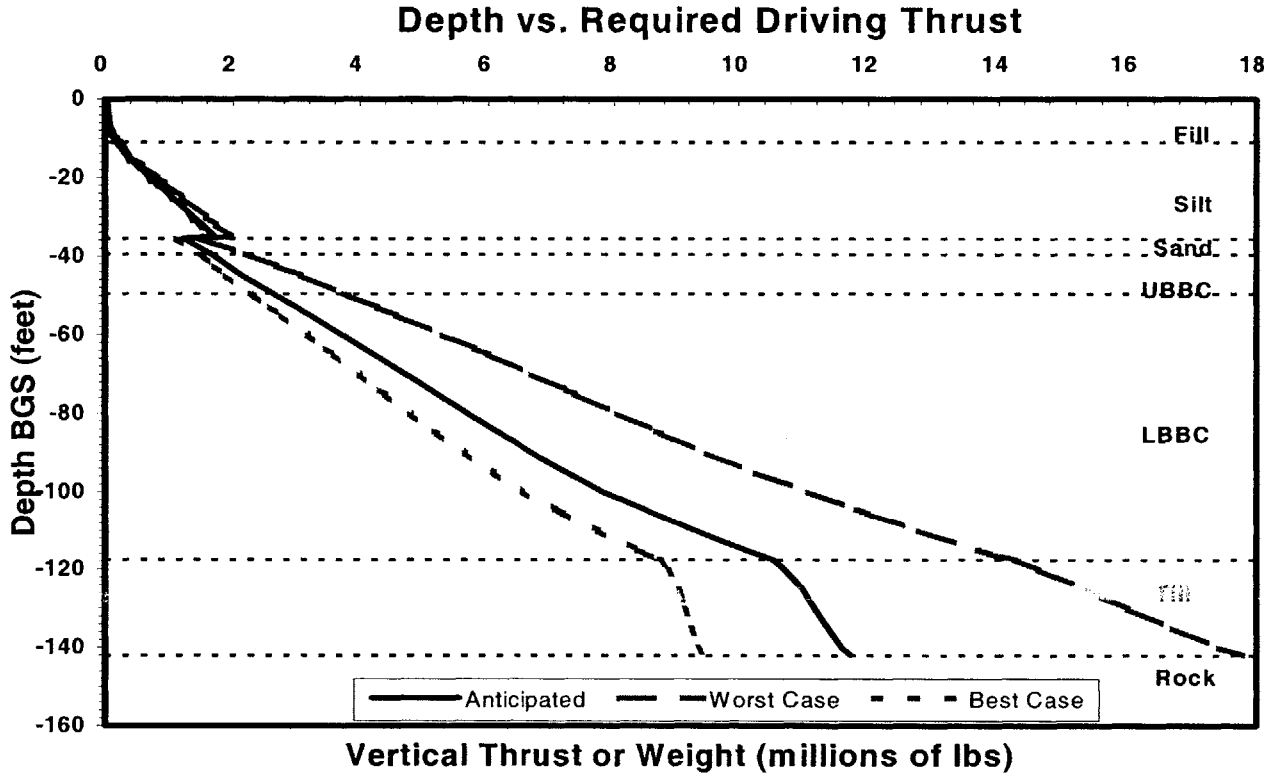

Figure 5-12 Anticipated driving thrust for the pneumatic caisson

The drop in required thrust at approximately 35 feet shown in Figure 5-12 is due to the reduction of required pneumatic chamber pressure, which reverts back to hydrostatic values when the sand layer is encountered.

The final empty weight of the designed pneumatic caisson was 2,631,507 pounds (from the sum of segment weights in Appendix G). In order to supply the additional weight to meet thrust requirements, it was decided to use steel shot as removable ballast within the stairwell annulus of the caisson. Industrial Supply (2001) provides steel shot ballasts up to 345 pcf in unit weight. Using the calculated volumes of the stairwell annulus minus the cross beams, the required thrust for the maximum thrust case could still not be reached. Therefore, shot was also placed within the annular space between the air and muck locks inside the egress wall, which allowed the maximum thrust requirement to be satisfied. A view showing the steel shot in the annular space is shown later in Figure 5-29 of Section 5.4.5. The calculated heights of steel shot ballast at the end of drive for each caisson segment can be found in Appendix G for best-case (bentonite) and worst-case scenarios.

Swatek (1975) states that heavy caissons drive the most smoothly, and are the easiest to keep within verticality when their center of gravity is kept in the lower portion of the caisson. The use of steel shot ballast also facilitates this situation.

5.3.4 Pressure Bulkhead

The airtight bulkhead at the top of the excavation chamber must provide enough headroom to allow mechanically-assisted excavation work to be conducted below it unencumbered. Megaw and Bartlett (1982) recommend that the bulkhead be positioned approximately 2.5m (8.2ft) above the cutting edge level. This height is based upon the assumption of hand excavation of soil materials at the face. In order to facilitate the anticipated type of excavation for the caisson, a chamber height between 9 and 11 feet is recommended. The schematics of the bulkhead within this report show a bulkhead height of 8 feet for simplicity. This pressure bulkhead also serves as the floor of the stairwell annulus and egress shaft above it, and will bear the full weight of those components as well as any ballast added to the caisson. It is anticipated that during construction, the steel shot ballast, having a porosity of 30%, could fill with rainwater, yielding a unit weight of 364 pcf. Keeping this in mind, the maximum volume of ballast that the caisson is capable of holding, as well as weight of the locks, egress wall, and the bulkhead itself were summed in spreadsheets found on p.123 of Appendix F. The depth of the bulkhead was initially assumed to

be 4 feet of reinforced concrete with 2% reinforcing steel. The total combined maximum factored load (L_T) on the bulkhead is equal to 28,240,078 lbs (weight of outer caisson wall is not included). The area of the bulkhead surface minus the three airlock and mucklock cutouts (A_B) was found to be 381.1 ft^2. Therefore, the simplified maximum uniform factored bulkhead loading (L_U) of 74,099 psf was calculated (for calculations, see Appendix F).

In order to approximate the actual required depth of the bulkhead, it was first approached as a circular plate. After the maximum moment on the circular plate was found, and was used in the design of a beam to solve for the approximate depth:

The bulkhead could be simplified into a circular plate, with a radius (r_a) of 12.00 feet, as described by Timoshenko (1959). The three holes through the bulkhead for the air and muck locks, each having a radius of 2.75 feet, were simplified into one hole of equivalent area, which had a radius (r_b) of 4.76 feet. Since the bulkhead is cast as part of the exterior caisson wall, it essentially has a clamped edge, which provides a resisting moment. Timoshenko's case 10 most accurately describes this bulkhead. Equation 25 was used to find the maximum moment (M_r) in the bulkhead, where r_a is the radius of the circular plate, r_b is the radius of the hole in the center of the plate, q is the uniform load L_U, and ν is the Poisson's ratio of the plate material (assumed 0.15 for concrete).

$$M_r = \frac{q}{16}(3+\upsilon)\left(r_a^2 - r_b^2\right) \qquad (25) \text{ (from Timoshenko, 1959)}$$

Once the maximum moment had been determined, the bulkhead was examined as a simply supported beam in order to estimate its depth. It was to be constructed of reinforced concrete. The depth determined through beam design of the bulkhead provided a conservative value. The methodology of Meyer (1996) was employed to design the beam using the maximum moment obtained from Timoshenko's equation (25). Various percentages of reinforcing steel were examined as well as depths to find the optimum beam depth. Using the following equations by Meyer, coupled with the Timoshenko M_r, the adequacy of various beam depths and reinforcement levels was analyzed for the bulkhead.

$$a = \frac{A_S f_y}{0.85 f_C' b} \qquad (26) \text{ (from Meyer, 1996)}$$

$$M_U = \phi A_S f_y \left(d - \frac{A_S f_y}{1.7 f_C' b} \right) \qquad (27) \text{ (from Meyer, 1996)}$$

Only beams which satisfied $M_U > M_r$ were considered. An assumption that a 2% steel ratio (ρ) would be used was made and used in (f_C) 5000 psi concrete. A value for beam width, b, was held at a constant of 1 foot. Also, a steel yield strength (f_y) of 65,000 psi was assumed for the steel reinforcement in the bulkhead. The result of the calculations, shown in Appendix F, was that a beam of 48" depth was more adequate to carry the maximum factored live and dead loads of the bulkhead. The resulting design of the pneumatic chamber and bulkhead segment is shown in Figure 5-13 and Figure 5-14.

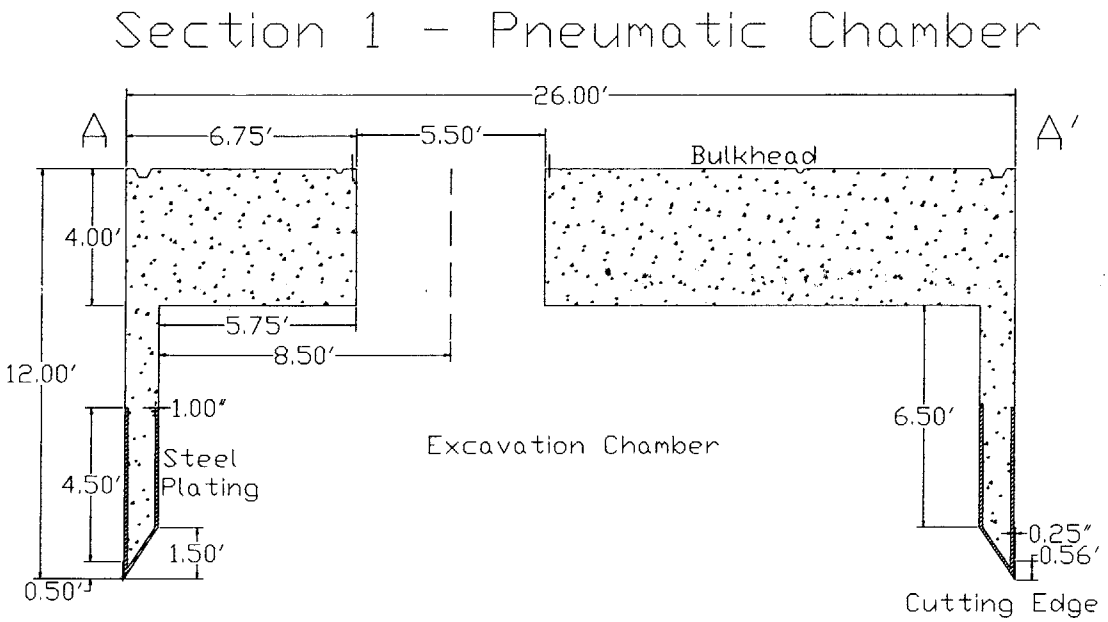

Figure 5-13 Vertical section of caisson segment 1

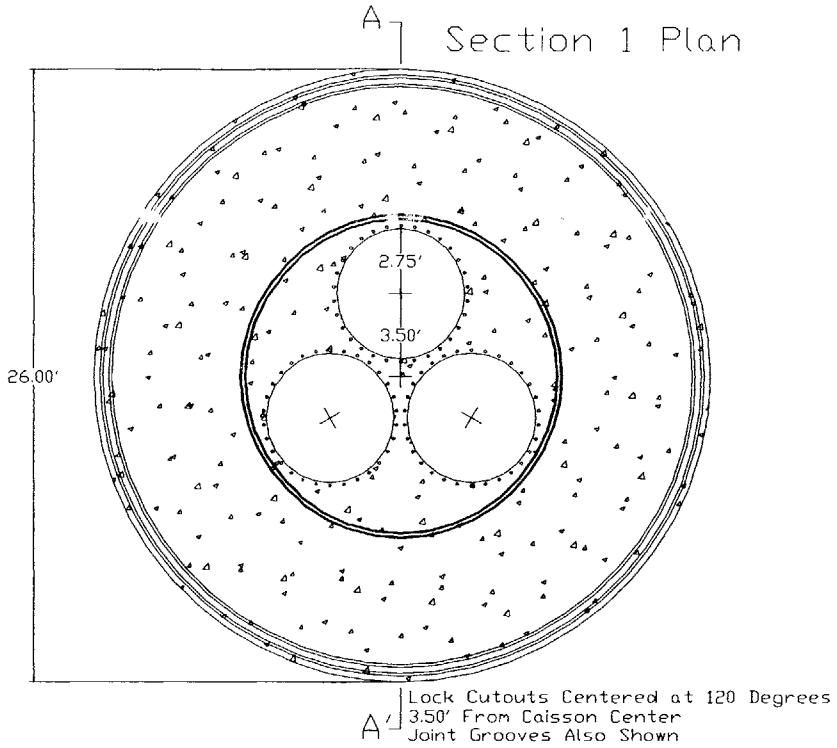

Figure 5-14 Horizontal section of caisson segment 1

5.3.5 Caisson Segments

The pneumatic caisson was designed as a segmental structure. The proposed caisson design, minus locks, is shown in Figure 5-15.

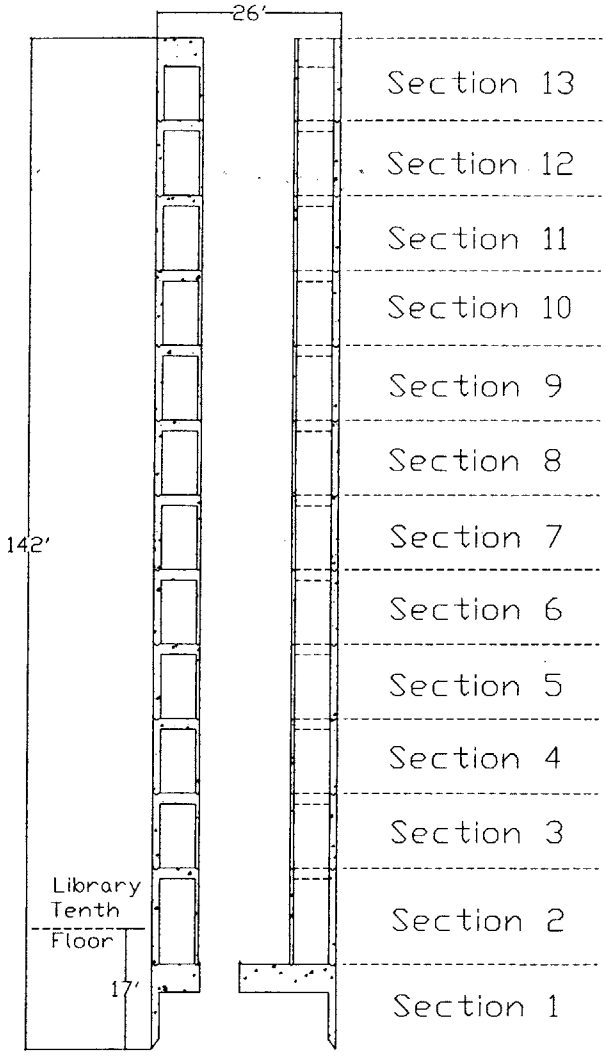

Figure 5-15 Vertical section of library shaft segmental pneumatic caisson

The stairwell that rests in this annulus makes 31.5 feet of vertical rise per revolution. A system of three cross beams was designed on levels spaced at 10.5 feet so that the stairwell could rest on the top of one out of the three beams in each group, passing though 120 degrees of the stairwell annulus between each beam group. The cross beam groups at one end of the segment essentially form an inverted channel. It is recognized that the free end of this channel will require stiffening elements until the segment is placed on the caisson. This bracing could take multiple forms, and is represented in subsequent schematics as temporary steel wires. The beams are 1.5 feet wide in plan view. The configuration of the crossbeam groups is shown in Figure 5-16 and Figure 5-17.

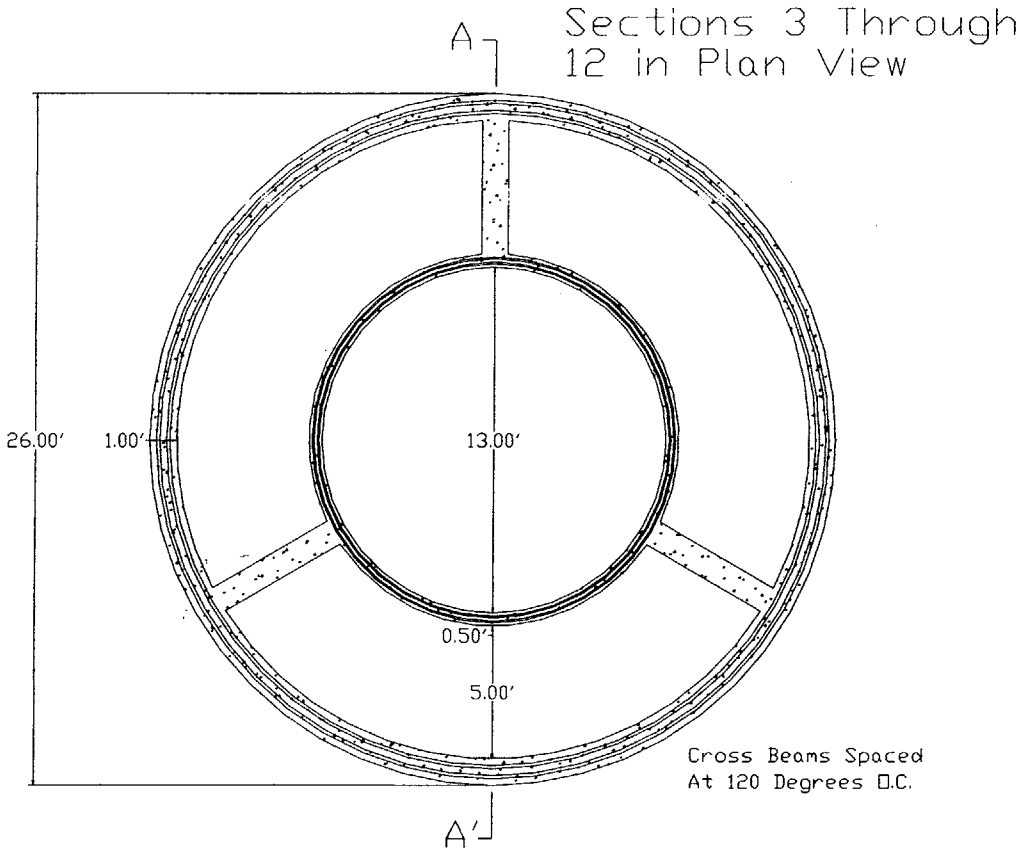

Figure 5-16 Horizontal section of segments 3 through 12 showing beam group layout

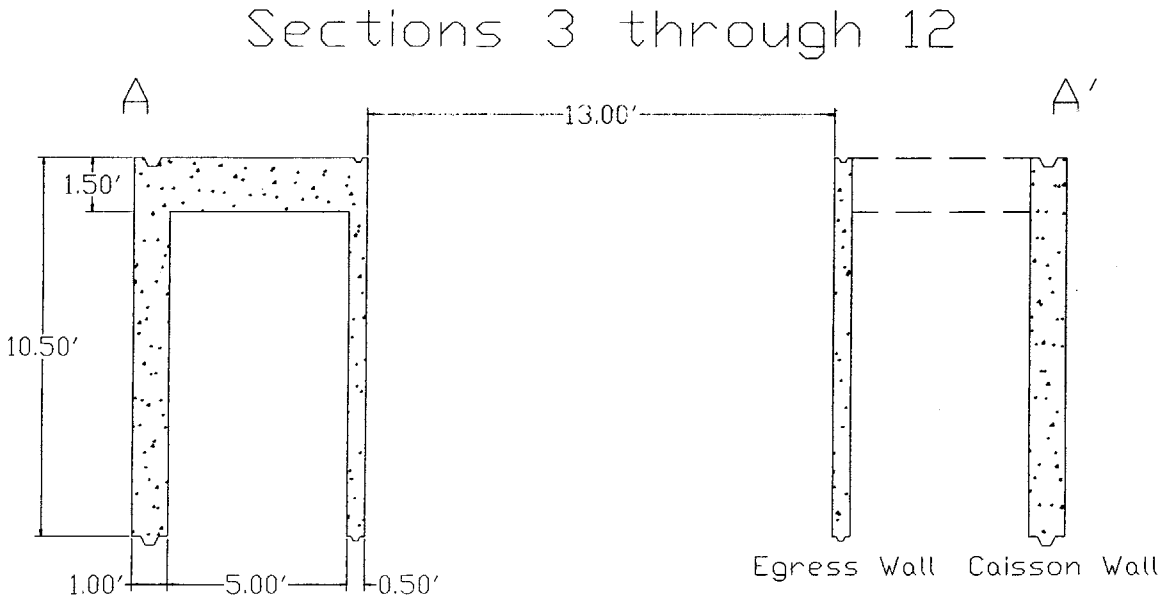

Figure 5-17 Vertical section of segments 3 through 12 showing beam group layout

Segments 3 through 12 are identical in dimension. Segment 1, at the leading edge of the caisson, was shown in Figure 5-13 and Figure 5-14. Segment 2 is slightly longer in dimension, but possesses the same plan section as Segments 3 through 12. Figure 5-18 shows segment 2 in vertical section and the elevations of the adjacent connector tunnel and library tenth floor.

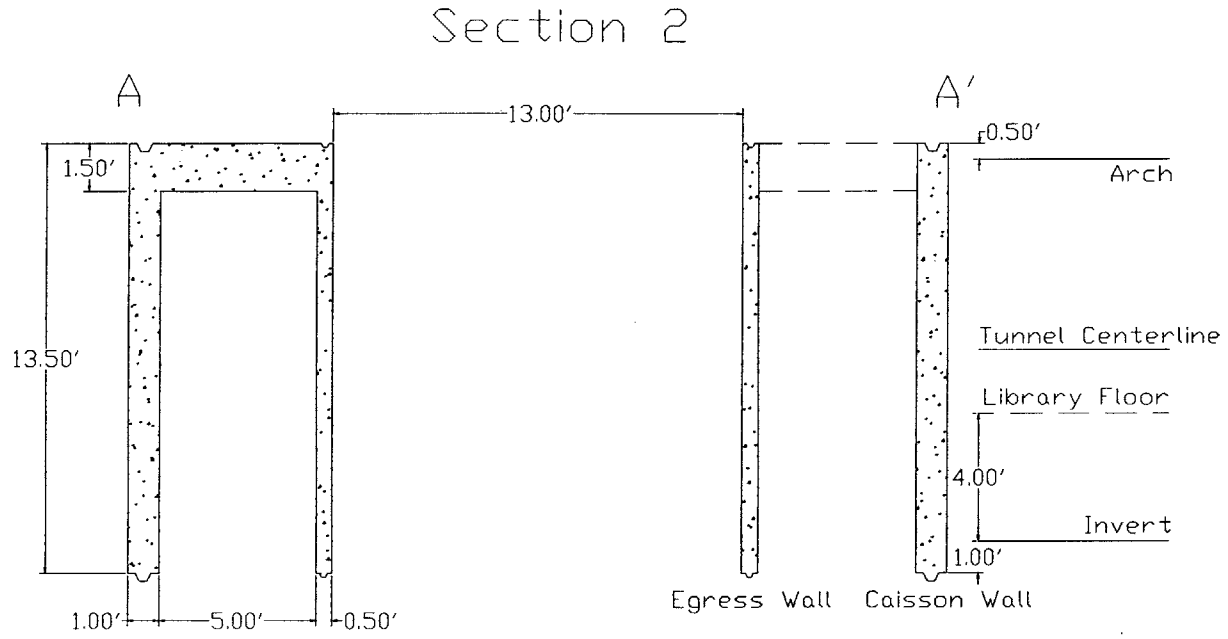

Figure 5-18 Vertical section of segment 2

Segment 13 was designed with a deepened crossbeam group in order to distribute the load of the overlying ventilation stage and mechanical egress cover. Flanges are also designed into the top of the segment to facilitate 6 inch thick concrete segments to cover the stairwell annulus and comprise the sidewalk on the surface. The plan section of the segment is identical to those of segments 3 through 12. Figure 5-19 shows segment 13 and the described sidewalk flanges in vertical section.

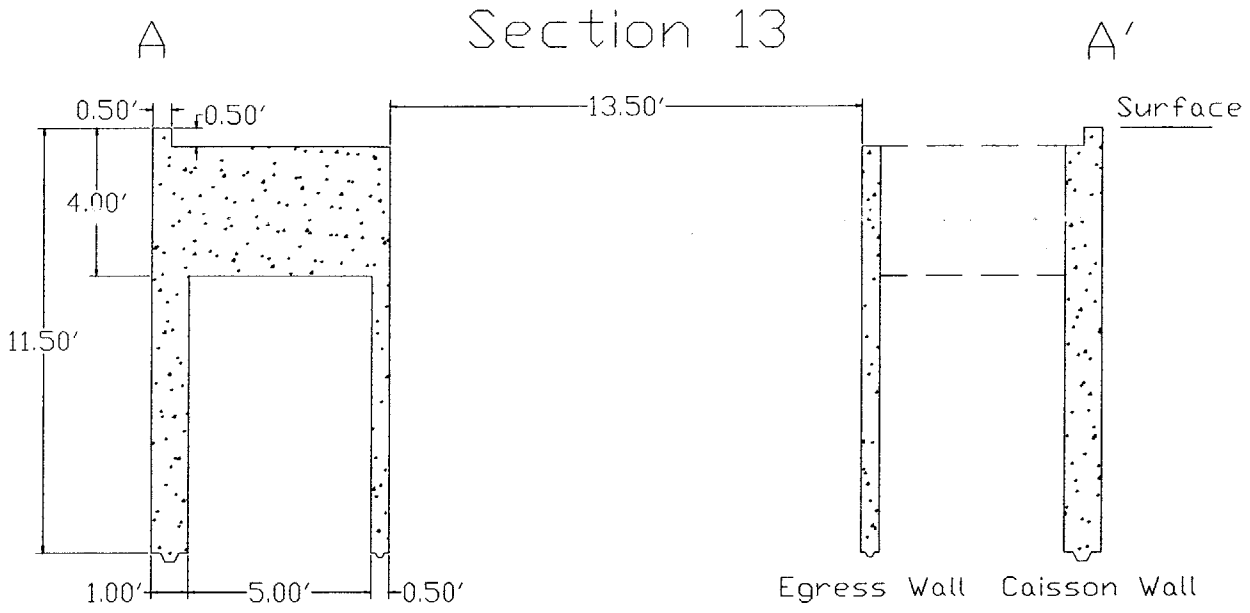

Figure 5-19 Vertical section of segment 13

The crossbeam groups of the segments 2 through 13 must all line up vertically when assembled; for this a keyway prevents misalignment during construction. The joints shown in the top and bottom of the caisson segments are designed to be supplemented with a sealant. Bolts or other connections capable of withstanding large vertical tensile forces that could be imparted by skin friction, which would pull the segments apart in the ground, should physically connect the segments. A detail of the joint minus the tensile connections is shown in Figure 5-20.

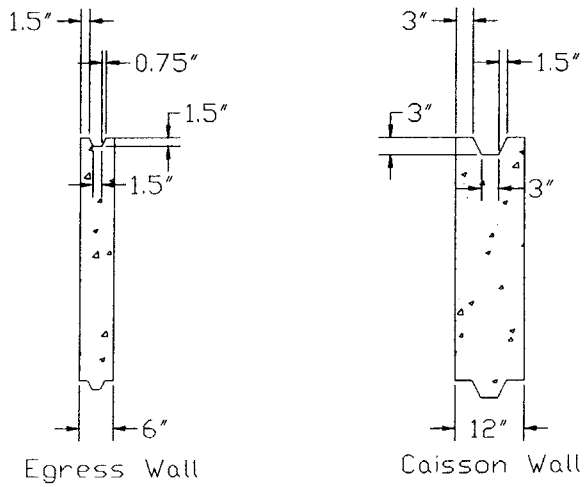

Figure 5-20 Detail of segment joints

The result is a segmental pneumatic caisson that can be precast on or off of the construction site, saving time spent in the construction of permanent or temporary liners on the site.

5.3.6 Air and Muck Locks

The airlocks used to convey workers and materials to and from the excavation face consist of both airlocks for workers and mucklocks for materials. Swatek (1975) states that caissons greater than 150 ft^2 should are commonly equipped with separate muck and man locks, and separate locks are preferable even for caissons of smaller areas. Considering that design excavation chamber pressures reach the maximum federal limit of 50 psi as described by Bickel et al (1996), the decompression time will be significant for crews returning to the surface; 209 minutes after working 2 hours under 50 psi. Therefore, to provide a continuous flow of workers to the excavation face, two worker airlocks are needed; one for entry, and one for exit, allowing the previous crew to decompress during the time the next crew can spend working at the face. An lower limit of just over 2 hours of working time is reached with two airlocks under 50 psi pressures.

The remaining lock is a mucklock. Various types of spoil removal systems have been used in the past that allow the chamber pressure to be maintained. Richardson and Mayo (1941) describe a 3 to 4 inch "blowpipe" which was used to blow sand and mud out of the excavation chamber to the surface using the differential pressure between the chamber and atmosphere to propel it upward, and is shown in Figure 5-21. This system is limited in the grain size it can convey to the surface and is considered a dangerous design because of its propensity to blowouts.

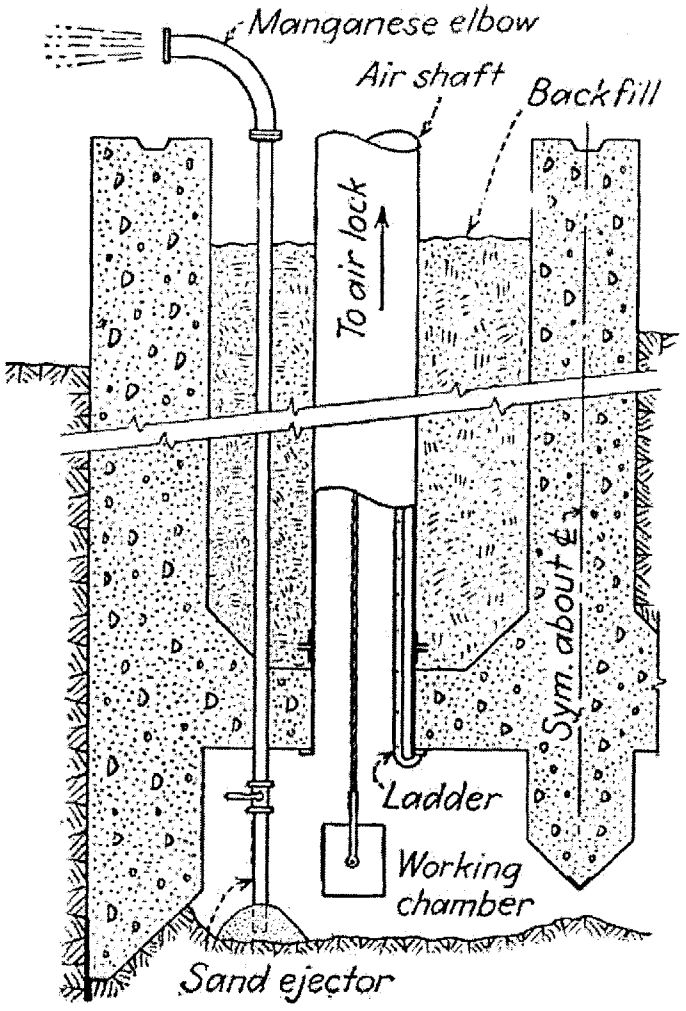

Figure 5-21 "Blowpipe" removal of sand and mud (from Richardson and Mayo, 1941)

Another mucklock system used in the Brooklyn Bridge Caisson involved the equalization of chamber pressure in an open shaft with water. A pipe would rest below water level in a pool at the face. Workers would shovel muck into the pool, which could then be removed by a clamshell from the surface through the water column. This method requires careful control of water levels to work properly. Robinson (1964) discusses the dangerous use of an open water column used to equalize chamber and atmospheric pressure in muck removal shafts, as shown in Figure 5-22.

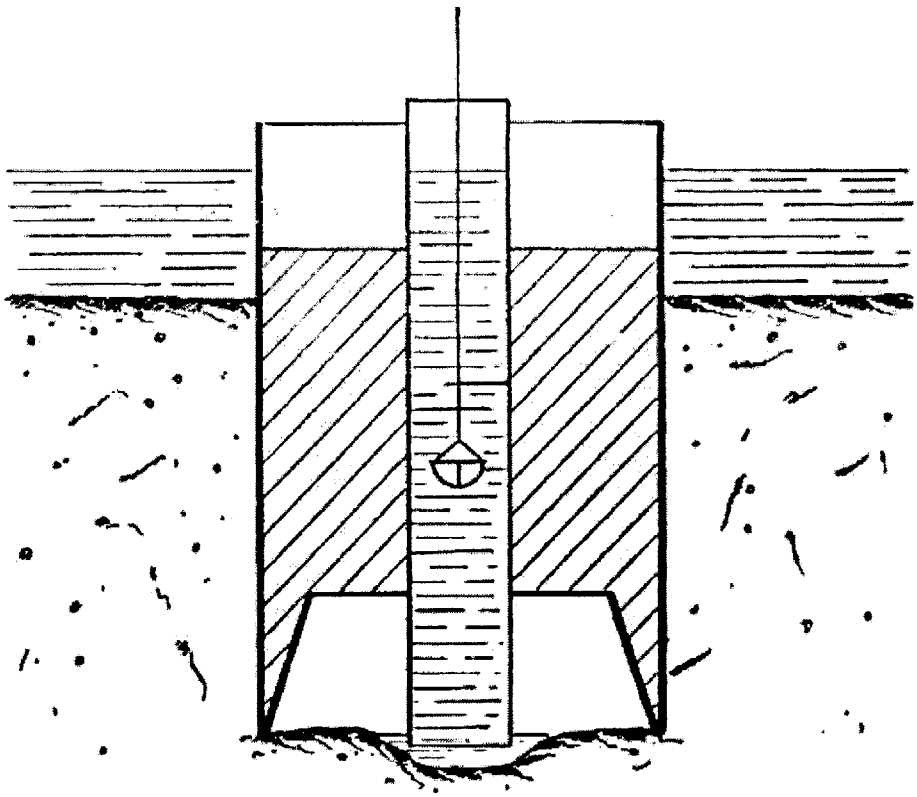

Figure 5-22 Open water column muck shaft in section (from Robinson, 1964)

The use of this type of muck lock system is only really practical and safe when used in large area caissons, where the volume of water will not significantly flood the excavation chamber if the bottom of the pipe was exposed and the water is released. McCullough (1972) describes the flooding caused by the water type muck locks in the Brooklyn Caisson.

> *"It was a neat, efficient system, so long as the water in the shafts stayed at the proper level. But if the volume of water in one shaft became too great-too heavy, that is, for the compressed air below to support it-then the water in the pit would flood out into the work area. Or, if for some reason, the volume of water decreased to the point where its weight was no longer enough to counteract the pressure in the chamber, then there would be a terrific release of air, or blowout, from below."*
>
> *...David McCullough, 1972*

The airlock and mucklock systems designed for the library shaft pneumatic caisson consist of 5.5 foot diameter, 24 foot length, 1 inch thick steel tubes with three inch bolted flanges. These internal and external dimensions were shown in Figure 5-6. The thickness of the steel tube was checked against the maximum lateral load imposed upon it by the steel shot ballast. The steel shot was assumed to possess a friction angle of 30 degrees, giving the material a K_O value of 0.50 as calculated in Equation 2 of Section 3.2. It was assumed that the worst-case condition would be that the steel shot would fill the entire height of the caisson, 130 feet. This imposed a vertical load of 44,850 psf and a resulting horizontal pressure of 22,425 psf. Using Lame's Equation (Equation 4) and half the yield stress used previously, (i.e. half of f_y = 65,000 psi) to provide a conservative buckling estimate, the minimum required thickness of the airlock walls, 0.507 inches, was calculated in Appendix F. The design assumed a steel wall thickness of 1 inch, which yields a factor of safety of 2.00 for the wall.

The tubes are capped with 1-inch thick bulkheads that have airtight doors that swing upward for the mucklock and downward for the airlocks (shown in Section 5.4, Figure 5-26 and Figure 5-29 respectively). The upward swinging doors of the mucklock are used to support an internal pulley system used to convey muck buckets from the chamber into the lock, where they are decompressed rapidly and removed to the surface. Steel pipe segments of identical dimensions in 12-foot lengths are used to extend the top of the locks to the current top elevation of the highest segment of the caisson. Larger design section drawings and details of the library pneumatic caisson shaft can be found included in Appendix H.

5.4 Construction Methodology

The construction and driving of the caisson can be divided into specific aspects. These aspects include the installation of guide piles, the launch of the caisson structure, the start of pressurization, the addition of subsequent segments, ballasting, deep face excavation, and the termination of caisson driving.

5.4.1 Guide Piles

The vertical alignment of the caisson within the ground is a key issue during construction. Swatek (1975) states that the first 20 to 30 feet of caisson sinking is the most important from the standpoint of control. He goes on to further state that caissons started with proper alignment within this depth range are more likely to stay that way over the rest of the drive.

Six guide piles comprised of W12x120 steel sections 20 to 30 feet in length will be driven under close vertical control to guide the caisson at the start of the drive. These six piles will be installed so that their flanges rest at the same radius as the outer edge of the cutting edge on segment 1. They are driven in a pattern 60 degrees apart, as shown in Figure 5-23 surrounding segment 1.

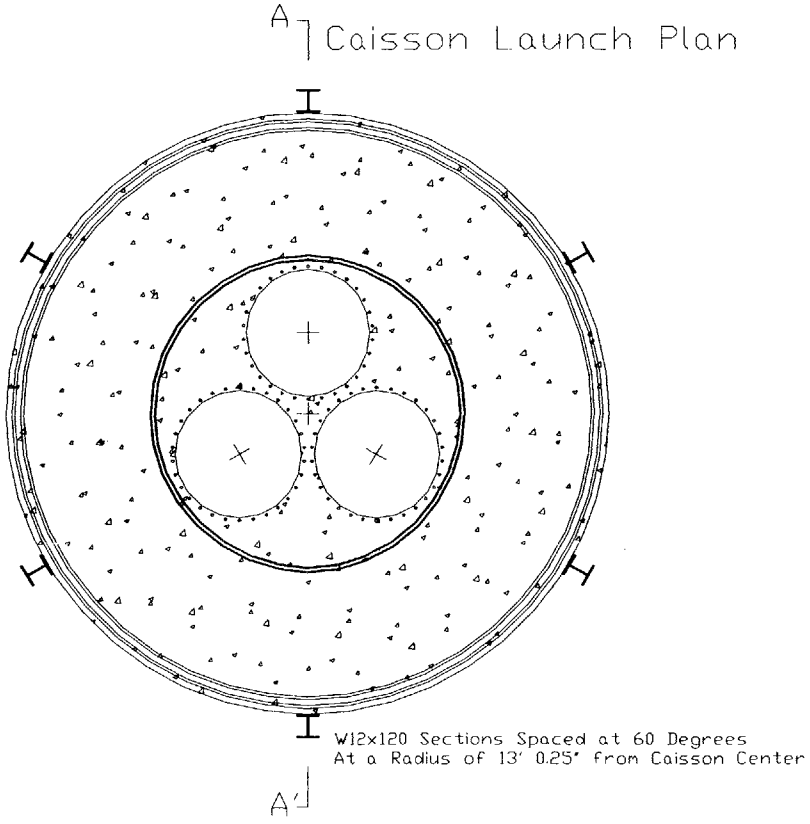

Figure 5-23 Guide pile layout in plan view

5.4.2 Caisson Launch

In order to minimize the friction on the caisson during the drive, the number of delays must be minimized. Therefore, whether the segments are being cast on or off of the construction site, at least four finished segments should be on site before the driving is allowed to begin to prevent stopping the caisson to wait for segments to be delivered or completed. The three locks should also be on site and ready for installation on the caisson once the water table is reached at a depth of 8 feet. Three full segments worth of steel shot ballast should also be available at the site to prevent delays dependent upon delivery. And finally, the guide piles must be installed before driving can begin.

To launch the sinking process of the caisson, segment 1 is place by crane into position within the guide piles. Levels are affixed to the sides and top of the pressure bulkhead to provide a means of vertical control. Excavation then begins in even rounds around the periphery of the opening, and is removed through the open cutouts in the overlying pressure bulkhead. Figure 5-23 depicts the launch and guided downward movement of segment 1 in vertical section.

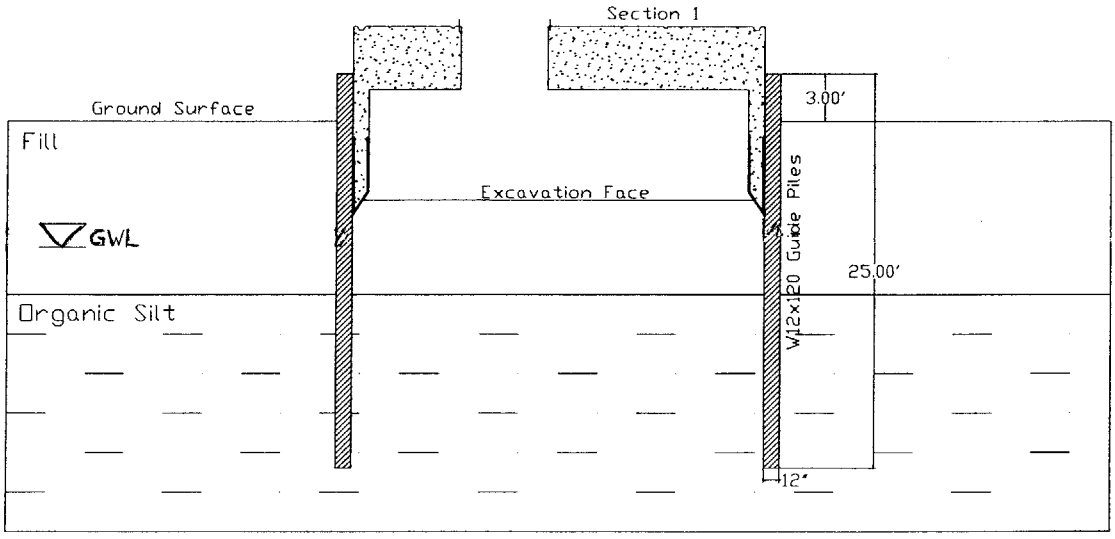

Figure 5-24 Vertical section of segment 1 launch and excavation

Excavation at the face is assisted by mechanization, such as a bobcat or other type of small excavation equipment, controlled by 3 to 4 workers, which is the upper limit due to the confined

area of the chamber. Workers excavate right up to the inside edge of the caisson cutting tip in even rounds to provide better control of vertical alignment. If the caisson needs to be lowered on a particular side to bring it back into verticality, excavation is concentrated under that side until alignment is regained. Obstructions, such as old piles or rubble, are removed using cutting or chiseling equipment. Bentonite slurry is introduced into the annulus behind the cutting edge of the caisson to reduce skin friction. Figure 5-25 from Megaw and Bartlett (1982) illustrates excavation within the caisson pneumatic chamber.

Figure 5-25 Manual excavation of soil within pneumatic chamber (from Megaw and Bartlett, 1982)

5.4.3 Start of Pressurization

When the tip of the segment 1 reaches a depth of 8 feet, segment 2 is placed atop segment 1 and affixed to it. Next, the two airlocks and one mucklock are installed within the egress wall of segment two, connected to the cutouts in the pressure bulkhead. The excavation chamber is then

pressurized to match the increasing pore pressures within the soil. If the face soil requires higher air pressures to achieve stability, then additional pressure over that of hydrostatic is employed. Section 5.2.1 details the design chamber pressures at various depths of the excavation face. The excavation process can be momentarily stopped while these components are installed, but this will be the only time excavation is stopped at the face.

Once pressurized, the times that crews can spend excavating at the face begins to decrease from a value of nearly 8 hours near the surface to shifts only two hours under the full 50 psi pressure near the end of the drive. The workers will not be able to spend their entire shift excavating at the face once the excavation chamber is pressurized. Time will also have to be spent in decompression. The higher the chamber pressure, the longer the decompression time required to prevent nitrogen narcosis. Decompression tables, such as the one shown in Table 5-7 provided in Bickel et al. (1996), are used to ensure that workers significantly reduce their chance of suffering this potentially fatal ailment.

Work Pressue, psig	Hours Under Pressure										
	1/2	1	1-1/2	2	3	4	5	6	7	8	Over 8
0-12	3	3	3	3	3	3	3	3	3	3	3
14	6	5	6	6	5	6	6	6	16	16	32
16	7	7	7	7	11	17	48	63	63	73	87
18	7	7	7	8	11	17	48	63	63	73	87
20	7	7	8	15	15	43	63	73	83	103	113
22	9	9	15	24	38	58	98	108	118	128	133
24	11	12	23	27	52	92	117	122	127	137	151
26	13	14	29	34	69	104	126	141	142	142	163
28	15	23	31	41	98	127	143	153	153	155	183
30	17	28	38	62	105	143	165	168	178	188	204
32	19	35	43	85	126	163	178	193	203	213	226
34	21	39	58	98	151	178	195	218	223	233	248
36	24	44	63	113	170	198	223	233	243	253	273
38	28	49	73	128	178	203	223	238	253	263	278
40	31	49	84	143	183	213	233	248	258	278	288
42	37	56	102	144	189	215	245	260	263	268	293
44	43	64	118	154	199	234	254	264	269	269	293
46	44	74	139	171	214	244	269	274	289	299	318
48	51	89	144	189	229	269	299	309	319	319	—
50	58	94	164	209	249	279	309	329	—	—	—

Notes: Working chamber pressures. Total decompression time, minutes; California Code of Regulations August 1985.

1. 14–22 psi require a two-step decompression;
   24–38 require a three-step decompression; and 40–50 require a four-step decompression.
2. When decompression exceeds 75 minutes, a special decompression chamber must be provided.
3. At least one physician, licensed in the state, must be available at all times to provide medical supervision. The physician must meet all requirements of the compressed air workers and be willing to enter the pressurized environment as needed.
4. See applicable regulations for additional details.

Table 5-7 Decompression tables (Table 6-4 of Bickel et al, 1996)

5.4.4 Additional Segments Added

Once pressurized, the excavation of the face continues downward, as does the caisson, until the top of each subsequent section comes within 4 feet of ground level, at which time a new segment is added and the more lock pipe extensions are installed. Bentonite slurry is being injected into the thin annulus around the caisson to reduce the increasing skin friction. The pneumatic chamber pressure is increased to match the design pressure profile shown in Section 5.2.1. Workers at the face place excavated material into buckets, which are hauled up into the muck lock, where depressurization and haulage to the surface occurs. Figure 5-26 shows a vertical section through the pneumatic caisson, which is comprised of segments 1 through 4 and displays the muck lock.

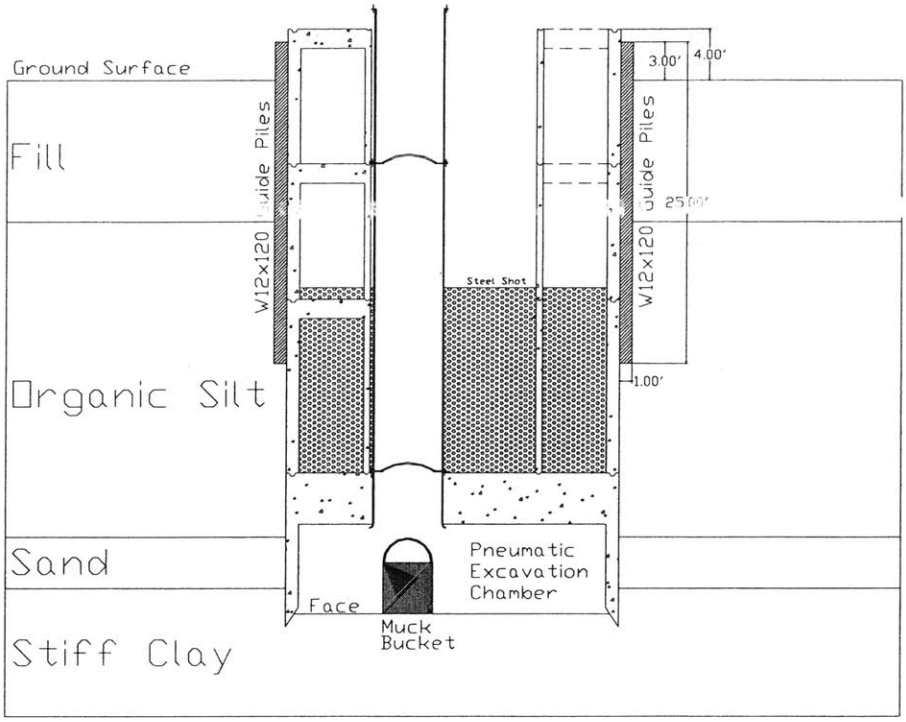

Figure 5-26 Vertical section showing caisson driving and mucklock

5.4.5 Ballasting

Additional weight in the form of steel shot ballast is added once the empty weight of the caisson is insufficient in providing the required thrust to continue sinking the caisson. Steel shot is fed into the annulus between the egress/locks and the stairwell area to meet the required thrust. The nature of the steel shot allows it to be recycled at the end of the construction process. It also eliminates the need for manual digging to remove the ballast, as a crane fitted with an electromagnet can pull large amounts of shot from the stairwell annulus after construction or if over-ballasting occurs. Any spills of ballast on the ground surface can be cleaned up employing the electromagnet.

Calculations to determine the weight of each segment and the cumulative weight of the caisson structure were conducted in spreadsheets contained in Appendix G. The cumulative weight of the caisson was plotted against the best and worst case required driving thrusts (TR), as shown in Figure 5-27, to determine if there was a depth interval that the caisson would not require ballast

in order to sink. The caisson structure, at shallow depths, provides enough weight to begin sinking operations without the addition of ballast.

Between approximately 15 and 20 feet below the ground surface, the weight of the caisson structure is no longer sufficient to provide the required driving thrust of both the best (20 feet) and worst-case (15 feet) scenarios. These points are indicated by the appropriate intersections shown in Figure 5-27. Beyond this depth, the minimum and maximum additional weights of steel shot required to continue sinking the caisson are shown in Figure 5-28 as the difference between the scenario curves and that of the caisson weight.

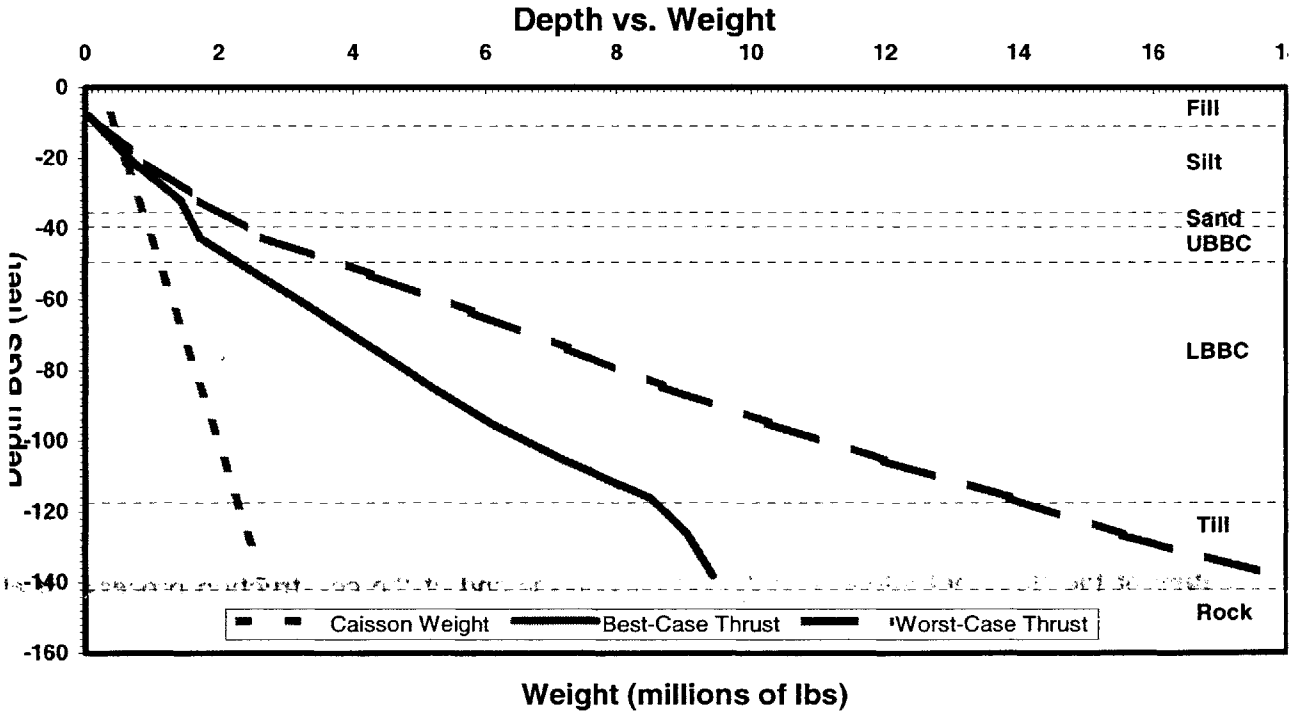

Figure 5-27 Caisson and driving weight as a function of depth

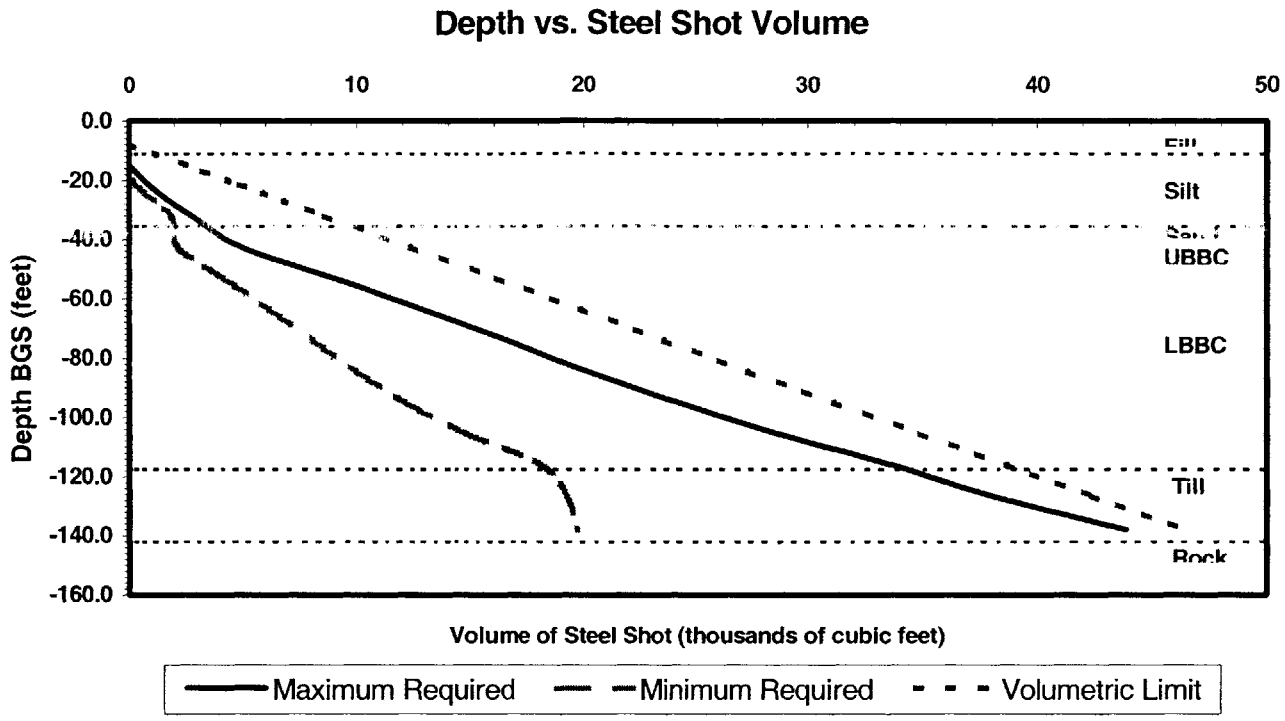

Figure 5-28 Limit, maximum, and minimum amounts of steel shot ballast

The available volume of each segment of the caisson into which the ballast could be placed was also calculated. From these calculations, the approximate heights of steel shot within the egress/locks annulus and the stairwell section at different depths were computed, and are shown in Appendix G for both best and worst-case scenarios (see also Fig 5-28). Figure 5-29 shows a vertical section of the caisson, segments 1 through four and also shows the steel shot ballast and worker airlock.

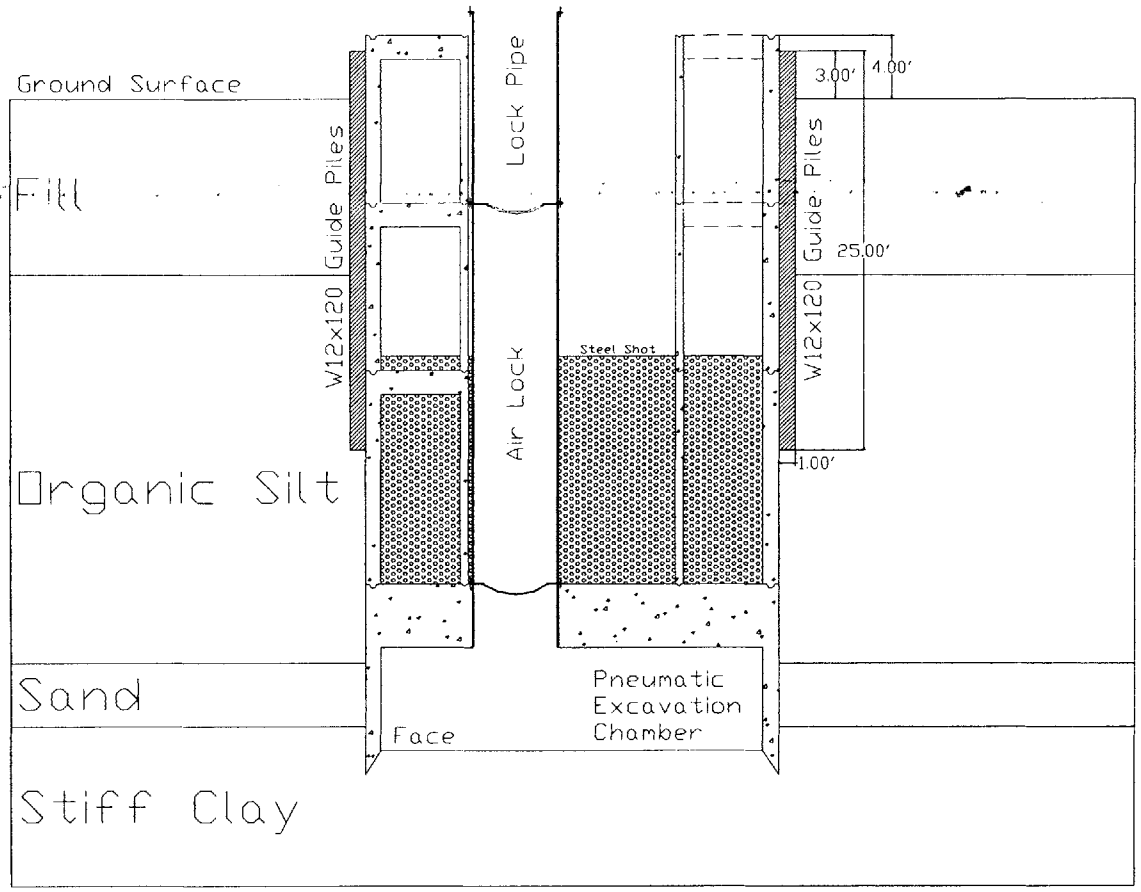

Figure 5-29 Vertical section of sinking caisson showing ballast and worker airlock

5.4.6 Deep Face Excavation

Excavation of the Boston Blue Clay has been shown to be possible using chamber pressures that match hydrostatic conditions at that elevation. If lateral movements or heaving of the face become noticeable, the weight of the caisson can be increased by adding additional ballast, causing the cutting edge to sink further beyond the excavation face, effectively deepening the depth of embedment of the sidewalls and increasing the length of future soil shear failures into the opening.

Excavation within the glacial till is creates the possibility of encountering particles of cobbles or larger size, which require chiseling or splitting equipment to remove. These fragments pose an obstruction to caisson sinking. Additional weight is not advised during face excavation through this material as the cutting edge may be damaged if hung up on an obstruction. Particles too

large to be conveyed through the muck lock must be split into pieces small enough to facilitate its removal from the pneumatic chamber. As chamber pressures increase, crew times at the face will be significantly reduced down to a maximum of approximately 2 hours, decreasing worker productivity and increasing costs at the same time. At a depth of approximately 123 feet below ground surface, 115 feet below the groundwater surface, the maximum allowed chamber pressure of 50 psi, the federally imposed limit, will be reached. Beyond this depth, the chamber pressure is held constant at 50 psi. The construction process has two options. The first is that if the glacial till has a low enough permeability, the excavation can continue and water seeping into the excavation chamber can be pumped to the surface. If, however, the till has a moderate to high hydraulic conductivity, the aquifer around the base of the excavation must be temporarily depressurized by wellpoints to reduce the pore pressures to those which can be matched by the chamber pressure limits. It should be noted that if exploratory borings indicate that the Cambridge Argillite contains numerous open fractures and is not more than approximately 150 feet from the surface then depressurization should be employed to prevent a blowout at the excavation face and possible significant water inflow.

5.4.7 Termination of Drive

When the final design depth of the caisson is reached at 142 feet below ground surface, the excavation operations stop. The pneumatic chamber remains at full operating pressure of 50 psi. The removal of ballast material begins immediately to take any weight away from the bottom edge of the caisson. The ballast material is removed by a craned fitted with an electromagnet and loaded onto trucks that return it for recycling. Meanwhile, the excavation face is covered with reinforcement steel brought down through the mucklock. Next, concrete is brought down through the mucklock and poured to form a 3-foot thick base slab at the chamber floor between the tapered portions of the cutting edge. This slab effectively forms a foundation on which the caisson will rest, shown in Figure 5-29, as well as sealing off the soil from the shaft itself.

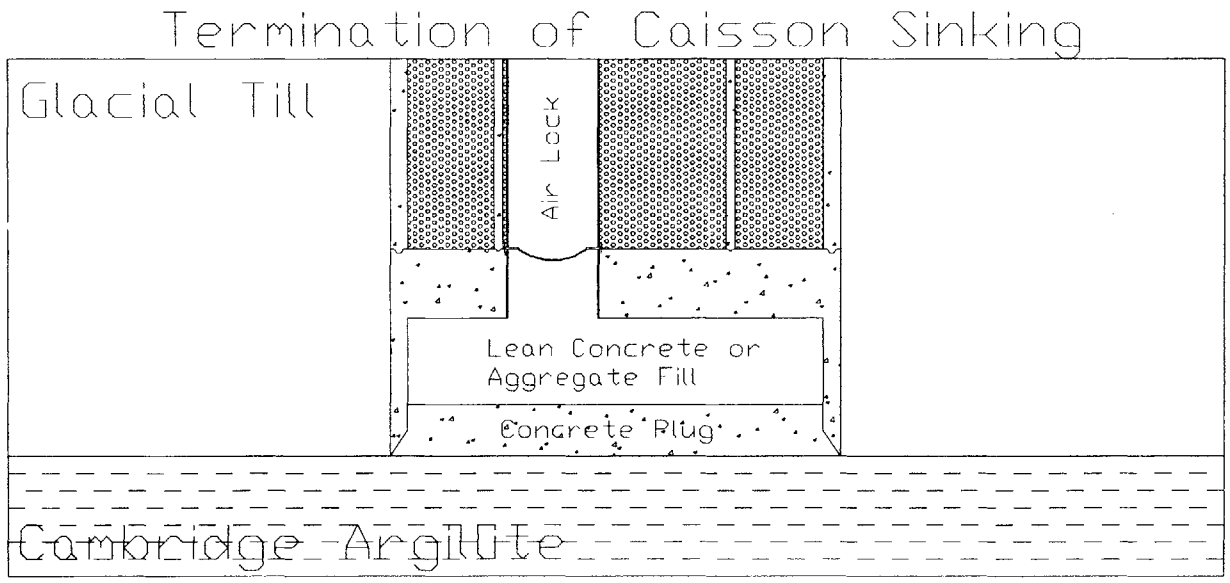

Figure 5-30 Shaft concrete plug at termination of sinking

Once the concrete slab has reached sufficient strength, the chamber pressure is vented back to atmospheric levels and the locks within the egress wall are removed. The remainder of the excavation chamber is filled with lean concrete to fill the void and cutouts to the top elevation of the bulkhead. The remainder of the steel shot ballast is removed, and the caisson installation is completed.

Installation of the connector tunnel will require partial demolition of the egress wall in order to gain access to the outer wall of the caisson, which will also have to be selectively demolished.

6 Evaluation of Methods

The secant pile shaft design proposed by Rehkopf et al (2001) is considered an in-situ construction method. Other in-situ construction methods, such as slurry panel or pile and lagging supported excavations, rely upon elements installed before the excavation begins. The disadvantages of installing elements prior to excavation can be avoided by the use of a pneumatic caisson alternative, proposed here, that can be considered to be a prefabricated structure. The secant pile and pneumatic caisson methods were evaluated regarding environmental impacts, stability, time of installation, and feasibility.

6.1 Environmental Impacts

The environmental impacts of each method were compared regarding both surface settlements and affects on local groundwater levels.

6.1.1 Settlement

The installation of a secant pile liner allows small borings to be made to construct the shaft wall. The use of casing to temporarily line the boring before concrete is tremied into the excavation will minimize any lateral soil movements into the excavation. However, if vibratory methods are used to remove the casing during the concrete pour, significant lateral movements of soil may occur. Due to the length of and time required to install a secant pile, it is likely that ground stresses will require the use of vibratory removal techniques, introducing the possibility of lateral movements into the boring, and subsequent significant surface settlements near the shaft.

The pneumatic caisson installation method provides face support to prevent the heave of the excavation face, and has stiff vertical walls to resist lateral soil movement. However, the over-cutting at the face and subsequent annulus that is formed around the exterior of the caisson wall does also introduce the possibility of lateral soil movement and surface settlement. Bentonite slurry within this annulus reduces the likelihood of this from occurring, and the annulus is grouted at the end of the drive to permanently fill this void space. Also, if skin friction is not significantly reduced, the positive skin friction could produce downdrag in soft cohesive soil layers, also causing surface settlement.

It is believed that with the use of bentonite slurry within the annulus, followed by grouting, skin friction will be reduced and ground movements will be notably less than those produced using the secant pile method.

6.1.2 Groundwater

The in-situ nature of the installation of the secant pile shaft is not likely to produce any notable change in groundwater levels adjacent to the opening. However, during excavation of the interior of the secant pile shaft, the excavation face provides a high head outlet for groundwater flow. If the secant piles do not overlap in a specific part of the shaft, then significant water inflows could occur at this point before the problem could be solved. This can affect the upper aquifer consisting of the organic silt and sands under the site. Near the base of the excavation, the length of groundwater flow paths are reduced while head energy is increasing. The result will be groundwater flow into the excavation base. If the glacial till is pervious, or the underlying Cambridge Argillite has a number of open fractures, significant groundwater pumping will be required to facilitate forming and construction of the floor of the shaft.

The pneumatic caisson counters groundwater inflow into the excavation by providing a pressure equal to or above the level of hydrostatic pressure at the excavation face. This means that inward head pressure is equal to or less than zero, at which point air drying of the soil near the face would occur as air escaped from the pneumatic chamber. If the glacial till possesses a low hydraulic conductivity, then the limited air pressure to counter hydrostatic levels at those depths will not cause any significant groundwater drawdown. If, however, the till has a moderate to high hydraulic conductivity, drawdown will occur either by flow into the excavation chamber or depressurization by pumping from surface groundwater wellpoints.

In either case, the drawdown of groundwater levels is limited to the lower aquifer comprised of the glacial till and Cambridge Argillite. Depressurization and dewatering of this interval of the geology has the potential for the most widespread impact, as drawdowns in this aquifer can have a large radius of influence. Therefore, both methods have the same potential for groundwater drawdown in the lower aquifer. The secant pile method does have a significantly higher chance

of lowering groundwater levels in the upper aquifer if overlaps are not continuous between all secant piles, particularly at shallow depths. Therefore, the pneumatic caisson is the preferred of the two methods regarding groundwater drawdown.

6.2 Stability

The secant pile method of shaft construction provides less structural control compared to the alternative proposed. The piles may not meet the required overlap of design, and could possibly leave a gap in the wall of the shaft, which will not be seen until the interior is excavated. Also, the sloughing and mixing of material from the wall of the pile into the concrete when the liner is withdrawn can significantly reduce the strength of the shaft liner, and may not be seen even after the interior is excavated. This can lead to an unstable opening. Essentially the installation of the temporary liner is done in the blind, and its condition or continuity cannot be guaranteed even after the center is excavated.

In contrast, the caisson segments are precast and installed in the ground by excavation. This means that the structural design and construction of the shaft liner can be closely controlled, ensuring high quality. This significantly increases the stability of the shaft structure itself. The soil is excavated by workers who can adapt and mitigate problems as they arise at the excavation face. Therefore the sinking operation and placement of the shaft structure in the ground also has a higher degree of control than the secant pile method. The result is a greater confidence in the stability of the shaft structure.

Soil stability issues are also better addressed with the pneumatic caisson, as face pressure can be adjusted to provide more support for the excavation, and workers can identify possible adversities before they become a problem.

Therefore, the pneumatic caisson provides a greater assurance of opening and structural stability when constructing the shaft.

6.3 Construction Time

The installation time of the secant pile shaft takes two to three months from start of drilling to the end of shaft excavation and permanent liner placement. This is due to the fact that essentially only one boring machine can be used due to the size of the shaft being constructed.

The installation of guide piles and preparation of the site for a pneumatic caisson would take one to two weeks. Assuming that a crew of 3 to 4 at the working face can excavate 32 cubic yards every eight hours using light excavation machinery (RS Means, 2000) in the pneumatic caisson, the structure would advance at a rate of 5 feet per day if excavation occurred around the clock. Excavation at depths where pneumatic pressures above 50 psi are required to counter hydrostatic pressure may be able to utilize remotely operated excavation equipment, eliminating the need for workers to be within the chamber itself. Utilizing either of these methods, the excavation and sinking operation could be completed within 1 to 1.5 months. The nature of the precast segments does not require site work to construct the liner within the excavation, but also comes at an additional cost.

Both methods have a similar construction duration, but construction quality is better controlled and assured for the pneumatic caisson method. The added quality will most likely also mean a higher cost for the shaft if the pneumatic caisson method is used.

6.4 Feasibility

The secant pile shaft construction method has the benefit of significantly reduced labor costs when compared to the pneumatic caisson method. Decompression times come at the expense of the time that workers can spend at excavating at the face in the pneumatic caisson method, causing a loss of productivity per unit dollar. However, the material costs would tend to slightly favor the precast segments of the caisson method, which requires little additional material to provide the specified shaft in the library design.

Construction of the connector tunnel would have to employ a method other than horizontal secant piles proposed by Rehkopf et al. (2001) due to the preexistence of the egress wall within the driven caisson. Use of this method to construct the connector tunnel from a pneumatic

caisson shaft is not feasible because the reduced clearances at the base of the shaft will not permit a boring machine enough room to drill secant piles at the radius required.

Furthermore, the low usage of the pneumatic caisson method in since World War II will limit the consideration of this option due to high labor costs and federal restrictions.

7 Conclusions and Recommendations

The pneumatic caisson method provides better quality control, lower chances of settlement, reduced likelihood of affecting upper aquifer groundwater levels, better excavation face stability, and similar construction times when compared to the secant pile method proposed by Rehkopf et al (2001). Constructing the shaft with the pneumatic caisson will be more expensive than the secant pile method, and poses complications for the construction of the connector tunnel if it is to be constructed using horizontal secant piles.

The analysis and design of the pneumatic caisson shaft has shown that it is possible to the depth required for the library deep egress shaft. The small diameter of the caisson meant that driving weight would be a critical issue due to the high surface area to volume ratio. Since this method is feasible in the geology present beneath McDermott Court, it is suggested and possible that the entire library structure proposed by Rehkopf et al (2001), essentially a circular caisson 140 feet tall and 200 feet wide, could be constructed using this method, allowing each floor of the library to be constructed at the surface and sunk to its design elevation. Basal stability issues would remain the same as the shaft caisson. Driving weight would not be a problem due to an increased volume to surface area ratio, and the face could be excavated with machinery. The design of a pressure bulkhead for such a structure seems to be the most identifiable obstacle to using this method for library construction. It is recommended that this alternative be examined for construction of the library structure due to its increased basal stability and the history of deep excavation failures/movements on MIT Campus.

Appendix A: Geotechnical Parameters

Site Geologic Conditions

Geologic column taken from Boring 1 and 1A of MIT Facilities Record # MG 14 S 01 00 Boring Logs
This boring is located proximal to the northern external stairs of Building 14
Ground water is assumed to exist at 8 feet BGS and aquitard reductions between aquifers are neglected
Ko estimated by 1-sinϕ for NC Soils (Jaky, 1944)
Ko values for OC Clay via communication with Professor CC Ladd of MIT
Su from Shansep and Recompression Triaxial Test Results via communication with Prof CC Ladd of MIT

$$u = \gamma_{WATER} D$$

$$\sigma_{VO} = \sum \gamma_{SOIL_i} H_i$$

$$\sigma_{VO}' = \sigma_{VO} - u$$

$$K_O = 1 - \sin\phi$$

$$\sigma_{HO}' = K_O \sigma_{VO}'$$

$$c_{HO} = \sigma_{HO}' + u$$

$$K_A = \frac{(1-\sin\phi)}{(1+\sin\phi)}$$

Rankine Active Coefficient

in feet			pcf		ft	psf	psf	psf	est.		psf	psf	psf Shansep	psf Recomp	psf Rankine
Depth BGS	**Soil**	**Geology**	γ_{SOIL}	ϕ	**Depth**	**u**	σ_{VO}	σ'_{VO}	**OCR**	Ko	σ'_{HO}	σ_{HO}	**Su**	**Su**	**Active**
0		Cinders, Sand, etc. (FILL)	110	32	0	0	0	0	1	0.470	0	0			0.307
5			110	32	-5	0	550	550	1	0.470	259	259			0.307
8		Top of ground water	110	32	-8	0	880	880	1	0.470	414	414			0.307
10			120	32	-10	125	1,100	975	1	0.470	458	583			0.307
11		Silt to Silt with some Sand (SILT)	100	30	-11	187	1,220	1,033	1	0.500	516	704	250	250	0.333
15			100	30	-15	437	1,620	1,183	1	0.500	592	1,028	250	250	0.333
17			100	30	-17	562	1,820	1,258	1	0.500	629	1,191	250	250	0.333
20			100	30	-20	749	2,120	1,371	1	0.500	686	1,434	250	250	0.333
21.5			100	30	-21.5	842	2,270	1,428	1	0.500	714	1,556	250	250	0.333
25			100	30	-25	1,061	2,620	1,559	1	0.500	780	1,840	250	250	0.333
30			100	30	-30	1,373	3,120	1,747	1	0.500	874	2,246	250	250	0.333
32			100	30	-32	1,498	3,320	1,822	1	0.500	911	2,409	250	250	0.333
35			100	30	-35	1,685	3,620	1,935	1	0.500	968	2,652	250	250	0.333
35.5		Hard coarse blue sand and gravel (SAND)	130	37	-35.5	1,716	3,670	1,954	1	0.398	778	2,494			0.249
39.5		Medium Clay (UBBC)	117	28	-39.5	1,966	4,190	2,224	4	1.040	2,313	4,279	1,630	1,500	0.361
40		Assumed OCR<=4, decr. Down	117	27	-40	1,997	4,249	2,252	3	0.839	1,889	3,886	1,630	1,500	0.376
42.5		Boston Blue Clay	117	27	-42.5	2,153	4,541	2,388	1	0.773	1,846	3,999	1,600	1,465	0.383
45			117	26	-45	2,309	4,834	2,525	2	0.707	1,785	4,094	1,570	1,425	0.390
49.5		Soft Blue Clay, OCR=1 (LBBC)	117	25	-49.5	2,590	5,360	2,770	1	0.577	1,600	4,189	1,516	1,350	0.406
50		Boston Blue Clay	117	24	-50	2,621	5,419	2,798	1	0.593	1,660	4,281	1,510	1,350	0.422
53			117	24	-53	2,808	5,770	2,962	1	0.593	1,757	4,565	1,490	1,350	0.422
55			117	24	-55	2,933	6,004	3,071	1	0.593	1,822	4,755	1,475	1,350	0.422
60			117	24	-60	3,245	6,589	3,344	1	0.593	1,984	5,228	1,440	1,350	0.422
63.5			117	24	-63.5	3,463	6,998	3,535	1	0.593	2,097	5,560	1,415	1,350	0.422
65			117	24	-65	3,557	7,174	3,617	1	0.593	2,146	5,702	1,405	1,350	0.422
70			117	24	-70	3,869	7,759	3,890	1	0.593	2,308	6,176	1,370	1,350	0.422
74			117	24	-74	4,118	8,227	4,108	1	0.593	2,437	6,556	1,342	1,350	0.422
75			117	24	-75	4,181	8,344	4,163	1	0.593	2,470	6,650	1,335	1,350	0.422

Continued on page 93

Continued from page 92

in feet			pcf		ft	psf	psf	psf	est.		psf	psf	psf Shansep	psf Recomp	psf Rankine
Depth BGS	**Soil**	**Geology**	γ_{SOIL}	ϕ	**Depth**	**u**	σ_{VO}	σ'_{VO}	**OCR**	K_O	σ'_{HO}	σ_{HO}	**Su**	**Su**	**Active**
80		Soft Blue Clay, OCR=1 (LBBC)	123	24	-80	4,493	8,929	4,436	1	0.593	2,632	7,124	1,300	1,350	0.422
84.5		Boston Blue Clay	123	24	-84.5	4,774	9,482	4,708	1	0.593	2,793	7,567	1,350	1,350	0.422
85			123	24	-85	4,805	9,544	4,739	1	0.593	2,811	7,616	1,370	1,350	0.422
90			123	24	-90	5,117	10,159	5,042	1	0.593	2,991	8,108	1,450	1,410	0.422
95			123	24	-95	5,429	10,774	5,345	1	0.593	3,171	8,600	1,530	1,470	0.422
100			123	24	-100	5,741	11,389	5,648	1	0.593	3,351	9,091	1,610	1,530	0.422
104.5		Soft Blue Clay	123	25	-104.5	6,022	11,942	5,920	1	0.577	3,418	9,440	1,682	1,584	0.406
105		with sand lenses	123	25	-105	6,053	12,004	5,951	1	0.577	3,436	9,489	1,690	1,590	0.406
105.5		Boston Blue Clay	123	25	-105.5	6,084	12,065	5,981	1	0.577	3,453	9,537	1,698	1,596	0.406
110			123	25	-110	6,365	12,619	6,254	1	0.577	3,611	9,976	1,770	1,650	0.406
115			123	25	-115	6,677	13,234	6,557	1	0.577	3,786	10,463	1,850	1,710	0.406
116			123	25	-116	6,739	13,357	6,617	1	0.577	3,821	10,560	1,862	1,734	0.406
117.5		Hard to medium blue sand, (TILL)	135	45	-117.5	6,833	13,541	6,708	2	0.586	3,930	10,762			0.172
120		gravel, and clay	135	45	-120	6,989	13,879	6,890	2	0.586	4,036	11,025			0.172
125		some boulders	135	45	-125	7,301	14,554	7,253	2	0.586	4,249	11,549			0.172
126.5			135	45	-126.5	7,394	14,756	7,362	1	0.586	4,314	11,708			0.172
130			135	45	-130	7,613	15,229	7,616	2	0.586	4,461	12,074			0.172
135			135	45	-135	7,925	15,904	7,979	2	0.586	4,674	12,599			0.172
140			135	45	-140	8,237	16,579	8,342	2	0.586	4,886	13,123			0.172
142		Cambridge Argillite (ROCK)	155	45	-142	8,362	16,849	8,487	2	0.586	4,972	13,333			0.172
145			155		-145	8,549	17,314	8,765							
150			155		-150	8,861	18,089	9,228			MAX	13,333	psf		
155			155		-155	9,173	18,864	9,691			MEDIAN	5,631	psf		
160			155		-160	9,485	19,639	10,154			AVG	6,093	psf		

Depth versus Undrained Strength of Boston Blue Clay

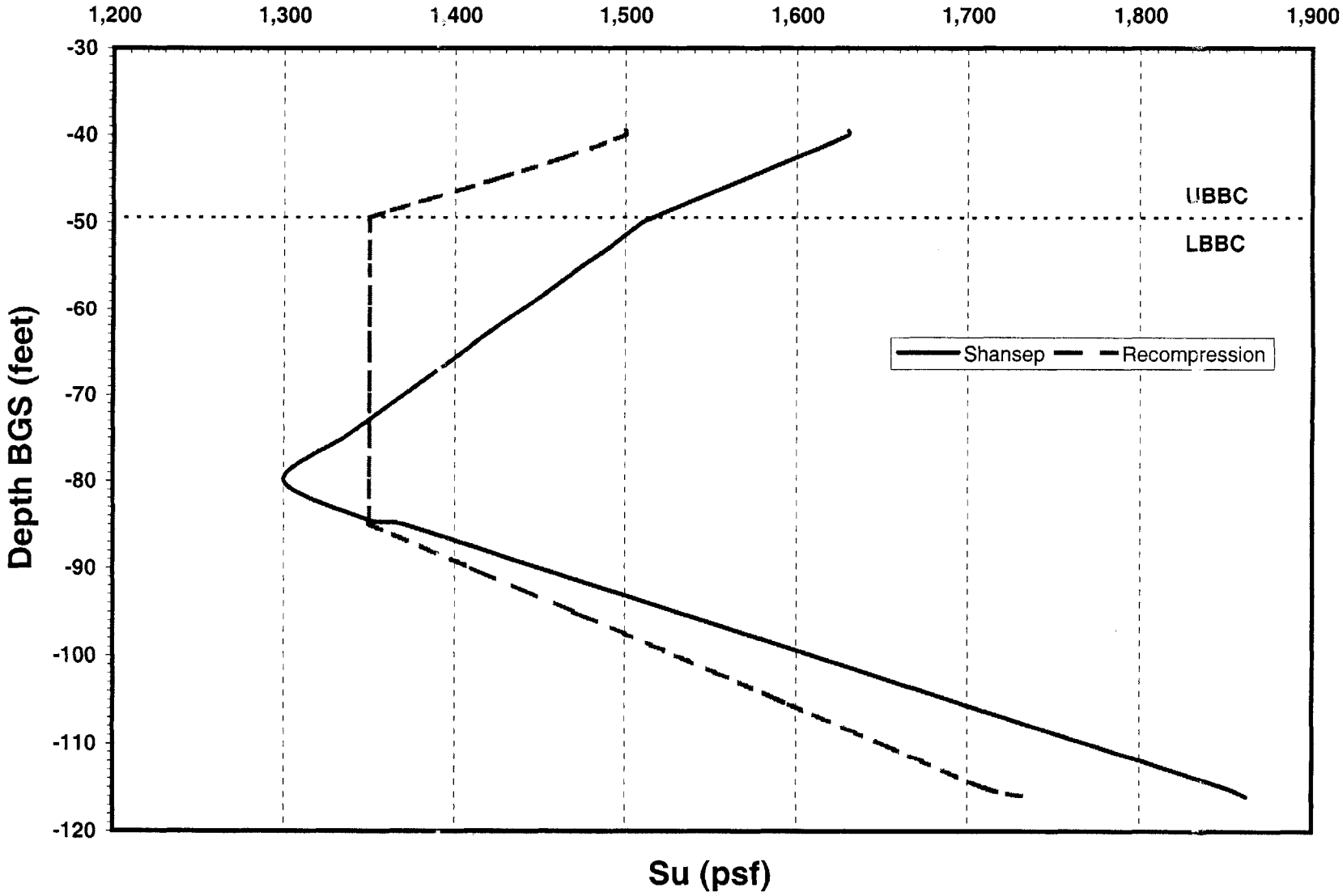

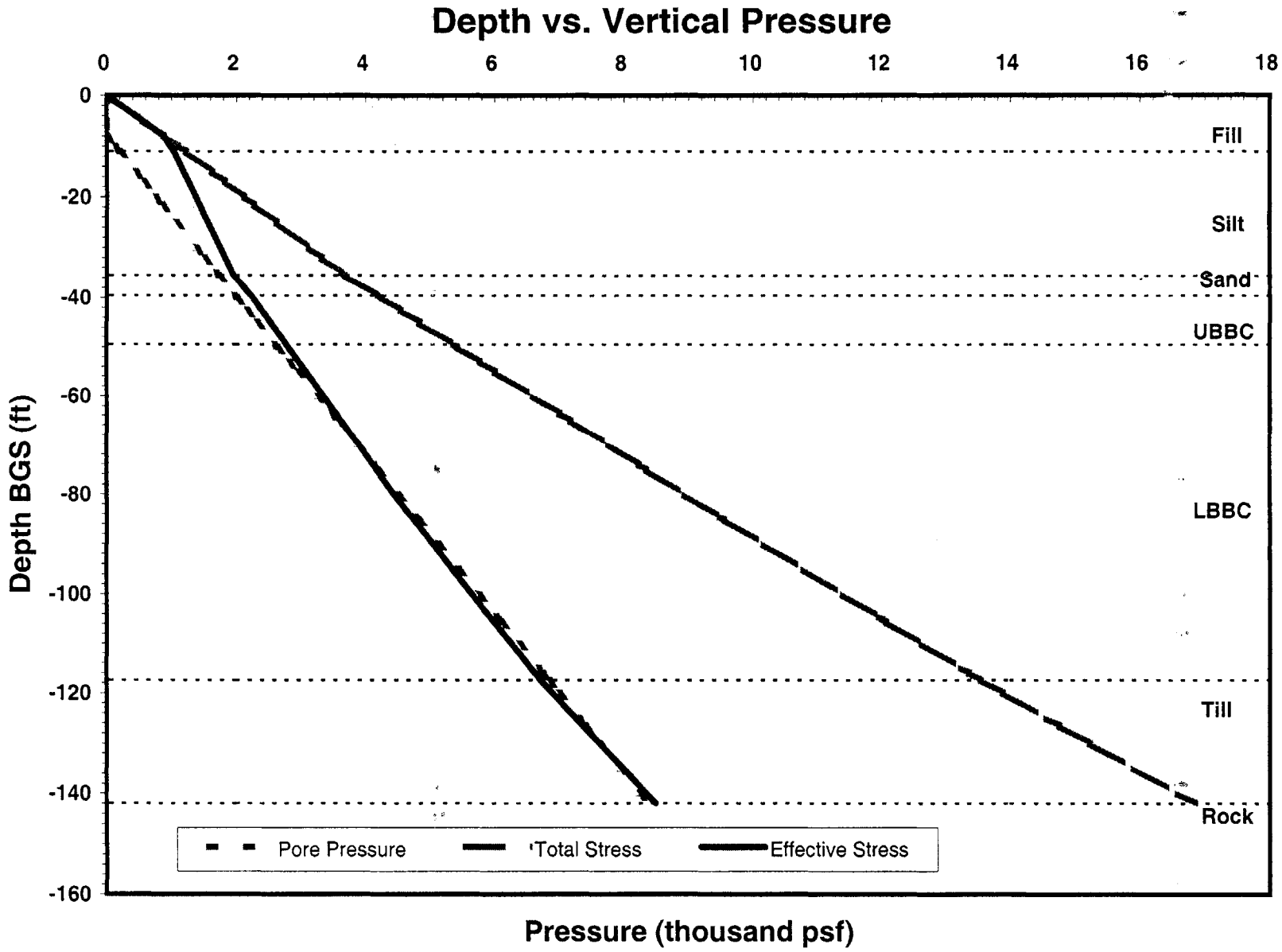
Depth vs. Vertical Pressure
0
2
4
6
8
10
12
14
16
18
0
-20
-40
-60
-80
-100
-120
-140
-160
Depth BGS (ft)
Fill
Silt
Sand
UBBC
LBBC
Till
Rock
Pore Pressure
Total Stress
Effective Stress
Pressure (thousand psf)

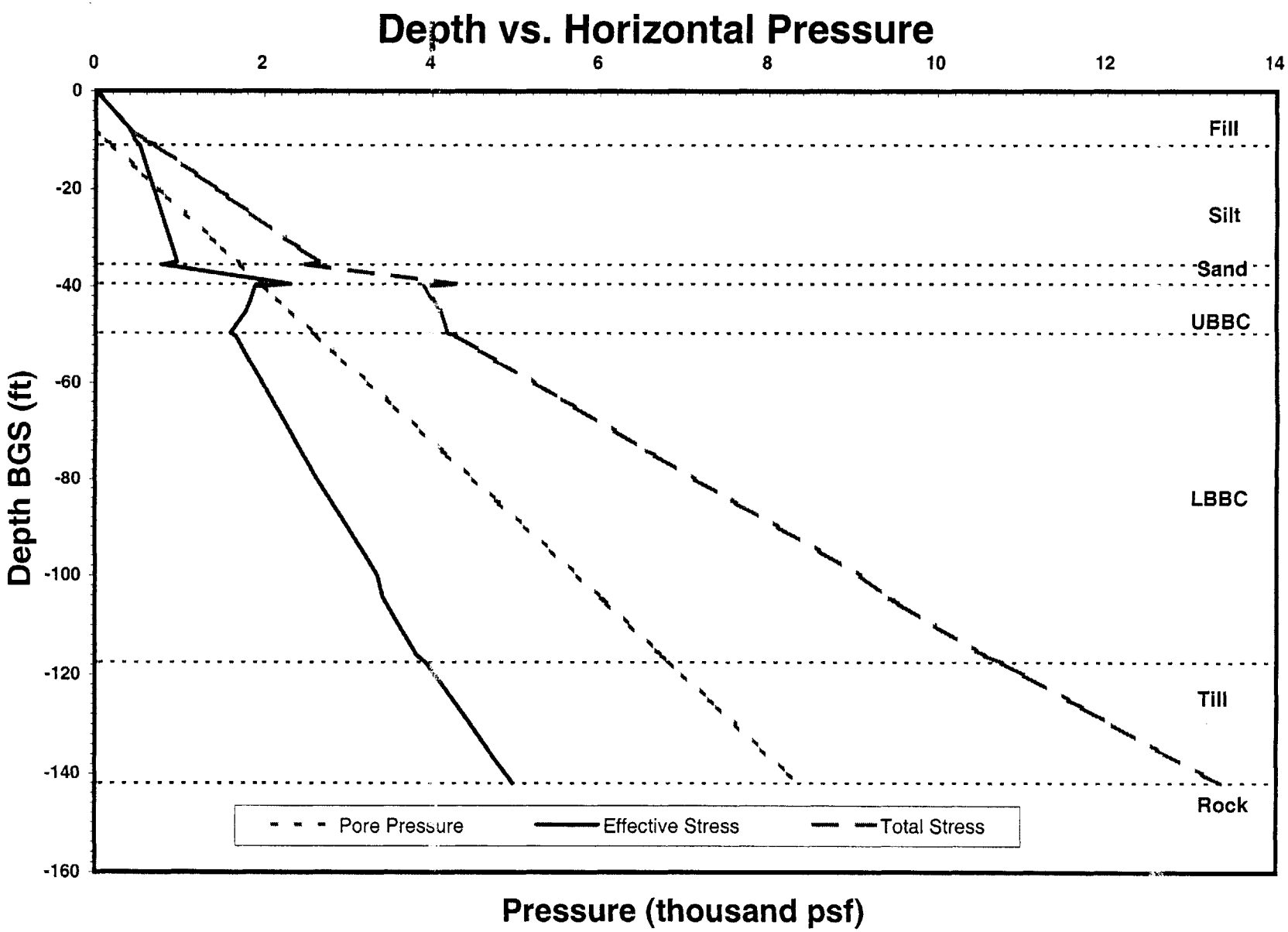
Depth vs. Horizontal Pressure
0
2
4
6
8
10
12
14
0
-20
-40
-60
-80
-100
-120
-140
-160
Depth BGS (ft)
Fill
Silt
Sand
UBBC
LBBC
Till
Rock
Pore Pressure
Effective Stress
Total Stress
Pressure (thousand psf)

Appendix B: Proposed Secant Pile Shaft Design

Vertical Secant Pile Shaft Design

Length of Shaft Centerline, **D**	140 ft	Secant pile factor of safety, **F**	2.00
Interior radius of secant piles, r_n	12.77 ft	Maximum vertical earth pressure, σ_{hmax}=**P**	21,000 psf
Thickness of perm liner, t_p	0.768 ft	Concrete strength, σ_t	5,000 psi
Interior radius of perm liner, r_f	12 ft	Concrete strength, σ_t	720,000 psf
Expected borehole deviation, $\%_{deviation}$	0.50%		
Deviation Distance, **d**	0.7 ft		

$r_n = r_f + t_p$ $\quad d = \%_{deviation} D_{borehole}$ $\quad r_i = r_f + t_p + \frac{1}{2} r_s$ $\quad n = \frac{2\pi r_i}{S}$

ft Pile Dia.	r_s (ft) Pile Rad.	r_i (ft) Installation Radius	t_{liner} (ft) Required Overlap	S (ft) Pile Spacing	l_{min} (ft) Min. Overlap	l_{avg} (ft) True Overlap	l_{max} (ft) Max. Overlap	n Number of Piles	$/LF	LF	Total Cost
2	1	13.768	0.881	0.395	0.881	1.961	1.729	218.8	$56	30626.4	$1,715,077
2.5	1.25	14.018	0.897	0.934	0.897	2.319	2.456	94.4	$71	13210.7	$937,960
3	1.5	14.268	0.913	1.458	0.913	2.622	2.999	61.5	$83	8611.2	**$714,732**
3.5	1.75	14.518	0.929	1.974	0.929	2.890	3.453	46.2	$141	6468.8	$912,107
4	2	14.768	0.945	2.487	0.945	3.133	3.850	37.3	$195	5224.6	$1,018,796
4.5	2.25	15.018	0.961	2.996	0.961	3.358	4.207	31.5	$252	4409.7	$1,111,242
5	2.5	15.268	0.977	3.504	0.977	3.567	4.536	27.4	$306	3833.8	$1,173,144
5.5	2.75	15.518	0.993	4.010	0.993	3.765	4.841	24.3	$344	3404.8	$1,171,264
6	3	15.768	1.009	4.515	1.009	3.952	5.128	21.9	$381	3072.7	$1,170,710
6.5	3.25	16.018	1.025	5.019	1.025	4.131	5.400	20.1	$425	2807.9	$1,193,356
7	3.5	16.268	1.041	5.522	1.041	4.302	5.658	18.5	$469	2591.7	$1,215,510

$l_{min} = 2\sqrt{r_s^2 - \left(\frac{S}{2} + d\right)^2}$ $\quad l_{avg} = 2\sqrt{r_s^2 - \left(\frac{S}{2}\right)^2}$ $\quad l_{max} = 2\sqrt{r_s^2 - \left(\frac{S}{2} - d\right)^2}$ $\quad S = 2\sqrt{r_S^2 - \left(\frac{t_f}{2}\right)^2} - d$ $\quad t_{liner} = r_n\left(\sqrt{\frac{\sigma_t}{\sigma_t - 2PF}} - 1\right)$

$714,732 Temp Liner

Temporary secant pile liner designed with 5000psi concrete
Permanent steel reinforced liner designed with FoS of 2.00 at a thickness of 0.768 feet of 5000 psi concrete

Means CM Tunnel Liner including reinforcement for 20 foot diameter, Earth 023000510 — $550 per linear foot

$74,250 Perm. Liner cost — **$74,250 Permanent Liner**

Shaft Excavation (avg) — $60 per cu yd — **$159,385** — **$159,385 Shaft Excavation**
Volume of Excavation — 2656.4 cu yd

Cost of Shaft per LF of depth
$6,774.05

Minimum Secant Pile Shaft Structural Cost (minus floorslab, stairwell, and topside)
$948,367

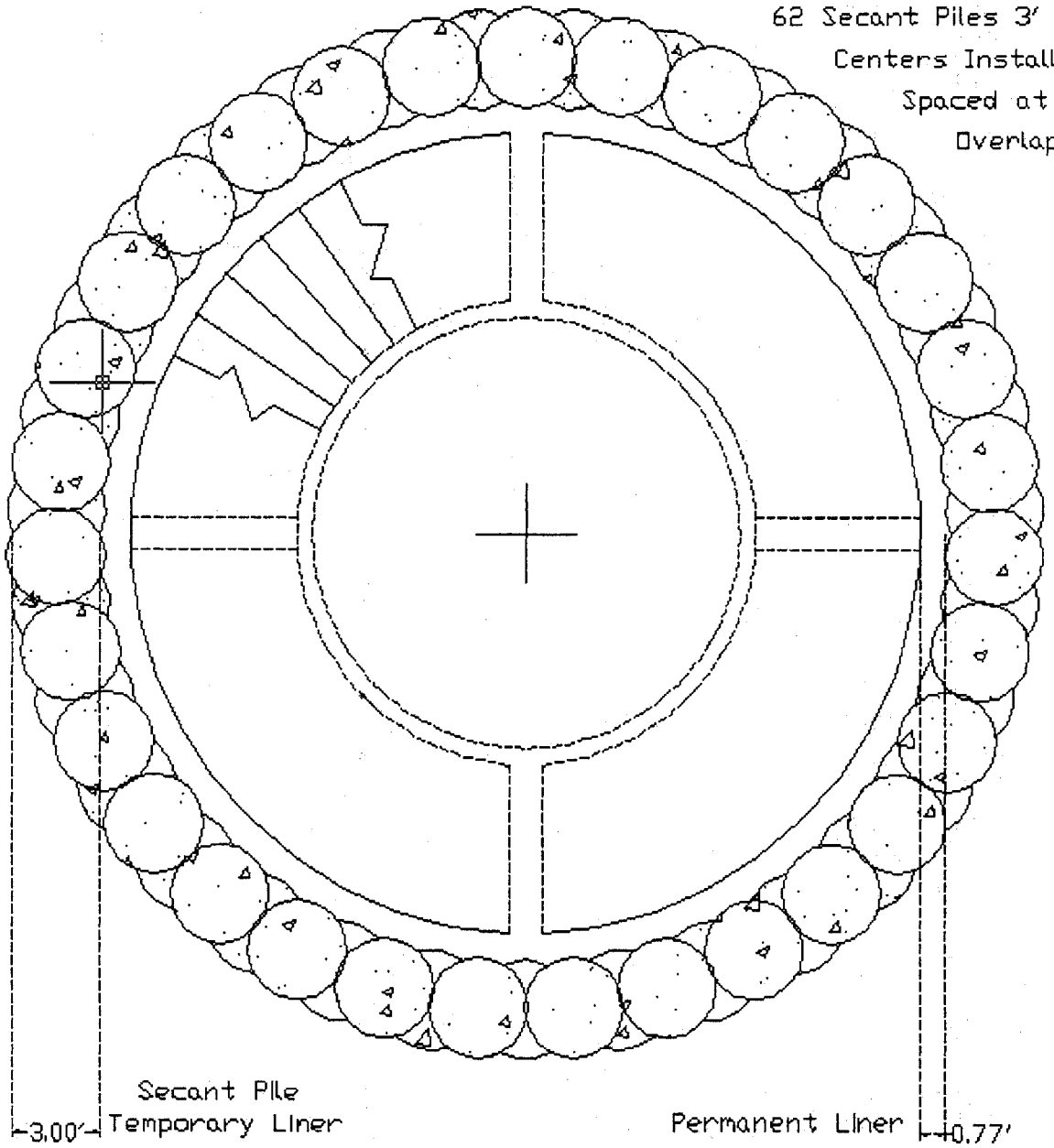

Proposed
Secant
Pile
Shaft
Design

Appendix C: Revised Secant Pile Shaft Design

Revised Vertical Secant Pile Shaft Design

Length of Shaft Centerline, **D**	140 ft	Secant pile factor of safety, **F**	2.00
Interior radius of secant piles, r_n	12.471 ft	Maximum horizontal earth pressure, σ_{hmax}=**P**	13,333 psf
Thickness of perm liner, t_p	0.471 ft	Concrete strength, σ_t	5000 psi
Interior radius of perm liner, r_f	12 ft	Concrete strength, σ_t	720,000 psf
Expected borehole deviation, $\%_{deviation}$	0.50%		
Deviation Distance, **d**	0.7 ft		

$r_n = r_f + t_p$ $\quad d = \%_{deviation} D_{borehole}$ $\quad r_i = r_f + t_p + \frac{1}{2} r_s$ $\quad n = \frac{2\pi r_i}{S}$

ft Pile Dia.	r_s (ft) Pile Rad.	r_i (ft) Installation Radius	t_{liner} (ft) Required Overlap	S (ft) Pile Spacing	l_{min} (ft) Min. Overlap	l_{avg} (ft) True Overlap	l_{max} (ft) Max. Overlap	n Number of Piles	$/LF	LF	Total Cost
2	1	13.471	0.528	0.529	0.528	1.929	1.800	160.0	$56	22403.1	$1,254,572
2.5	1.25	13.721	0.538	1.041	0.538	2.273	2.474	82.8	$71	11589.9	$822,886
3	1.5	13.971	0.548	1.550	0.548	2.569	2.996	56.7	$83	7931.1	**$658,279**
3.5	1.75	14.221	0.558	2.055	0.558	2.833	3.438	43.5	$141	6086.5	$858,191
4	2	14.471	0.568	2.560	0.568	3.074	3.828	35.5	$195	4973.3	$969,786
4.5	2.25	14.721	0.577	3.063	0.577	3.297	4.182	30.2	$252	4227.9	$1,065,420
5	2.5	14.971	0.587	3.565	0.587	3.505	4.507	26.4	$306	3693.6	$1,130,227
5.5	2.75	15.221	0.597	4.067	0.597	3.702	4.810	23.5	$344	3291.7	$1,132,336
6	3	15.471	0.607	4.569	0.607	3.889	5.095	21.3	$381	2978.4	$1,134,753
6.5	3.25	15.721	0.617	5.071	0.617	4.067	5.364	19.5	$425	2727.2	$1,159,055
7	3.5	15.971	0.627	5.572	0.627	4.237	5.621	18.0	$469	2521.3	$1,182,502

$l_{min} = 2\sqrt{r_s^2 - \left(\frac{S}{2} + d\right)^2}$ $\quad l_{avg} = 2\sqrt{r_s^2 - \left(\frac{S}{2}\right)^2}$ $\quad l_{max} = 2\sqrt{r_s^2 - \left(\frac{S}{2} - d\right)^2}$ $\quad S = 2\sqrt{r_s^2 - \left(\frac{t_l}{2}\right)^2} - d$ $\quad t_{liner} = r_n\left(\sqrt{\frac{\sigma_t}{\sigma_t - 2PF}} - 1\right)$

$658,279 Temp Liner

Temporary secant pile liner designed with 5000psi concrete
Permanent steel reinforced liner designed with FoS of 2.00 at a thickness of 0.471 feet of 5000 psi concrete

Means CM Tunnel Liner including reinforcement for 20 foot diameter, Earth 023000510 — $550 per linear foot
$74,250 Perm. Liner cost — **$74,250 Permanent Liner**

Shaft Excavation (avg) — $60 per cu yd — **$152,002** — **$152,002 Shaft Excavation**
Volume of Excavation — 2533.4 cu yd

Cost of Shaft per LF of depth
$6,318.08

Minimum Secant Pile Shaft Structural Cost (minus floorslab, stairwell, and topside)
$884,532

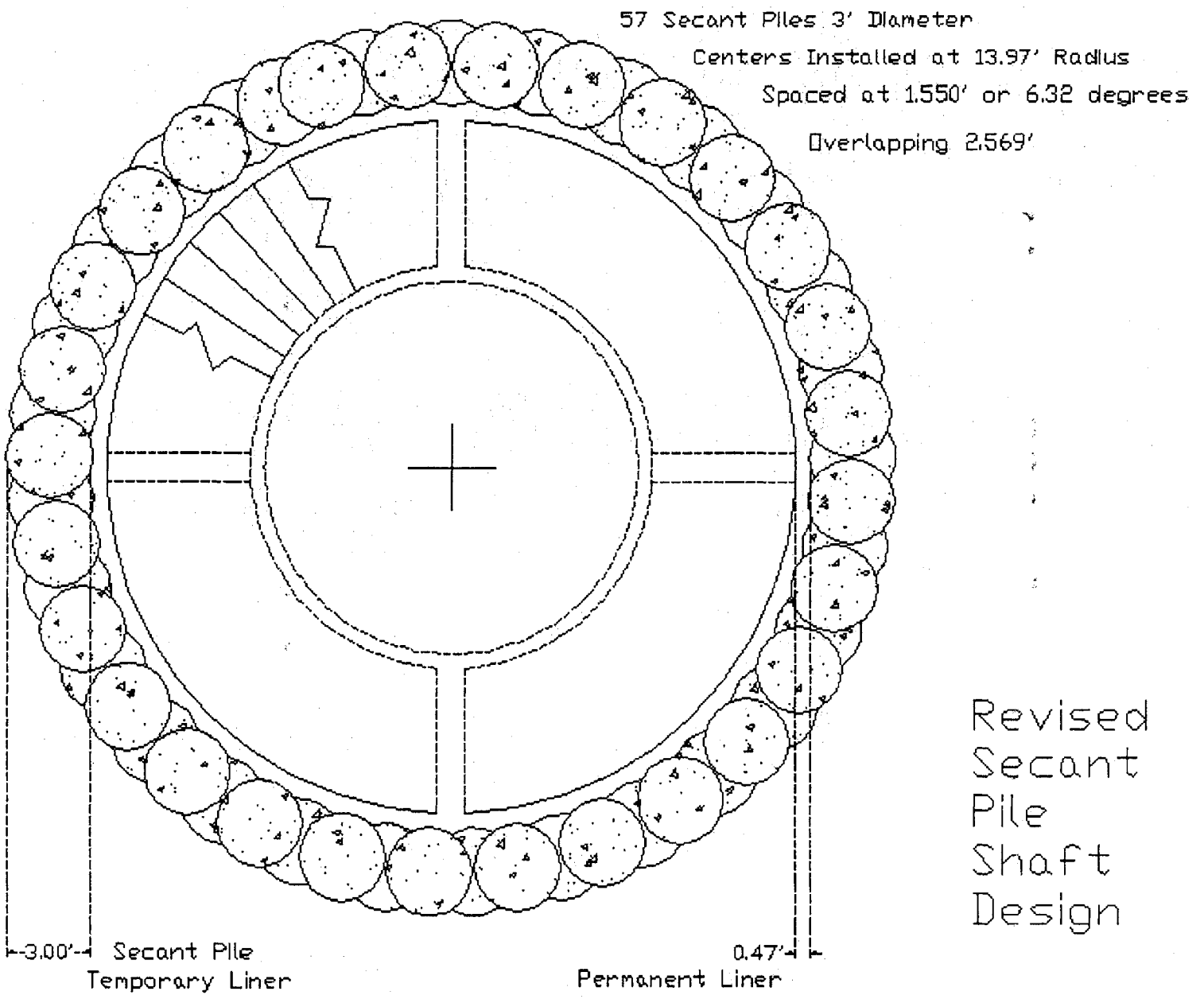

Revised Secant Pile Shaft Design

Appendix D: Basal Stability Calculations

Basal Stability Calculations

Treat excavation face stability as the base of a braced excavation

Critical Case is deep excavation in soft clay from 50 to 100 feet BGS
Assume 2 feet of soil is left above cutting edge in soft clay
UBC Calculated Bjerrum & Eide Undrained Bearing Capacity for Clay
Po is excavation chamber air pressure
Modified Bjerrum & Eide calculation was derived

Appendix D
Spreadsheet page layout

p.106	p.108	p.110
p.107	p.109	p.111

Minimum Basal Factor of Safety, FS_{REQ} = 1.25

Maximum Allowable Air Pressure, P_{max} = 50 psi

Nc value used for cohesive soil **6.2**

Soil height in Chamber, H_s = 1.50 ft

Width of Chamber, **B** = 24 ft

p_D is the design pneumatic chamber pressure

p_C is the cohesive soil stability pressure

H_S was set to zero once its insignificane was determined

"Air Drying" indicates air is migrating into surrounding ground

Soil	Geology	pcf γ	φ	ft **Depth** D	psf u	psf σvo	psf **Shansep** Su	psf **Recomp** Su	**Cohesionless** Nq	Nγ
		110	32	0	0	0			23.180	30.210
	FILL	110	32	-5	0	550			23.180	30.210
		110	32	-8	0	880			23.180	30.210
		120	32	-10	125	1,100			23.180	30.210
	SILT	100	30	-11	187	1,220	250	250		
		100	30	-15	437	1,620	250	250		
		100	30	-17	562	1,820	250	250		
		100	30	-20	749	2,120	250	250		
		100	30	-21.5	842	2,270	250	250		
		100	30	-26	1,061	2,620	250	250		
		100	30	-30	1,373	3,120	250	250		
		100	30	-32	1,498	3,320	250	250		
		100	30	-35	1,685	3,620	250	250		
	SAND	130	37	-35.5	1,716	3,670	0	0	42.920	66.190
	UBBC	117	28	-38.5	1,966	4,190	1,630	1,500		
		117	27	-40	1,997	4,249	1,630	1,500		

Continued on page 107

Continued from page 106

Soil	Geology	pcf γ	ϕ	ft Depth	psf u	psf σ_{vo}	psf Shansep S_u	psf Recomp S_u	Cohesionless N_q	N_γ
		117	26.5	-42.5	2,153	4,541	1,600	1,465		
		117	26	-45	2,309	4,834	1,570	1,425		
	LBBC	117	25	-49.5	2,590	5,360	1,516	1,350		
		117	24	-50	2,621	5,419	1,510	1,350		
		117	24	-53	2,808	5,770	1,490	1,350		
		117	24	-55	2,933	6,004	1,475	1,350		
		117	24	-60	3,245	6,589	1,440	1,350		
		117	24	-63.5	3,463	6,998	1,415	1,350		
		117	24	-65	3,557	7,174	1,405	1,350		
		117	24	-70	3,869	7,759	1,370	1,350		
		117	24	-74	4,118	8,227	1,342	1,350		
		117	24	-75	4,181	8,344	1,335	1,350		
		123	24	-80	4,493	8,929	1,300	1,350		
		123	24	-84.5	4,774	9,482	1,350	1,350		
		123	24	-85	4,805	9,544	1,370	1,350		
		123	24	-90	5,117	10,159	1,450	1,410		
		123	24	-95	5,429	10,774	1,530	1,470		
		123	24	-100	5,741	11,389	1,610	1,530		
		123	25	-104.5	6,022	11,942	1,682	1,584		
		123	25	-105	6,053	12,004	1,690	1,590		
		123	25	-105.5	6,084	12,065	1,698	1,596		
		123	25	-110	6,365	12,619	1,770	1,650		
		123	25	-115	6,677	13,234	1,850	1,710		
		123	25	-116	6,739	13,357	1,862	1,734		
	TILL	135	45	-117.5	6,833	13,541			134.870	271.750
		135	45	-120	6,989	13,879			134.870	271.750
		135	45	-125	7,301	14,554			134.870	271.750
		135	45	-126.5	7,394	14,756			134.870	271.750
		135	45	-130	7,613	15,229			134.870	271.750
		135	45	-135	7,925	15,904			134.870	271.750
		135	45	-140	8,237	16,579			134.870	271.750
	ROCK	155	45	-142	8,362	16,849			134.870	271.750

Peck (1969) Stability Factor, Nt

Nt	Condition
1	Stable
>1	Small Creep
>3	Creeping, usually slow enough to permit tunneling
>6	May produce general shear failure. Clay likely to invade tail space too quickly to handle

$$N_t = \frac{(\sigma_{VO} - p_O)}{s_U}$$

p_C is the cohesive soil stability pressure

p_{CH} is p_C with additional H_S overburden

p_{MAX} is the 50 psi federal limit

u is the hydrostatic pore pressure

$$p_C = \frac{(FS_{REQ}\sigma_{VC}) - q_{ULT}}{144}$$

$$p_{CH} = \frac{\left|(FS_{REQ}\sigma_{VO}) - q_{ULT} - (H_S\gamma_{SOIL})\right|}{144}$$

$$p_{MAX} > p_D = MAX\,(p_C, p_{CH}, u)$$

REVERSE BEARING CAPACITY PROBLEM

Bjerrum & Eide (1956) Cohesive Soils

$$q_{ULT} = N_C s_U + p_O$$

$p_D > u$ Air Drying

$p_D = u$ Hydrostatic

$p_D < u$ Inflow or Pump

Modified Bjerrum & Eide Equation (Cohesive Soils)

$$q_{ULT} = N_C s_U + p_D + \gamma_{SOIL} H_S$$

Terzaghi Equation (Cohesionless Soil, neglect c')

$$q_{ULT} = N_q(H_S\gamma_{SOIL} + p_O) + \frac{1}{2}\gamma_{SOIL} B N_\gamma$$

$$FS = \frac{q_{ULT}}{\sigma_{VO}}$$

Shansep S_U Used

ft	psf $H_S = 0$ $p_O = 0$	$H_S = 0$ $p_O = 0$	psi $H_S = 0$	psi With H_S=1.5 ft		psi	$H_S = 0$ With p_D		Cohesive Soils Peck (1969) Stability	
D	q_{ULT}	FS	p_C required	p_{CH} required	psi u	Design Chamber p_D	new FS'	Pneumatic Condition	N_t	Condition
0.0	39877				0.0	0.0		Hydrostatic		
-5.0	39877	72.50			0.0	0.0	79.46	Hydrostatic		
-8.0	39877	45.32			0.0	0.0	49.66	Hydrostatic		
-10.0	43502	39.55			0.9	0.9	45.97	Hydrostatic		
-11.0	1550	1.27	-0.2	-1.4	1.3	1.3	1.55	Hydrostatic	4.13	Creeping
-15.0	1550	[illegible]	3.3	2.3	3.0	3.3	1.33	Air Drying	4.58	Creeping
-17.0	1550	[illegible]	5.0	4.0	3.9	5.0	1.32	Air Drying	4.38	Creeping
-20.0	1550	[illegible]	7.6	6.6	5.2	7.6	1.31	Air Drying	4.08	Creeping
-21.5	1550	[illegible]	8.9	7.9	5.9	8.9	1.31	Air Drying	3.93	Creeping
-25.0	1550	[illegible]	12.0	10.9	7.4	12.0	1.30	Air Drying	3.58	Creeping
-30.0	1550	[illegible]	16.3	15.3	9.5	16.3	1.29	Air Drying	3.08	Creeping
-32.0	1550	[illegible]	18.1	17.0	10.4	18.1	1.29	Air Drying	2.88	Small Creep
-35.0	1550	[illegible]	20.7	19.6	11.7	20.7	1.28	Air Drying	2.58	Small Creep
-35.5	103256	28.14			11.9	11.9	50.48	Hydrostatic		
-39.5	10106	2.41	-33.8	-35.2	13.7	13.7	2.92	Hydrostatic	1.36	Small Creep
-40.0	10106	2.38	-33.3	-34.5	13.9	13.9	2.88	Hydrostatic	1.38	Small Creep

Continued on page 109

Contined from page 108

Shansep S_u Used

ft	psf $H_S = 0$ $p_O = 0$	$H_S = 0$ $p_O = 0$	psi $H_S = 0$	psi With H_S=1.5 ft	psi	psi Design	$H_S = 0$ With p_D	Pneumatic	Cohesive Soils Peck (1969) Stability	
D	q_{ULT}	FS	p_C required	p_{CH} required	u	p_D	new FS'	Condition	N_t	Condition
-42.5	9920	2.18	-29.5	-30.7	15.0	15.0	2.69	Hydrostatic	1.49	Small Creep
-45.0	9734	2.01	-25.6	-26.9	16.0	16.0	2.52	Hydrostatic	1.61	Small Creep
-49.5	9399	1.75	-18.7	-20.0	18.0	18.0	2.26	Hydrostatic	1.83	Small Creep
-50.0	9362	1.73	-18.0	-19.2	18.2	18.2	2.24	Hydrostatic	1.85	Small Creep
-53.0	9238	1.60	-14.1	-15.3	19.5	19.5	2.11	Hydrostatic	1.99	Small Creep
-55.0	9145	1.52	-11.4	-12.6	20.4	20.4	2.04	Hydrostatic	2.08	Small Creep
-60.0	8928	1.36	-4.8	-6.0	22.5	22.5	1.87	Hydrostatic	2.32	Small Creep
-63.5	8773	1.25	-0.2	-1.4	24.1	24.1	1.77	Hydrostatic	2.50	Small Creep
-65.0	8711	[illegible]	1.8	0.6	24.7	24.7	1.73	Hydrostatic	2.57	Small Creep
-70.0	8494	[illegible]	8.4	7.1	26.9	26.9	1.61	Hydrostatic	2.84	Small Creep
-74.0	8320	[illegible]	13.6	12.4	28.6	28.6	1.53	Hydrostatic	3.06	Creeping
-75.0	8277	[illegible]	14.9	13.7	29.0	29.0	1.51	Hydrostatic	3.12	Creeping
-80.0	8060	[illegible]	21.5	20.3	31.2	31.2	1.42	Hydrostatic	3.41	Creeping
-84.5	8370	[illegible]	24.2	22.9	33.2	33.2	1.40	Hydrostatic	3.49	Creeping
-85.0	8494	[illegible]	23.9	22.6	33.4	33.4	1.41	Hydrostatic	3.46	Creeping
-90.0	8990	[illegible]	25.8	24.5	35.5	35.5	1.40	Hydrostatic	3.48	Creeping
-95.0	9486	[illegible]	27.6	26.4	37.7	37.7	1.40	Hydrostatic	3.49	Creeping
-100.0	9982	[illegible]	29.5	28.3	39.9	39.9	1.39	Hydrostatic	3.51	Creeping
-104.5	10428	[illegible]	31.2	30.0	41.8	41.8	1.39	Hydrostatic	3.52	Creeping
-105.0	10478	[illegible]	31.4	30.2	42.0	42.0	1.39	Hydrostatic	3.52	Creeping
-105.5	10528	[illegible]	31.6	30.3	42.3	42.3	1.39	Hydrostatic	3.52	Creeping
-110.0	10974	[illegible]	33.3	32.0	44.2	44.2	1.39	Hydrostatic	3.53	Creeping
-115.0	11470	[illegible]	35.2	33.9	46.4	46.4	1.38	Hydrostatic	3.54	Creeping
-116.0	11544	[illegible]	35.8	34.5	46.8	46.8	1.38	Hydrostatic	3.55	Creeping
-117.5	440235	32.51			47.5	47.5	102.58	Hydrostatic		
-120.0	440235	31.72			48.5	48.5	101.61	Hydrostatic		
-125.0	440235	30.25			50.7	50.0	98.85	Water Inflow or Pump		
-126.5	440235	29.83			51.4	50.0	97.49	Water Inflow or Pump		
-130.0	440235	28.91			52.9	50.0	94.47	Water Inflow or Pump		
-135.0	440235	27.68			55.0	50.0	90.46	Water Inflow or Pump		
-140.0	440235	26.55			57.2	50.0	86.78	Water Inflow or Pump		
-142.0	440235	26.13			58.1	50.0	85.63	Water Inflow or Pump		

$$p_C = \frac{(FS_{REQ}\sigma_{VO}) - q_{ULT}}{144}$$

$$p_{CH} = \frac{\left|(FS_{REQ}\sigma_{VO}) - q_{ULT} - (H_S\gamma_{SOIL})\right|}{144}$$

$$p_{MAX} > p_D = MAX\ (p_O, p_{CH}, u)$$

$p_D > u$ Air Drying

$p_D = u$ Hydrostatic

$p_D < u$ Water Inflow or Pump

$$N_t = \frac{(\sigma_{VO} - p_O)}{s_U}$$

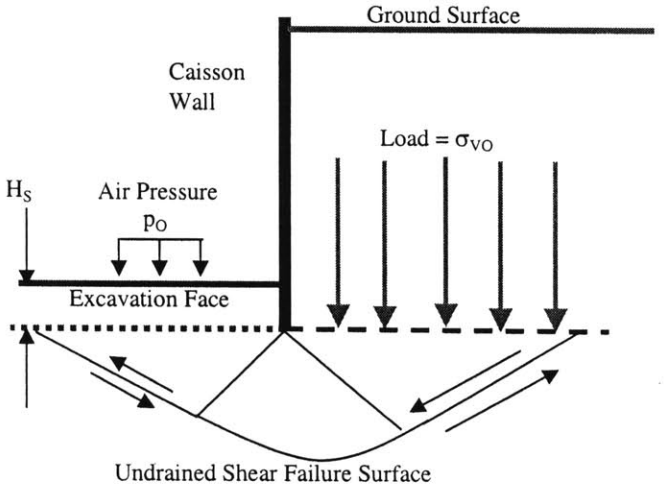

Recompression S_u Used

ft	psf $H_S = 0$ $P_O = 0$	$H_S = 0$ $p_O = 0$	psi $H_S = 0$	psi With H_S=1.5 ft		psi	$H_S = 0$		Cohesive Soils	
			Clay Stability	Clay Stability	psi	Design Chamber	With p_D	Pneumatic	Peck (1969) Stability	
D	Clay q_{ULT}	FS	p_C required	p_{CH} required	u	p_D	new FS'	Condition	Nt	Condition
0.0	39877				0.0	0.0		Hydrostatic		
-5.0	39877	72.50			0.0	0.0	79.46	Hydrostatic		
-8.0	39877	45.32			0.0	0.0	49.66	Hydrostatic		
-10.0	43502	39.55			0.9	0.9	45.97	Hydrostatic		
-11.0	1550	1.27	-0.2	-1.4	1.3	1.3	1.55	Hydrostatic	4.13	Creeping
-15.0	1550	[illegible]	3.3	2.3	3.0	3.3	1.33	Air Drying	4.58	Creeping
-17.0	1550	[illegible]	5.0	4.0	3.9	5.0	1.32	Air Drying	4.38	Creeping
-20.0	1550	[illegible]	7.6	6.6	5.2	7.6	1.31	Air Drying	4.08	Creeping
-21.5	1550	[illegible]	8.9	7.9	5.9	8.9	1.31	Air Drying	3.93	Creeping
-25.0	1550	[illegible]	12.0	10.9	7.4	12.0	1.30	Air Drying	3.58	Creeping
-30.0	1550	[illegible]	16.3	15.3	9.5	16.3	1.29	Air Drying	3.08	Creeping
-32.0	1550	[illegible]	18.1	17.0	10.4	18.1	1.29	Air Drying	2.88	Small Creep
-35.0	1550	[illegible]	20.7	19.6	11.7	20.7	1.28	Air Drying	2.58	Small Creep
-35.5	103256	28.14			11.9	11.9	50.48	Hydrostatic		
-39.5	9300	2.22	-28.2	-29.6	13.7	13.7	2.73	Hydrostatic	1.48	Small Creep
-40.0	9300	2.19	-27.7	-28.9	13.9	13.9	2.69	Hydrostatic	1.50	Small Creep

Continued on page 111

Continued from page 110

Recompression S_u Used

ft	psf $H_S = 0$ $P_O = 0$	$H_S = 0$ $p_O = 0$	psi $H_S = 0$	psi With H_S=1.5 ft	psi	psi Design Chamber	$H_S = 0$ With p_D		Cohesive Soils Peck (1969) Stability	
D	Clay q_{ULT}	FS	p_C required	p_{CH} required	u	p_D	new FS'	Pneumatic Condition	Nt	Condition
-42.5	9083	2.00	-23.7	-24.9	15.0	15.0	2.51	Hydrostatic	1.63	Small Creep
-45.0	8835	1.83	-19.4	-20.6	16.0	16.0	2.34	Hydrostatic	1.77	Small Creep
-49.5	8370	1.56	-11.6	-12.8	18.0	18.0	2.07	Hydrostatic	2.05	Small Creep
-50.0	8370	1.54	-11.1	-12.3	18.2	18.2	2.06	Hydrostatic	2.07	Small Creep
-53.0	8370	1.45	-8.0	-9.3	19.5	19.5	1.96	Hydrostatic	2.19	Small Creep
-55.0	8370	1.39	-6.0	-7.2	20.4	20.4	1.91	Hydrostatic	2.27	Small Creep
-60.0	8370	1.27	-0.9	-2.2	22.5	22.5	1.79	Hydrostatic	2.48	Small Creep
-63.5	8370	1.20	2.6	1.4	24.1	24.1	1.71	Hydrostatic	2.62	Small Creep
-65.0	8370	1.17	4.1	2.9	24.7	24.7	1.68	Hydrostatic	2.68	Small Creep
-70.0	8370	1.08	9.2	8.0	26.9	26.9	1.60	Hydrostatic	2.88	Small Creep
-74.0	8370	1.02	13.3	12.1	28.6	28.6	1.54	Hydrostatic	3.04	Creeping
-75.0	8370	1.00	14.3	13.1	29.0	29.0	1.52	Hydrostatic	3.08	Creeping
-80.0	8370	0.93	19.4	18.2	31.2	31.2	1.46	Hydrostatic	3.29	Creeping
-84.5	8370	0.88	24.2	22.9	33.2	33.2	1.40	Hydrostatic	3.49	Creeping
-85.0	8370	0.87	24.7	23.4	33.4	33.4	1.40	Hydrostatic	3.51	Creeping
-90.0	8742	0.83	27.5	26.2	35.5	35.5	1.38	Hydrostatic	3.58	Creeping
-95.0	9114	0.79	30.2	28.9	37.7	37.7	1.36	Hydrostatic	3.64	Creeping
-100.0	9486	0.76	33.0	31.7	39.9	39.9	1.35	Hydrostatic	3.69	Creeping
-104.5	9821	0.73	35.5	34.2	41.8	41.8	1.34	Hydrostatic	3.74	Creeping
-105.0	9858	0.72	35.7	34.5	42.0	42.0	1.34	Hydrostatic	3.74	Creeping
-105.5	9895	0.72	36.0	34.7	42.3	42.3	1.34	Hydrostatic	3.75	Creeping
-110.0	10230	0.70	38.5	37.2	44.2	44.2	1.33	Hydrostatic	3.79	Creeping
-115.0	10602	0.68	41.2	40.0	46.4	46.4	1.32	Hydrostatic	3.83	Creeping
-116.0	10751	0.67	41.3	40.0	46.8	46.8	1.32	Hydrostatic	3.82	Creeping
-117.5	440235	32.51			47.5	47.5	102.58	Hydrostatic		
-120.0	440235	31.72			48.5	48.5	101.61	Hydrostatic		
-125.0	440235	30.25			50.7	50.0	98.85	Water Inflow or Pump		
-126.5	440235	29.83			51.4	50.0	97.49	Water Inflow or Pump		
-130.0	440235	28.91			52.9	50.0	94.47	Water Inflow or Pump		
-135.0	440235	27.68			55.0	50.0	90.46	Water Inflow or Pump		
-140.0	440235	26.55			57.2	50.0	86.78	Water Inflow or Pump		
-142.0	440235	26.13			58.1	50.0	85.63	Water Inflow or Pump		

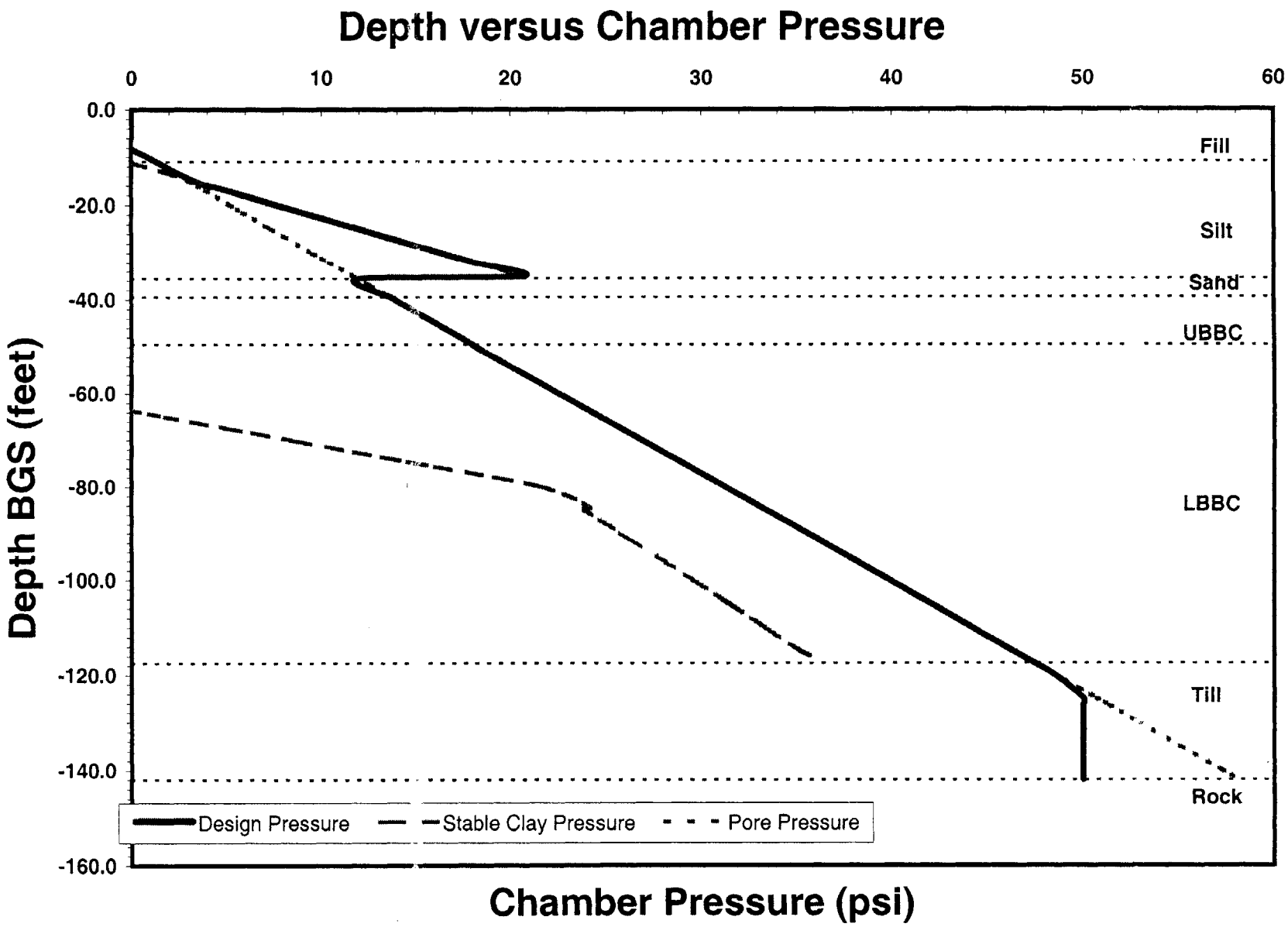
Depth versus Chamber Pressure
0
10
20
30
40
50
60
0.0
-20.0
-40.0
-60.0
-80.0
-100.0
-120.0
-140.0
-160.0
Depth BGS (feet)
Fill
Silt
Sand
UBBC
LBBC
Till
Rock
Design Pressure
Stable Clay Pressure
Pore Pressure
Chamber Pressure (psi)

Appendix E: Soil Skin Friction Calculations

Caisson Driving

Length	142 ft
Outer Radius	13 ft
Outer Circumference, **P**	81.68 ft
Caisson Wall Area, A_{WALL}	78.54 ft²
Wall Thickness, **B**	1 feet
Percentage of End Bearing at tip, **G**	25.00%
Pneumatic Chamber Plan Area, A_{BULK}	452 ft²

Friction data from NAVFAC (1982) 18-30

Material w/formed concrete	ϕ_M
clean gravel or gravel-sand mix	24
clean sand, silty sand and gravel	20
silty sand, gravel, or sand with silt or clay	17

Assumed based on Coller et al Information

Bentonite slurry friction reduction in cohesionless soils	50% R_{COHL}
Bentonite slurry friction reduction in cohesive soils	25% R_{COH}

N_γ and N_C values for cohesionless soils from Vesic (1973)

N_C for cohesive soils for strip footings from Skempton (1951)

F is unit skin friction

TF is cumulative skin friction

TR is thrust

q_{ULT} is the bearing capacity

Appendix E
Spreadsheet page layout

p.114	p.116
p.115	p.117

Soil	Geology	pcf γ_{SOIL}	ϕ	ft **Depth** D	psf u	psf σ_{vo}	psf σ'_{vo}	K_o	psf **Rankine Active**	psf σ'_{ho}	psf σ_{ho}	psf **Shansep Su**	α	low psf **short term Skin Friction** F_{LOW}	high psf **short term Skin Friction** F_{HIGH}
		110	32	0	0	0	0	0.470	0.307	0	0			0.00	0.00
	FILL	110	32	-5	0	550	550	0.470	0.307	259	259			51.67	79.04
		110	32	-8	0	880	880	0.470	0.307	414	414			82.67	126.47
		120	32	-10	125	1,100	975	0.470	0.307	458	583			91.61	140.15
	SILT	100	30	-11	187	1,220	1,033	0.500	0.333	516	704	250	0.58	145.00	250.00
		100	30	-15	437	1,620	1,183	0.500	0.333	592	1,028	250	0.58	145.00	250.00
		100	30	-17	562	1,820	1,258	0.500	0.333	629	1,191	250	0.58	145.00	250.00
		100	30	-20	749	2,120	1,371	0.500	0.333	686	1,434	250	0.58	145.00	250.00
		100	30	-21.5	842	2,270	1,428	0.500	0.333	714	1,556	250	0.58	145.00	250.00
		100	30	-25	1,061	2,620	1,559	0.500	0.333	780	1,840	250	0.58	145.00	250.00
		100	30	-30	1,373	3,120	1,747	0.500	0.333	874	2,246	250	0.58	145.00	250.00
		100	30	-32	1,498	3,320	1,822	0.500	0.333	911	2,409	250	0.58	145.00	250.00
		100	30	-35	1,685	3,620	1,935	0.500	0.333	968	2,652	250	0.58	145.00	250.00
	SAND	130	37	-35.5	1,716	3,670	1,954	0.398	0.249	778	2,494			216.26	346.41
	UBBC	117	28	-39.5	1,966	4,190	2,224	1.040	0.361	2,313	4,279	1,630	0.46	749.80	1630.00
		117	27	-40	1,997	4,249	2,252	0.839	0.376	1,889	3,886	1,630	0.46	749.80	1630.00
		117	27	-42.5	2,153	4,541	2,388	0.773	0.383	1,846	3,999	1,600	0.46	736.00	1600.00
		117	26	-45	2,309	4,834	2,525	0.707	0.390	1,785	4,094	1,570	0.46	722.20	1570.00
	LBBC	117	25	-49.5	2,590	5,360	2,770	0.577	0.406	1,600	4,189	1,516	0.64	970.24	1516.00
		117	24	-50	2,621	5,419	2,798	0.593	0.422	1,660	4,281	1,510	0.64	966.40	1510.00
		117	24	-53	2,808	5,770	2,962	0.593	0.422	1,757	4,565	1,490	0.64	953.60	1490.00
		117	24	-55	2,933	6,004	3,071	0.593	0.422	1,822	4,755	1,475	0.64	944.00	1475.00
		117	24	-60	3,245	6,589	3,344	0.593	0.422	1,984	5,228	1,440	0.64	921.60	1440.00
		117	24	-63.5	3,463	6,998	3,535	0.593	0.422	2,097	5,560	1,415	0.64	905.60	1415.00
		117	24	-65	3,557	7,174	3,617	0.593	0.422	2,146	5,702	1,405	0.64	899.20	1405.00
		117	24	-70	3,869	7,759	3,890	0.593	0.422	2,308	6,176	1,370	0.64	876.80	1370.00
		117	24	-74	4,118	8,227	4,108	0.593	0.422	2,437	6,556	1,342	0.64	858.88	1342.00

Continued on page 115

Continued from page 114

Soil	Geology	pcf		ft		psf	psf		psf		psf	psf		low psf short term Skin	high psf short term Skin
		γ_{SOIL}	ϕ	**Depth**	psf	psf	psf		**Rankine**	psf	psf	**Shansep**		**Friction**	**Friction**
				D	**u**	σvo	$\sigma'vo$	K_o	**Active**	$\sigma'ho$	σho	**Su**	α	F_{LOW}	F_{HIGH}
	LBBC	117	24	-75	4,181	8,344	4,163	0.593	0.422	2,470	6,650	1,335	0.64	854.40	1335.00
		123	24	-80	4,493	8,929	4,436	0.593	0.422	2,632	7,124	1,300	0.64	832.00	1300.00
		123	24	-84.5	4,774	9,482	4,708	0.593	0.422	2,793	7,567	1,350	0.64	864.00	1350.00
		123	24	-85	4,805	9,544	4,739	0.593	0.422	2,811	7,616	1,370	0.64	876.80	1370.00
		123	24	-90	5,117	10,159	5,042	0.593	0.422	2,991	8,108	1,450	0.64	928.00	1450.00
		123	24	-95	5,429	10,774	5,345	0.593	0.422	3,171	8,600	1,530	0.64	979.20	1530.00
		123	24	-100	5,741	11,389	5,648	0.593	0.422	3,351	9,091	1,610	0.64	1030.40	1610.00
		123	25	-104.5	6,022	11,942	5,920	0.577	0.406	3,418	9,440	1,682	0.85	1429.70	1682.00
		123	25	-105	6,053	12,004	5,951	0.577	0.406	3,436	9,489	1,690	0.85	1436.50	1690.00
		123	25	-105.5	6,084	12,065	5,981	0.577	0.406	3,453	9,537	1,698	0.85	1443.30	1698.00
		123	25	-110	6,365	12,619	6,254	0.577	0.406	3,611	9,976	1,770	0.85	1504.50	1770.00
		123	25	-115	6,677	13,234	6,557	0.577	0.406	3,786	10,463	1,850	0.85	1572.50	1850.00
		123	25	-116	6,739	13,357	6,617	0.577	0.406	3,821	10,560	1,862	0.85	1582.70	1862.00
	TILL	135	45	-117.5	6,833	13,541	6,708	0.586	0.172	3,930	10,762			418.91	1430.25
		135	45	-120	6,989	13,879	6,890	0.586	0.172	4,036	11,025			430.24	1468.94
		135	45	-125	7,301	14,554	7,253	0.586	0.172	4,249	11,549			452.91	1546.34
		135	45	-126.5	7,394	14,756	7,362	0.586	0.172	4,314	11,708			459.71	1570.13
		135	45	-130	7,613	15,229	7,616	0.586	0.172	4,461	12,074			475.58	1623.73
		135	45	-135	7,925	15,904	7,979	0.586	0.172	4,674	12,599			498.25	1701.13
		135	45	-140	8,237	16,579	8,342	0.586	0.172	4,886	13,123			520.92	1778.52
	ROCK	155	45	-142	8,362	16,849	8,487	0.586	0.172	4,972	13,333			529.99	1809.48
		155													

Cohesionless Soils

$$F_{LOW-COHL} = K_A \sigma'_{VO} \tan \phi_M$$

$$F_{HIGH-COHL} = K_O \sigma'_{VO} \tan \phi_M$$

$$q_{ULT-COHL} = \frac{1}{2} \gamma_{SOIL} B N_\gamma$$

Cohesive Soils

$$F_{LOW-COH} = s_U \alpha$$

$$F_{HIGH-COH} = s_U$$

$$q_{ULT-COH} = N_C s_U$$

$$\Delta D = D_i - D_{(i-1)}$$

$$TF_{LOW} = \sum (\Delta D) P F_{LOW} \qquad TF_{HIGH} = \sum (\Delta D) P F_{HIGH}$$

$$TF_{BENT} = \sum (\Delta D) P (1 - R) F_{LOW}$$

$$TR_{LOW} = TF_{LOW} + (q_{ULT} GA_{WALL}) + (A_{BULK} p_D)$$

$$TR_{HIGH} = TF_{HIGH} + (q_{ULT} GA_{WALL}) + (A_{BULK} p_D)$$

$$TR_{BENT} = TF_{BENT} + (q_{ULT} GA_{WALL}) + (A_{BULK} p_D)$$

R values from page 114
G from page 114

Bentonite Cumulative Total Best Case Friction TF_{BENT}	lbs short term Friction TF_{LOW}	lbs long term Friction TF_{HIGH}	Cohesionless $N\gamma$	Cohesionless Nq	Clays Nc	psf q_{ULT}	$A_{WALL}{}^{*}q_{ULT}$ lbs End Bearing	psf Design Chamber p_D	lbs Best Case Driving Force TR_{BENT}	lbs low Driving Force TR_{LOW}	lbs high Driving Force TR_{HIGH}	ft Depth BGS
0	0	0	30.21	23.18	35.49	1662	130,505	0	32,626	32,626	32,626	0.0
10,550	21,101	32,283	30.21	23.18	35.49	1662	130,505	0	43,177	53,727	64,909	5.0
20,679	41,358	63,274	30.21	23.18	35.49	1662	130,505	0	53,305	73,984	95,900	8.0
28,162	56,323	86,170	30.21	23.18	35.49	1813	142,369	125	120,212	148,374	178,220	10.0
37,044	68,167	106,590			5.2	1300	102,107	187	147,259	178,381	216,805	11.0
72,576	115,542	188,272			5.2	1300	102,107	475	312,988	355,955	428,684	15.0
90,342	139,230	229,113			5.2	1300	102,107	725	443,852	492,740	582,623	17.0
116,990	174,761	290,374			5.2	1300	102,107	1,100	640,147	697,918	813,530	20.0
130,315	192,527	321,004			5.2	1300	102,107	1,288	738,294	800,507	928,984	21.5
161,405	233,981	392,476			5.2	1300	102,107	1,725	967,305	1,039,881	1,198,376	25.0
205,819	293,200	494,578			5.2	1300	102,107	2,350	1,294,463	1,381,844	1,583,222	30.0
223,585	316,887	535,419			5.2	1300	102,107	2,600	1,425,327	1,518,629	1,737,161	32.0
250,233	352,419	596,680			5.2	1300	102,107	2,975	1,621,622	1,723,807	1,968,068	35.0
254,650	361,251	610,828	66.19	42.92	55.63	4302	337,924	1,716	1,115,433	1,222,034	1,471,611	35.5
438,384	606,231	1,143,392			5.2	8476	665,740	1,966	1,494,038	1,661,884	2,199,045	39.5
461,351	636,853	1,209,962			5.2	8476	665,740	1,997	1,531,119	1,706,621	2,279,730	40.0
574,072	787,147	1,536,689			5.2	8320	653,487	2,153	1,711,349	1,924,425	2,673,966	42.5
684,679	934,623	1,857,289			5.2	8164	641,234	2,309	1,889,466	2,139,411	3,062,076	45.0
952,150	1,291,252	2,414,521			5.2	7883	619,179	2,590	2,278,455	2,617,557	3,740,826	49.5
981,751	1,330,720	2,476,190			5.2	7852	616,728	2,621	2,321,558	2,670,527	3,815,997	50.0
1,157,007	1,564,395	2,841,307			5.2	7748	608,560	2,808	2,579,460	2,986,847	4,263,759	53.0
1,272,669	1,718,610	3,082,268			5.2	7670	602,433	2,933	2,750,047	3,195,989	4,559,647	55.0
1,554,960	2,094,999	3,670,375			5.2	7488	588,138	3,245	3,169,911	3,709,950	5,285,326	60.0
1,749,134	2,353,897	4,074,903			5.2	7358	577,927	3,463	3,460,334	4,065,097	5,786,104	63.5
1,831,763	2,464,069	4,247,047			5.2	7306	573,843	3,557	3,584,286	4,216,592	5,999,570	65.0
2,100,332	2,822,161	4,806,566			5.2	7124	559,548	3,869	3,990,427	4,712,256	6,696,661	70.0
2,310,796	3,102,780	5,245,033			5.2	6978	548,112	4,118	4,310,949	5,102,932	7,245,186	74.0

Continued on page 117

Continued from page 116

Bentonite Cumulative Total Best Case Friction TF_{BENT}	lbs short term Friction TF_{LOW}	lbs long term Friction TF_{HIGH}	Cohesionless N_γ	Cohesionless N_q	Clays Nc	psf q_{ULT}	$A_{WALL}{}^{*}q_{ULT}$ lbs End Bearing	psf Design Chamber p_D	lbs Best Case Driving Force TR_{BENT}	lbs low Driving Force TR_{LOW}	lbs high Driving Force TR_{HIGH}	ft Depth BGS
2,363,138	3,172,569	5,354,078			5.2	6942	545,253	4,181	4,390,805	5,200,236	7,381,745	75.0
2,617,984	3,512,364	5,885,009			5.2	6760	530,958	4,493	4,783,223	5,677,603	8,050,248	80.0
2,856,168	3,829,942	6,381,224			5.2	7020	551,379	4,774	5,153,543	6,127,318	8,678,600	84.5
2,883,025	3,865,751	6,437,176			5.2	7124	559,548	4,805	5,196,557	6,179,284	8,750,709	85.0
3,167,277	4,244,754	7,029,368			5.2	7540	592,222	5,117	5,630,123	6,707,601	9,492,215	90.0
3,467,211	4,644,667	7,654,232			5.2	7956	624,897	5,429	6,079,373	7,256,828	10,266,393	95.0
3,782,829	5,065,491	8,311,769			5.2	8372	657,571	5,741	6,544,305	7,826,966	11,073,244	100.0
4,176,962	5,591,001	8,930,017			5.2	8746	686,978	6,022	7,072,821	8,486,860	11,825,875	104.5
4,220,963	5,649,669	8,999,038			5.2	8788	690,245	6,053	7,131,753	8,560,459	11,909,828	105.0
4,265,172	5,708,615	9,068,386			5.2	8830	693,513	6,084	7,190,894	8,634,336	11,994,107	105.5
4,679,926	6,261,620	9,718,979			5.2	9204	722,920	6,365	7,740,030	9,321,724	12,779,084	110.0
5,161,592	6,903,841	10,474,534			5.2	9620	755,594	6,677	8,371,011	10,113,260	13,683,953	115.0
5,258,550	7,033,119	10,626,625			5.2	9682	760,495	6,739	8,497,423	10,271,992	13,865,499	116.0
5,284,213	7,084,445	10,801,863	271.75	134.87	133.87	18343	1,440,744	6,833	8,735,492	10,535,724	14,253,142	117.5
5,328,142	7,172,302	11,101,827	271.75	134.87	133.87	18343	1,440,744	6,989	8,849,994	10,694,154	14,623,679	120.0
5,420,628	7,357,275	11,733,365	271.75	134.87	133.87	18343	1,440,744	7,200	9,038,025	10,974,672	15,350,761	125.0
5,448,791	7,413,600	11,925,741	271.75	134.87	133.87	18343	1,440,744	7,200	9,066,188	11,030,997	15,543,138	126.5
5,516,772	7,549,562	12,389,943	271.75	134.87	133.87	18343	1,440,744	7,200	9,134,169	11,166,959	16,007,340	130.0
5,618,516	7,753,051	13,084,698	271.75	134.87	133.87	18343	1,440,744	7,200	9,235,913	11,370,448	16,702,095	135.0
5,724,890	7,965,798	13,811,061	271.75	134.87	133.87	18343	1,440,744	7,200	9,342,287	11,583,195	17,428,458	140.0
5,768,180	8,052,378	14,106,664	271.75	134.87	133.87	21061	1,654,187	7,200	9,438,937	11,723,136	17,777,422	142.0

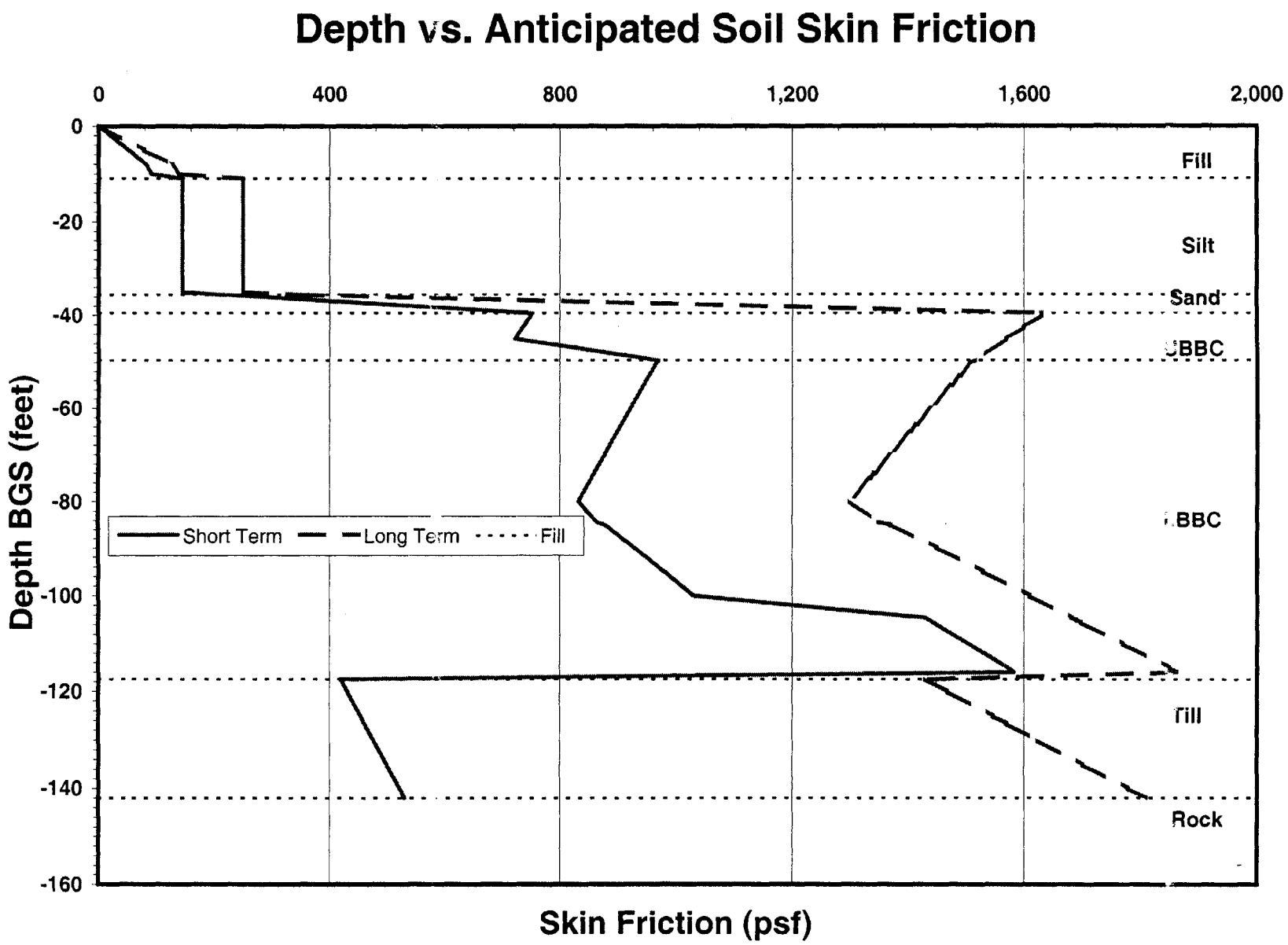
Depth vs. Anticipated Soil Skin Friction
0
400
800
1,200
1,600
2,000
0
-20
-40
-60
-80
-100
-120
-140
-160
Depth BGS (feet)
Skin Friction (psf)
Short Term
Long Term
Fill
Fill
Silt
Sand
UBBC
LBBC
Fill
Rock

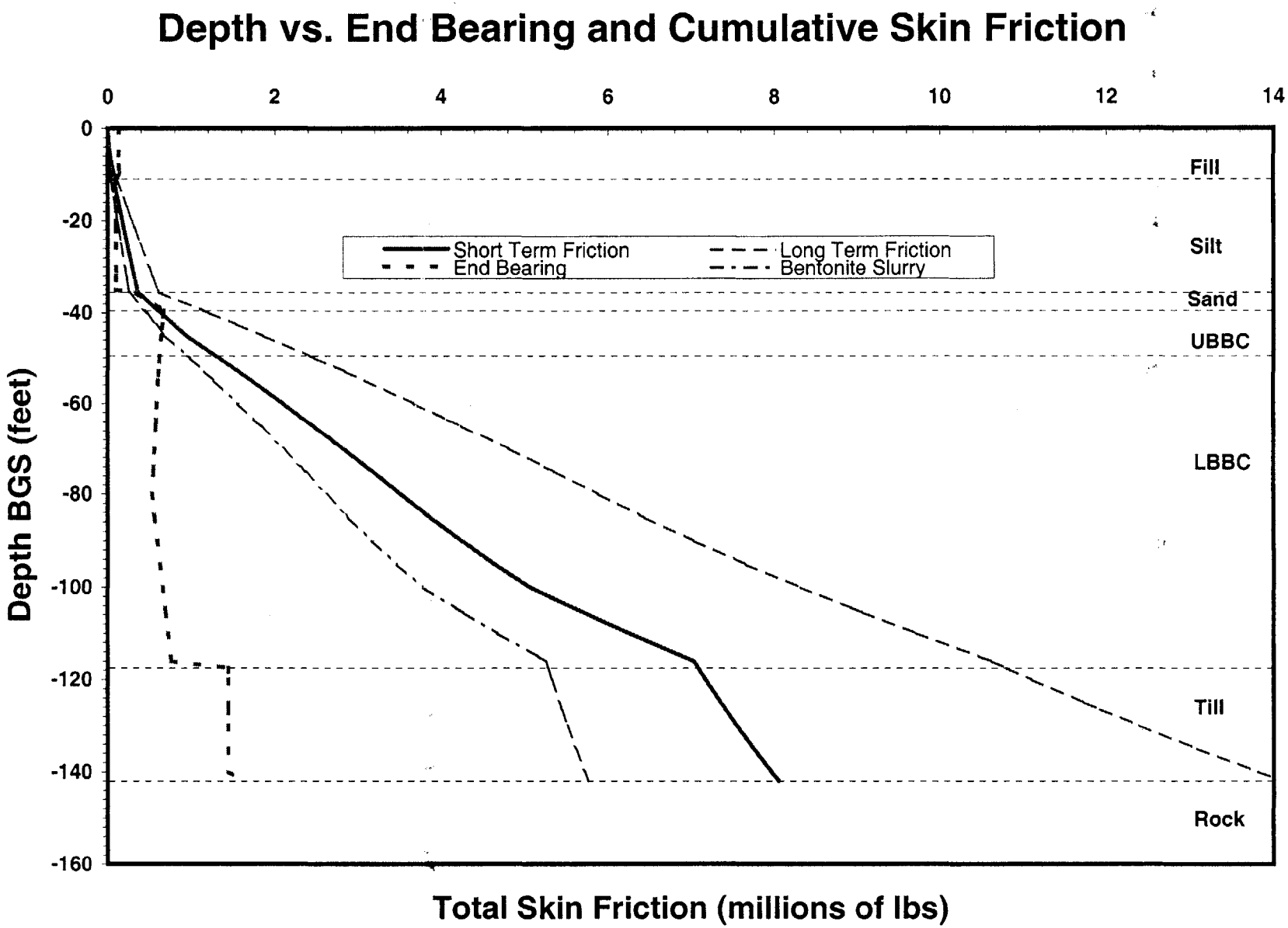
Depth vs. End Bearing and Cumulative Skin Friction
0
2
4
6
8
10
12
14
0
-20
-40
-60
-80
-100
-120
-140
-160
Depth BGS (feet)
Short Term Friction
End Bearing
Long Term Friction
Bentonite Slurry
Fill
Silt
Sand
UBBC
LBBC
Till
Rock
Total Skin Friction (millions of lbs)

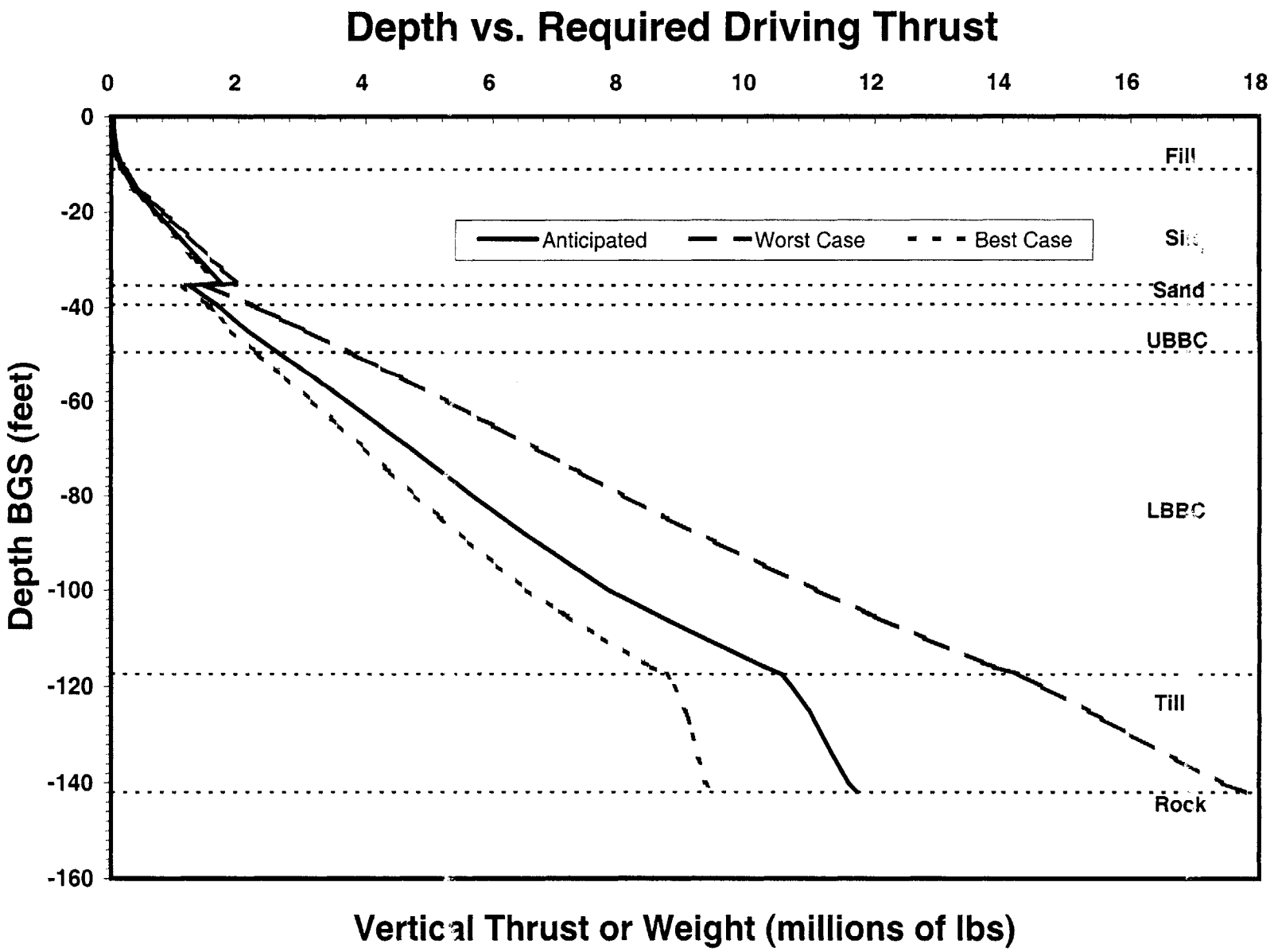
Depth vs. Required Driving Thrust
0
2
4
6
8
10
12
14
16
18
0
-20
-40
-60
-80
-100
-120
-140
-160
Depth BGS (feet)
Anticipated
Worst Case
Best Case
Fill
Silt
Sand
UBBC
LBBC
Till
Rock
Vertical Thrust or Weight (millions of lbs)

Appendix F: Structural Design Calculations

Caisson Design

Appendix F

Spreadsheet page layout

Design Assumptions:

1. Segmental caisson comprised of 10' tall cast-on-surface segments or precast segments.
2. Liner (caisson) constructed with moderate strength concrete, σ_t = σ_t 720000 psf
3. External horizontal pressure (P) on lining equals the in situ horizontal stress σ_{ho}
4. Resulting minimum factor of safety of liner design, F_{liner} = F_{liner} 4.06
5. The liner inner radius, r_i = r_i 12.00 ft
6. Concrete unit weight, γ_C = $\gamma_{CONCRETE}$ 150 pcf
7. Concrete has a modulus of elasticity, E = 580,393,246 psf
8. Steel unit weight γ_{STEEL} 490 pcf
9. Dry unit weight of steel shot ballast, γ_S γ_{SHOT} 345.0 pcf

Wall Design

ft BGS

Segment Depth Interval Top	Bottom	psf MAX σ_{ho} (P)	Minimum Segment t_{liner} (ft) Liner Thickness
0	10	583	0.040
10	20	1,434	0.098
20	30	2,246	0.155
30	40	4,279	0.300
40	50	4,281	0.300
50	60	5,228	0.370
60	70	6,176	0.441
70	80	7,124	0.513
80	90	8,108	0.589
90	100	9,091	0.667
100	110	9,976	0.738
110	120	11,025	0.823
120	130	12,074	0.911
130	140	13,123	1.000

$$t_{liner} = r_i\left(\sqrt{\frac{\sigma_t}{\sigma_t - 2PF_{liner}}} - 1\right)$$

$$t_{liner} = \sqrt{\frac{L_C F}{\pi\sigma_t} + r_i^2} - r_i$$

$$L_C = 1.4(W_M + 0.5W_C + W_B + W_W) + 1.6(W_A + W_L + W_{SS})$$

Max. Weight of Caisson, L_C	30,614,550 lbs
Caisson Wall Concrete σ_t	720,000 psf
Wall Comp. factor of safety, F	1.85
Required Wall Area	78.523 ft²
Required Wall Thickness	1.000 ft

Component Weights

Depth Before Chamber Pressure Applied		8 ft
Estimated Chamber and Roof Height		12 ft
Caisson Length		142 ft
Internal Length		130 ft
Caisson Wall Outer Radius, r_o		13.00 ft
Caisson Wall Inner Radius, r_i		12.00 ft
Caisson Wall Area (concrete)	$A = \pi(r_o^2 - r_i^2)$	78.544 ft
Caisson Wall Dead Weight, W_W		1,672,989 lbs
Mechanical Egress Outer Radius	$W = \gamma HA$	7.00 ft
Mechanical Egress Inner Radius		6.50 ft
Mechanical Egress Wall Area (concrete)		21.206 ft²
Mechanical Egress Wall Dead Weight, W_M		413,513 lbs
Number of Steel Airlocks		2
Steel Airlock Outer Radius		2.75 ft
Steel Airlock Inner Radius		2.67 ft
Steel Airlock Area		1.362 ft²
Steel Airlock Dead Weight, W_A		173544 lbs
Mucklock Length Required for Equilibrium		115.3846154 ft
Steel Mucklock Outer Radius		2.75 ft
Steel Mucklock Inner Radius		2.67 ft
Steel Mucklock Area		1.362 ft²
Steel Mucklock Dead Weight, W_L		86772 lbs
Total Load of Cross Beams (p.123), W_C		46,125 lbs
Total Load of Bulkhead (p.125), W_B		234,559 lbs
Total Weight of Steel Shot (p.123), W_{SS}		17,017,819 lbs

Calculation of Caisson Loadings

$$A_{Locks} = \pi r^2 = \pi 2.75^2 = 23.758\,ft^2$$

$$A_{MECH} = \pi r^2 = \pi 6.5^2 = 132.732\,ft^2$$

$$A_{INT} = A_{MECH} - 3A_{Locks} = 61.458\,ft^2$$

$$A_{ANN} = \pi\left(r_o^2 - r_i^2\right) = \pi\left(12^2 - 7^2\right) = 298.452\,ft^2$$

Steel Shot Porosity

$$n = 1 - \left(\frac{\gamma_{SHOT}}{\gamma_{STEEL}}\right)$$

Saturated Steel Shot Unit Weight

$$\gamma_{SS} = \gamma_{SHOT} + n\gamma_{WATER}$$

Height of A_{INT} and A_{ANN} areas, **H** 130 ft

Iteration Required to find weight of Bulkhead, W_B

$$V = H\left(A_{ANN} + A_{INT}\right)$$

Dead Loads		
Dead Load of Egress Wall, W_M	413,513	lbs
Dead Load of Cross-Beams, W_C	23,063	lbs
Dead Load of Floor/Bulkhead, W_B	234,559	lbs
Dead Load Safety Factor	1.4	
Total Factored Dead Loads on Bulkhead	595,062	lbs

Live Loads		
Live Load of Air and Muck Locks, (W_A + W_L)	260,316	lbs
Live Load of Steel Shot Ballast, W_{SS}	17,017,819	lbs
Live Load Safety Factor	1.6	
Total Factored Live Loads on Bulkhead	27,645,016	lbs
Total Factored Live and Dead Loads on Bulkhead, L_T	28,240,078	lbs

Weight of all components of the caisson (bulkhead, egress walls, half of cross beams, locks, and steel shot)
Weight of caisson external wall and half of cross beams load carried by those walls not included

Cross Beam Group

concrete	Cap Cross Beam Group	Beam Group	
Number of Beams in Group	3	3	
Beam Width	1.00	1.00	ft
Beam Length	5.00	5.00	ft
Beam Depth	4.00	1.50	ft
Beam Volume	20.00	7.50	ft^3
Beam Group Volume	60.00	22.50	ft^3
Number of Beam Groups	1	11	
Total Weight of Beam Groups		37,125	lbs
Weight of Cap Beam Group	9,000		
Total Load of Cross Beams, W_C		46,125	lbs

Absolute Worst Case Bulkhead Loading
(Caisson Full To Top With Saturated Steel Shot)

Saturated Steel Shot Unit Weight, γ_{SS}	364	pcf
Maximum volume of steel shot possible in caisson, V	46,788	ft^3
Maximum weight of Shot on Bulkhead, W_{SS}	17,017,819	lbs
Total Factored Live and Dead Loads, L_T	28,240,078	lbs
Area of Bulkhead, A_B	381.115	ft^2
Design uniform floor load on bulkhead, L_U	74,099	psf
Total Vertical Bulkhead Loading	17,017,819	lbs
Bulkhead Diameter	24	ft
Bulkhead Area	452	ft^2
Bulkhead Perimeter	75.3984	ft

Design of the Bulkhead

Timoshenko (1959) p. 61

Circular plate with circular hole at center, case 10

Strength of reinforcing steel in concr	9,711,726	psf
Factor of safety for steel	1.15	
Equivalent radius of center hole (r_b)	4.76	ft
Radius of plate (r_a)	12.00	ft
a/b	2.5	
q=L_U	74,099	
$\nu_{CONCRETE}$	0.17	

$$M_R = \frac{q}{16}(3+\nu)\left(r_a^2 - r_b^2\right)$$

M_R for concrete	1,769,724	ft-lbs

From Christian Meyer (design of simply supported beam p.165)

$A_S = \rho bd$ ρ = % of steel by section area $A_{EQ} = MA_S$

$$a = \frac{A_S f_y}{0.85 f_C' b} \qquad M_U = \phi A_S f_y \left(d - \frac{A_S f_y}{1.7 f_C' b}\right)$$

$$I = \frac{\left(ba^2\right)}{12} + \left(ba\left(\frac{a}{2}\right)^2\right) + \left(A_{EQ}(d-a)^2\right) \qquad \sigma_{MAX} = \frac{M_{ULT} a}{I}$$

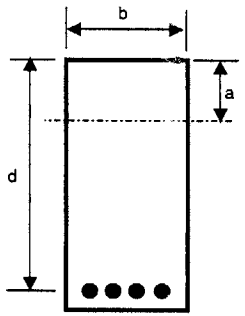

Total Factored Loads on Slab	17,017,819	lbs
Bulkhead Perimeter to Resist Shear	75.3984	feet
Shear Force per Foot of Perimeter	225705.3094	lbs/ft
Concrete compressive strength (f_C')	5000	psi
Steel yield strength (f_Y)	65,000	psi
Beam width (b)	12	inches
ϕ	0.9	
M	7	

	T_B			Meyer Beam Cap	Timoshenko				psi	
	inches	in2	inches	in-lb	in-lb					
ρ	**d**	**A_S**	**a (eq. 4.9)**	**M_{ULT} (eq. 4.9a)**	**M_R (Timoshenko)**	**Difference**	**A_{EQ}**	**I**	**σ_{MAX}**	
0.035	38.3	16.0817	20.4963	26,381,106	21,236,690	24.22%	112.572	70083.41392	7715.319531	Insufficient
0.035	34.3	14.3864	18.3356	21,112,176	21,236,690	-0.59%	100.705	50173.59988	7715.319531	Insufficient
0.03	40.3	14.5151	18.4997	26,382,539	21,236,690	24.23%	101.606	73701.32037	6622.240136	Insufficient
0.03	36.1	12.9833	16.5473	21,107,805	21,236,690	-0.61%	90.883	52743.0192	6622.240136	Insufficient
0.025	43.1	12.9347	16.4854	26,387,807	21,236,690	24.26%	90.543	82131.87088	5296.539575	Insufficient
0.025	38.6	11.5693	14.7452	21,110,643	21,236,690	-0.59%	80.985	58770.44311	5296.539575	Insufficient
0.02	**47.1**	**11.3043**	**14.4074**	**26,384,195**	**21,236,690**	**24.24%**	**79.130**	**96542.88423**	3937.400465	Sufficient
0.02	42.1	10.1118	12.8876	21,111,405	21,236,690	-0.59%	70.783	69100.34147	3937.400465	Sufficient
0.015	53.2	9.5732	12.2012	26,368,665	21,236,690	24.17%	67.013	119822.7734	2685.038701	Sufficient
0.015	47.6	8.5650	10.9162	21,107,200	21,236,690	-0.61%	59.955	85812.99983	2685.038701	Sufficient
0.01	63.8	7.6552	9.7566	26,383,696	21,236,690	24.24%	53.586	160183.9015	1606.997126	Sufficient
0.01	57.1	6.8466	8.7261	21,104,799	21,236,690	-0.62%	47.927	114600.6886	1606.997126	Sufficient

Design of the Bulkhead (cont')

Thickness of Reinforced Steel Floor/Bulkhead

(using max moment of Timoshenko and simplified beam calcs of Meyer)
2% Steel by Section Area

Bulkhead Thickness, T_B	4 feet
No. of #8 rebar	14
No. of #10 rebar	9
No. of #12 rebar	6
No. of #14 rebar	5

Rebar	in^2	Number
8	0.785	14
10	1.230	9
12	1.767	6
14	2.405	5

steel	2%
Unit Weight of Bulkhead	156.8 pcf
Total Dead Load of Bulkhead, W_B	234,559 lbs

Airlock and Mucklock Wall Design

Maximum Possible Height of Steel Shot Ballast, H_{SHOT}	130 ft	$\sigma_V = \gamma_{SHOT} H_{SHOT}$
Maximum Vertical Pressure of Shot at Bulkhead, σ'_V	44,850 psf	
Assumed Steel Shot Friction Angle (after sand), ϕ	30 degrees	$t = a\left(\sqrt{\frac{\sigma_t}{\sigma_t - 2PF}} - 1\right)$
Resulting K_O of Steel Shot	0.500	
Maximum Horizontal Pressure on Airlock Walls, σ'_H	22,425 psf	Lame' Equation
Airlock Steel Wall Yield Strength, σ_t	2,900,000 psf	
Airlock Factor of Safety	2	$K_O = 1 - \sin\phi$
Inner Radius of Airlock Wall, **a**	2.67 ft	
Thickness of Steel Airlock Wall Required, t	0.042 ft	$\sigma_H' = K_O \sigma_V'$
Thickness of Steel Airlock Wall Required, t	0.507 inches	

Airlock Wall 1" Thick Has Sufficient Thickness to Overcome Lateral Loading of Steel Shot

Airlock and Mucklock Wall Design

$$W = W_W + W_M + W_A + W_L + W_B + W_C$$

Worst Case		
Full Lateral Loading and Friction		
Total Weight of Caisson Structure, W	2,627,502	lbs
Maximum Required Thrust for Caisson Driving, T_{MAX}	17,777,422	lbs
Maximum Weight of Ballast Required for Driving, (T_{MAX} - W_C)	15,149,919	lbs
Mechanical Shaft Area Minus Locks	61.458	ft^2
Height of Steel Shot Dead Weight in Center Shaft	100.0	ft
Maximum Dead Load of Steel Shot in Center Shaft	2,120,285	lbs
Maximum Pressure of Steel Shot in Center Shaft	34,500	psf
Remaining Weight of Ballast Required In Annulus	13,029,634	lbs
Caisson Interal Annulus Area	298.452	ft^2
Maximum Pressure of Ballast on Floor of Annulus	43,657	psf
Steel Shot Ballast Unit Weight	345	pcf
Maximum Height of Ballast in Annulus	126.5	ft
Factor of Safety of Mechanical Egress Wall	2.00	
Maximum Lateral Force on Mechanical Egress Wall	24,796	psf
Ballast Minimum Angle of Friction	28.94	degrees

Anticipated Working Friction (neglects bentonite)		
Construction Lateral Loading and Friction		
Total Weight of Caisson Structure, W	2,627,502	lbs
Maximum Required Thrust for Caisson Driving, T_{MAX}	11,723,136	lbs
Maximum Weight of Ballast Required for Driving, (T_{MAX} - W_C)	9,095,633	lbs
Mechanical Shaft Area Minus Locks	61.458	ft^2
Height of Steel Shot Dead Weight in Center Shaft	60.0	ft
Maximum Dead Load of Steel Shot in Center Shaft	1,272,171	lbs
Maximum Pressure of Steel Shot in Center Shaft	20,700	psf
Remaining Weight of Ballast Required In Annulus	7,823,462	lbs
Caisson Interal Annulus Area	298.452	ft^2
Maximum Pressure of Ballast on Floor of Annulus	26,213	psf
Steel Shot Ballast Unit Weight	345	pcf
Maximum Height of Ballast in Annulus	76.0	ft
Factor of Safety of Mechanical Egress Wall	2.00	
Maximum Lateral Force on Mechanical Egress Wall	24,796	psf
Ballast Minimum Angle of Friction	28.94	degrees

Loading Shot to Equal Heights on Each Side of Mechanical Egress Wall Minimizes This Pressure

APPENDIX G: Ballasting and Simplified Settlement

Section Design

Appendix G

Spreadsheet page layout

Cross Beam Group Spacing	10.5 ft O.C.	
Height of Topside Egress Connector	7.5 ft O.C.	
Height of Beam Groups	1.5 ft	
Caisson surface exposure when next segment is placed		4 ft

Segment Dimensioning and Numbering

Determination of Caisson Segment Lengths

Caisson Features	ft **Bottom**	ft **Distance From Tip Top**	ft **Center**	ft **Section Joints**	ft **Segment Length, L**	**Section Number**
Cap Cross Beams	138.0	142.0	140.0	142.0	11.5	13
Cross Beam Group 11	129.0	130.5	129.8	130.5	10.5	12
Cross Beam Group 10	118.5	120.0	119.3	120.0	10.5	11
Cross Beam Group 9	108.0	109.5	108.8	109.5	10.5	10
Cross Beam Group 8	97.5	99.0	98.3	99.0	10.5	9
Cross Beam Group 7	87.0	88.5	87.8	88.5	10.5	8
Cross Beam Group 6	76.5	78.0	77.3	78.0	10.5	7
Cross Beam Group 5	66.0	67.5	66.8	67.5	10.5	6
Cross Beam Group 4	55.5	57.0	56.3	57.0	10.5	5
Cross Beam Group 3	45.0	46.5	45.8	46.5	10.5	4
Cross Beam Group 2	34.5	36.0	35.3	36.0	10.5	3
Cross Beam Group 1	24.0	25.5	24.8	25.5	13.5	2
Library 10th Level El.		17.0				
Bulkhead	8.0	12.0	10.0	12.0	12.0	1
Pneumatic Chamber	0.0	8.0	4.0			

Calculated Weights and Volumes for Ballast Estimation

Ballast Estimation found on spreadsheet pages 131-133

	Cap Beam Group	**Beam Group**	
No. of Beams	3	3	
Beam Width	1.00	1.00	ft
Beam Length	5.00	5.00	ft
Beam Depth	4.00	1.50	ft
Beam Volume	20.00	7.50	ft^3
Group Volume	60.00	22.50	ft^3

Height Above Bulkhead	130	ft
Weight of Steel Shot, γ_{SHOT}	345	pcf
Weight of Beam Group, W_C	3,375	lbs
Volume of Beam Group, V_C	22.50	ft^3
Volume of Stair Annulus, A_{ANN}	298.45	ft^3/ft
Annular Space between locks, A_{INT}	61.46	ft^3/ft
Weight of Caisson Wall, W_W	11,782	lbs/ft
Weight of Egress Wall, W_M	3,181	lbs/ft
Weight of Bulkhead, W_B	234,559	lbs
Weight of Lock Pipe	667	lbs/ft
Length of Airlock Pipe Section	12	ft
Lock Extension Pipe Weight, W_{LE}	8,010	lbs
Length of Air and Muck Locks, H_L	24	ft
Weight per Lock, W_L	16,019	lbs
Number of Locks, N_L	3	
Cap Cross Beams, W_{CC}	9,000	lbs
Cap Cross Beams Volume, V_{CC}	60.00	ft^3

Simple Settlement Calculation

$$\rho_{MAX} = \frac{H_C \pi \left(r_i^{\,2} - (r_c - t)^2 \right)}{\pi \left(r_i^{\,2} - r_c^{\,2} \right)}$$

			15	20	25	30	50	100
		ft^3			**Building 62**			
in	ft	**Resulting**	r_i = 15ft	r_i = 20ft	r_i = 25ft	r_i = 30ft	r_i = 50ft	r_i = 100ft
t	**t**	**Void**	ρ_{MAX}	ρ_{MAX}	ρ_{MAX}	ρ_{MAX}	ρ_{MAX}	ρ_{MAX}
0	0.000	0.000	0.000	0.000	0.000	0.000	0.000	0.000
0.0625	0.005	59.571	4.063	0.985	0.499	0.311	0.098	0.023
0.125	0.010	119.167	8.128	1.970	0.998	0.623	0.195	0.046
0.1875	0.016	178.786	12.195	2.956	1.498	0.934	0.293	0.069
0.25	**0.021**	**238.429**	**16.263**	**3.943**	**1.997**	**1.246**	**0.391**	**0.093**
0.3125	0.026	298.096	20.333	4.929	2.497	1.558	0.488	0.116
0.375	0.031	357.787	24.404	5.916	2.997	1.870	0.586	0.139
0.4375	0.036	417.501	28.477	6.904	3.497	2.182	0.684	0.162
0.5	0.042	477.240	32.552	7.891	3.998	2.494	0.782	0.185
0.5625	0.047	537.002	36.628	8.880	4.498	2.806	0.880	0.209
0.625	0.052	596.788	40.706	9.868	4.999	3.118	0.978	0.232
0.6875	0.057	656.598	44.786	10.857	5.500	3.431	1.076	0.255
0.75	0.063	716.432	48.867	11.847	6.001	3.744	1.174	0.278
0.8125	0.068	776.290	52.950	12.836	6.503	4.056	1.272	0.302
0.875	0.073	836.171	57.035	13.827	7.004	4.369	1.370	0.325
0.9375	0.078	896.077	61.121	14.817	7.506	4.682	1.468	0.348
1	0.083	956.006	65.208	15.808	8.008	4.995	1.567	0.371

r_C 13 ft

H_C is the height of the caisson

H_C = 140 ft

r_c is the radius of the caisson

r_i is the radius of settlement influence

t is the cutting edge thickness

V is the volume of the annulus behind the cutting edge

ρ_{MAX} soil settlement in a radius of influence into a void created by cutting edge

Nearest structure (Building 62) is at a radius of 25 feet from the caisson centerline

Calculation shows max amount of settlement (assumes no change in soil volume)

Calculation is considered a long term maximum estimate

Void filled with bentonite slurry helps keep it open until sinking complete

A 0.25 Inch wide cutting edge was selected

Ballast Estimation

Weights and Volumes from p.129

Continued on page 132 ⟶

Section Number	ft **Section Length** **L (from p.128)**	ft **Length Above Bulkhead**	lbs **Empty Weight** W_{SEG}	lbs **Locks** W_{LOCKS}	ft **Tot. Length of Locks** H_B	ft^3 **Addl. Vol. For Steel Shot** $V_{SEG-SHOT}$
1	12.0	0.0	375,939	0	0	0
2	13.5	13.5	205,369	48,058	24	4,836
3	10.5	24.0	160,481	0	24	3,757
4	10.5	34.5	160,481	24,029	36	3,757
5	10.5	45.0	160,481	24,029	48	3,757
6	10.5	55.5	160,481	24,029	60	3,757
7	10.5	66.0	160,481	24,029	72	3,757
8	10.5	76.5	160,481	24,029	84	3,757
9	10.5	87.0	160,481	24,029	96	3,757
10	10.5	97.5	160,481	24,029	108	3,757
11	10.5	108.0	160,481	0	108	3,757
12	10.5	118.5	160,481	24,029	120	3,757
13	11.5	130.0	181,069	24,029	132	4,079

$$W_{SEG1} = L(W_W + W_B) \qquad W_{SEG13} = L(W_W + W_M) + W_{CC} \qquad W_{LOCKS} = N_L W_L + N_L W_{LE} \frac{(H_B - H_L)}{12}$$

$$W_{SEG2-12} = L(W_W + W_M) + W_C \qquad V_{SEG-SHOT} = \sum L_{SEG} (A_{ANN} + A_{INT}) - \{V_C : V_{CC}\}$$

W_{SEG1} is the weight of caisson segment 1

$W_{SEG2-12}$ is the weight of caisson segments 3 through 12

W_{SEG13} is the weight of caisson segment 13

W_{LOCKS} is the weight of weight of additional locks or pipe extensions required with that segment

$V_{SEG-SHOT}$ is the volumetric capacity of the segment available to hold steel shot ballast

Ballast Estimation (cont')

Continued from page 131

Continued on page 133

lbs **Addl. Weight of Ballast Available** $W_{SEG-SHOT}$	ft^3 **Tot. Vol. Avail. for Steel Shot** V_{SHOT}	lbs **Caisson Total Empty Weight** W_C	lbs **Tot. Weight of Ballast Available** W_{SHOT}	ft **Excavation Face Depth**	lbs **Thrust Minimum** TR_{BENT}
0	0	375,939	0	-8.0	53,305
1,668,516	4,836	629,366	1,668,516	-21.5	738,294
1,296,010	8,593	789,847	2,964,526	-32.0	1,425,327
1,296,010	12,349	974,357	4,260,536	-42.5	1,711,349
1,296,010	16,106	1,158,867	5,556,546	-53.0	2,579,460
1,296,010	19,862	1,343,377	6,852,556	-63.5	3,460,334
1,296,010	23,619	1,527,888	8,148,565	-74.0	4,310,949
1,296,010	27,376	1,712,398	9,444,575	-84.5	5,153,543
1,296,010	31,132	1,896,908	10,740,585	-95.0	6,079,373
1,296,010	34,889	2,081,418	12,036,595	-105.5	7,190,894
1,296,010	38,645	2,241,899	13,332,605	-116.0	8,497,423
1,296,010	42,402	2,426,410	14,628,615	-126.5	9,066,188
1,407,241	46,481	2,631,507	16,035,856	-138.0	9,438,937

$W_{SEG-SHOT} = \gamma_{SHOT} V_{SEG-SHOT}$ $V_{SHOT} = \sum V_{SEG-SHOT}$ $W_{SHOT} = \sum W_{SEG-SHOT}$ **Appendix E**

$W_C = \sum (W_{SEG} + W_{LOCKS})$

Weights and Volumes from p.129

$W_{SEG-SHOT}$ is the weight of steel shot ballast that the segment is capable of holding

V_{SHOT} is the total volumetric capacity of the assembly of the caisson available to hold steel shot ballast

W_{SHOT} is the total weight of steel shot ballast that can be held by the caisson assembly

W_C is the empty weight of the caisson assembly (empty segments and locks) without ballast

$V_{REQ-MIN}$ is the volume of steel shot ballast needed to meet the minimum thrust requirement

$V_{REQ-MAX}$ is the volume of steel shot ballast needed to meet the maximum thrust requirement (p.133)

$$V_{REQ-MAX} = \frac{TR_{MAX} - W_C}{\gamma_{SHOT}}$$

$H_{MAX-MIN}$ is the maximum height of steel shot ballast in the lock annulus (INT) for the minimum thrust requirement (p.133)

$H_{MAX-MAX}$ is the maximum height of steel shot ballast in the lock annulus (INT) for the maximum thrust requirement (p.133)

$H_{INT-MIN}$ is the estimated height of steel shot ballast in the lock annulus (INT) to meet the minimum thrust requirement (p.133)

Ballast Estimation (cont')

Continued from page 132

lbs Thrust Maximum TR_{HIGH}	$\frac{TR_{HIGH}}{\gamma_{SHOT}} < V_{SHOT}$ MAX Drivable	ft_3 MIN Ballast $V_{REQ-MIN}$	ft_3 MAX Ballast $V_{REQ-MAX}$	MINIMUM CASE ft Height in Lock Annulus $H_{INT-MIN}$	MINIMUM CASE ft Height in Caisson Annulus $H_{INT-MAX}$	MAXIMUM CASE ft Height in Lock Annulus $H_{ANN-MIN}$	MAXIMUM CASE ft Height in Caisson Annulus $H_{ANN-MAX}$
95,900	YES	-935	-812	-2.6	-2.6	-2.3	-2.3
928,984	YES	316	868	0.9	0.9	2.4	2.4
1,737,161	YES	1,842	2,746	5.1	5.1	7.6	7.6
2,673,966	YES	2,136	4,926	5.9	5.9	13.7	13.7
4,263,759	YES	4,118	9,000	11.4	11.4	25.0	25.0
5,786,104	YES	6,136	12,877	17.0	17.0	35.8	35.8
7,245,186	YES	8,067	16,572	22.4	22.4	46.0	46.0
8,678,600	YES	9,974	20,192	27.7	27.7	56.1	56.1
10,266,393	YES	12,123	24,259	33.7	33.7	67.4	67.4
11,994,107	YES	14,810	28,732	41.1	41.1	79.8	79.8
13,865,499	YES	18,132	33,692	50.4	50.4	93.6	93.6
15,543,138	YES	19,246	38,020	53.5	53.5	100.0	106.8
17,777,422	YES	19,732	43,901	54.8	54.8	100.0	126.5

Appendix E

$$V_{REQ-MIN} = \frac{TR_{BENT} - W_C}{\gamma_{SHOT}}$$

when $H_{INT} < H_{MAX}$

$$H_{INT-MIN} = H_{ANN-MIN} = \frac{V_{REQ-MIN}}{A_{ANN} + A_{INT}}$$

when $H_{INT-MAX} = H_{MAX-MAX}$

$$H_{ANN-MIN} = \frac{V_{REQ-MIN} - (H_{MAX} A_{INT})}{A_{ANN}}$$

$H_{MAX-MIN}$ 60 ft

$H_{MAX-MAX}$ 100 ft

$$H_{INT-MAX} = H_{ANN-MAX} = \frac{V_{REQ-MAX}}{A_{ANN} + A_{INT}}$$

$$H_{ANN-MAX} = \frac{V_{REQ-MAX} - (H_{MAX} A_{INT})}{A_{ANN}}$$

Weights and Volumes from p.129

$H_{INT-MAX}$ is the estimated height of steel shot ballast in the lock annulus (INT p.129) to meet the maximum thrust requirement

$H_{ANN-MIN}$ is the estimated height of steel shot ballast in the stairwell annulus (ANN p.129) to meet the minimum thrust requirement

$H_{ANN-MAX}$ is the estimated height of steel shot ballast in the stairwell annulus (ANN p.129) to meet the maximum thrust requirement

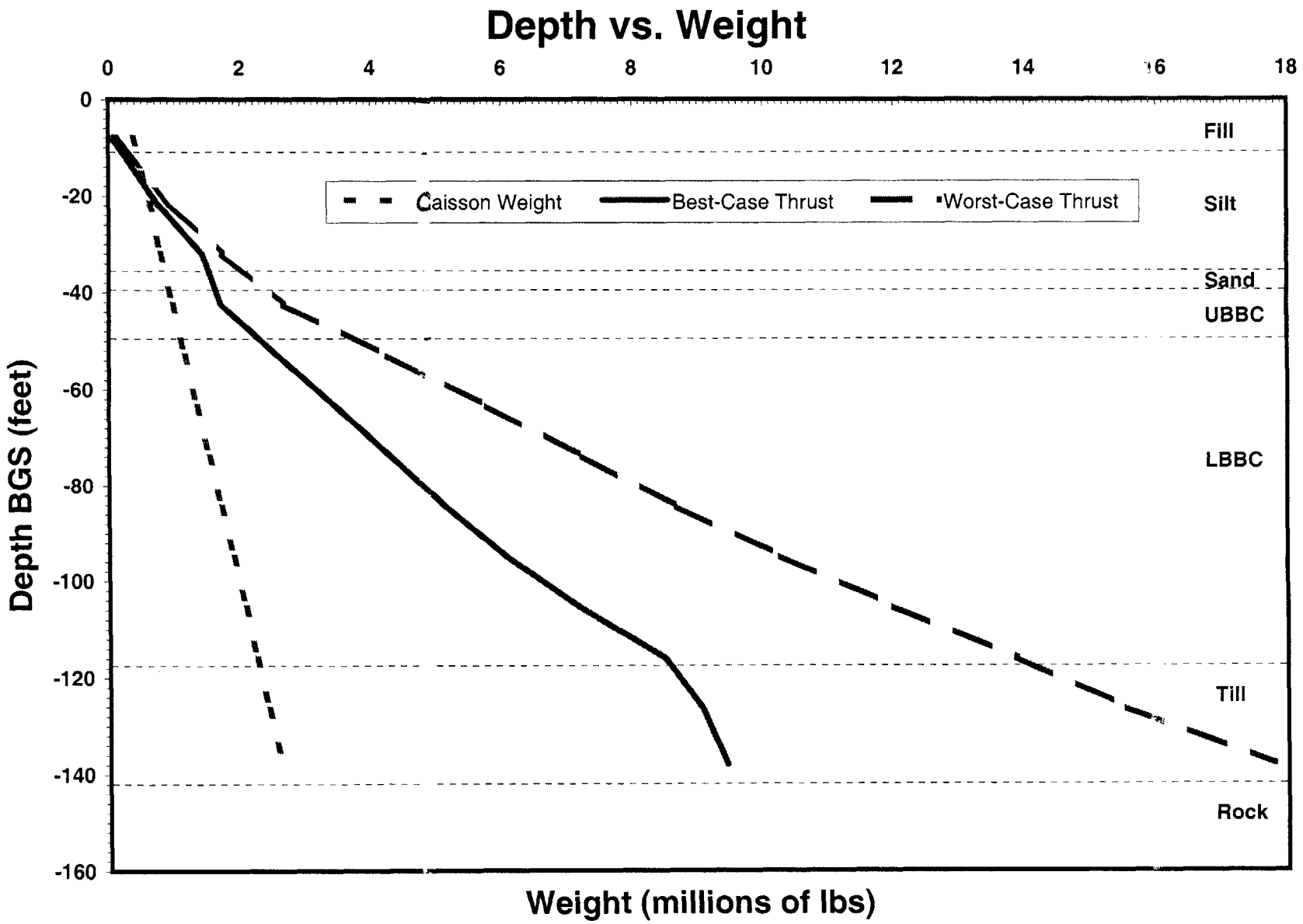
Depth vs. Weight
0
2
4
6
8
10
12
14
16
18
0
-20
-40
-60
-80
-100
-120
-140
-160
Depth BGS (feet)
Caisson Weight
Best-Case Thrust
Worst-Case Thrust
Fill
Silt
Sand
UBBC
LBBC
Till
Rock
Weight (millions of lbs)

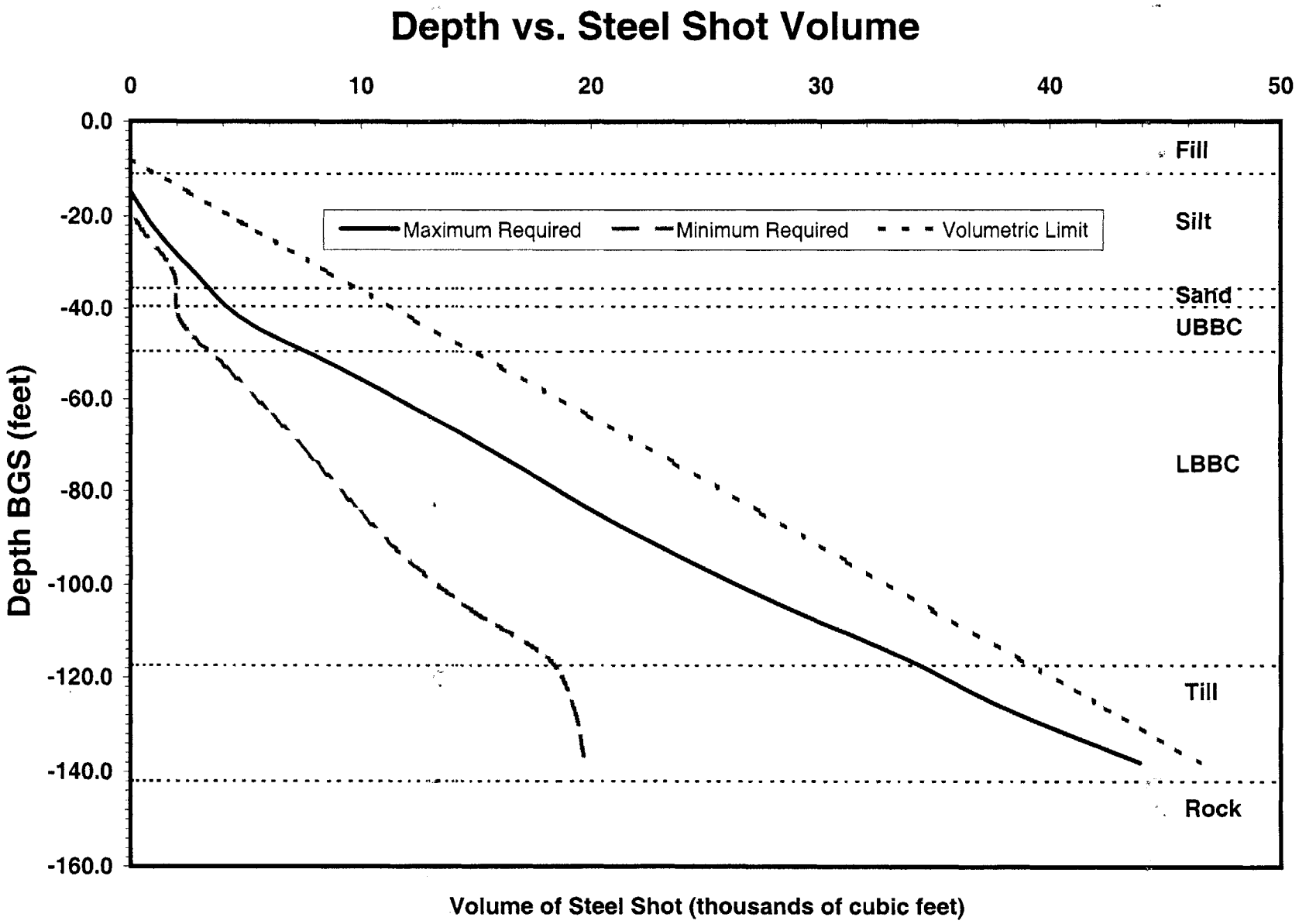
Depth vs. Steel Shot Volume
0
10
20
30
40
50
0.0
-20.0
-40.0
-60.0
-80.0
-100.0
-120.0
-140.0
-160.0
Depth BGS (feet)
Maximum Required
Minimum Required
Volumetric Limit
Fill
Silt
Sand
UBBC
LBBC
Till
Rock
Volume of Steel Shot (thousands of cubic feet)

Appendix H: Pneumatic Caisson Plans and Drawings

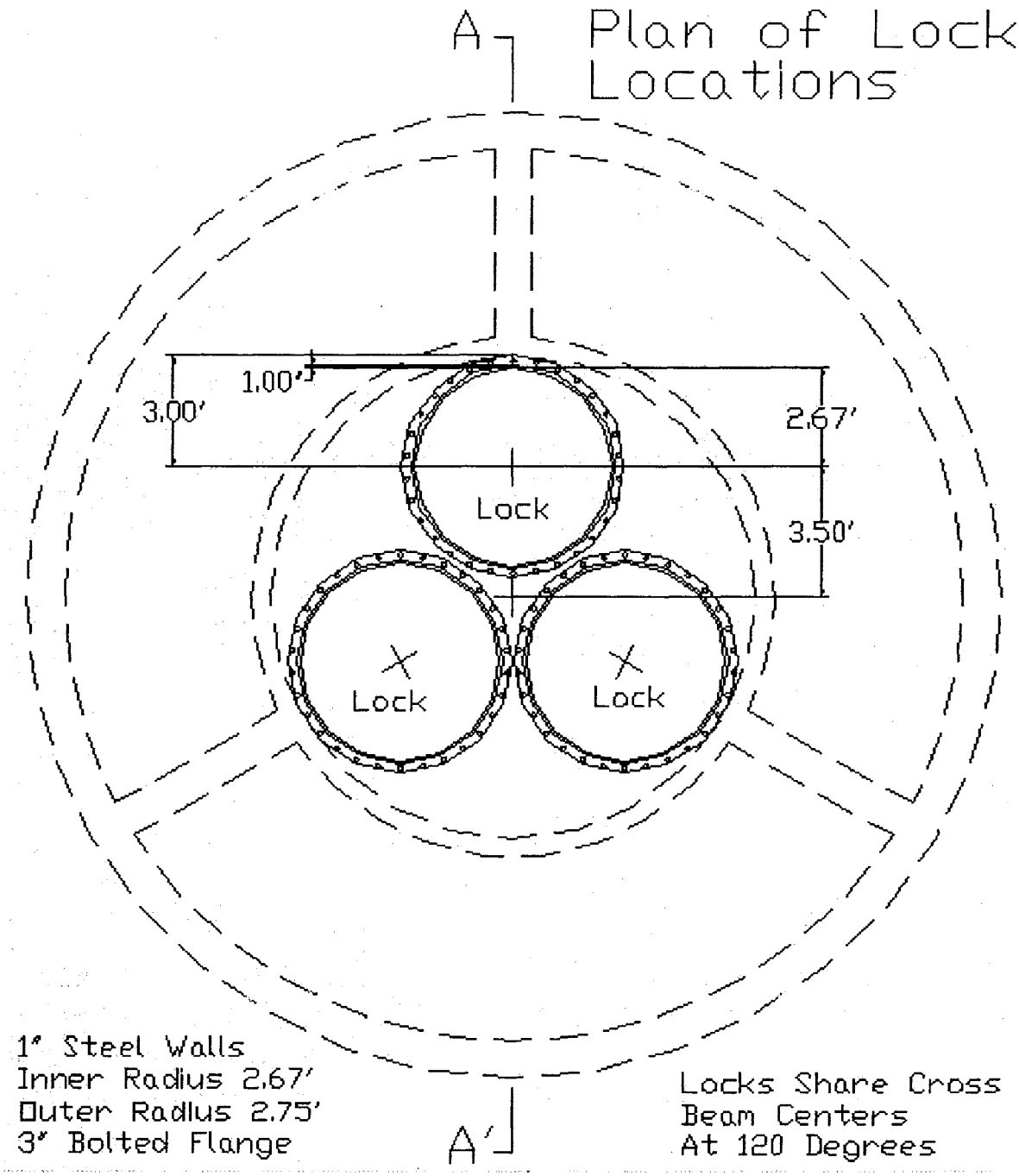
A
Plan of Lock Locations
1.00'
3.00'
2.67'
3.50'
Lock
Lock
Lock
A'
1" Steel Walls
Inner Radius 2.67'
Outer Radius 2.75'
3" Bolted Flange
Locks Share Cross Beam Centers At 120 Degrees

Cutting Edge Detail

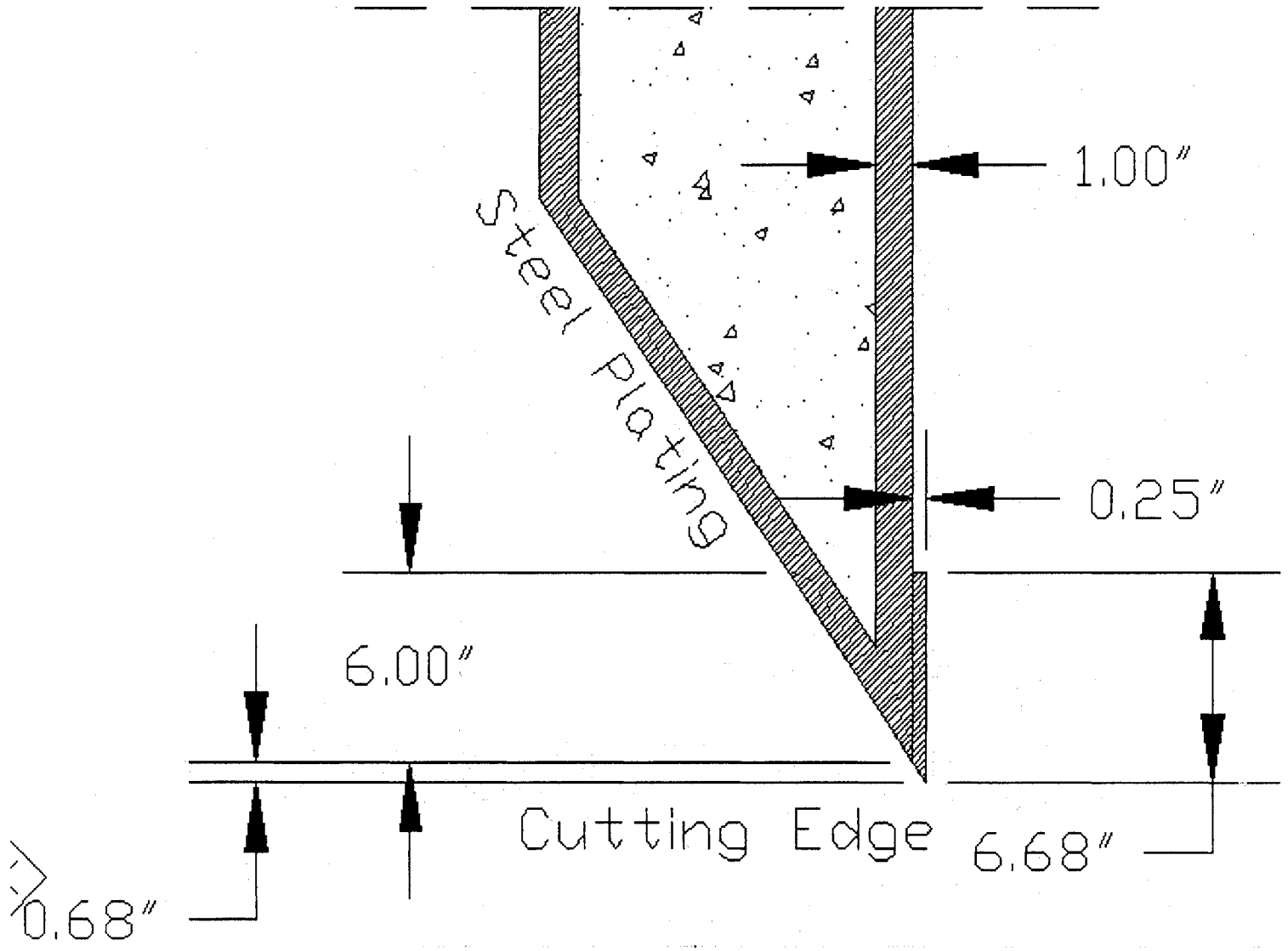

Section 1 - Pneumatic Chamber

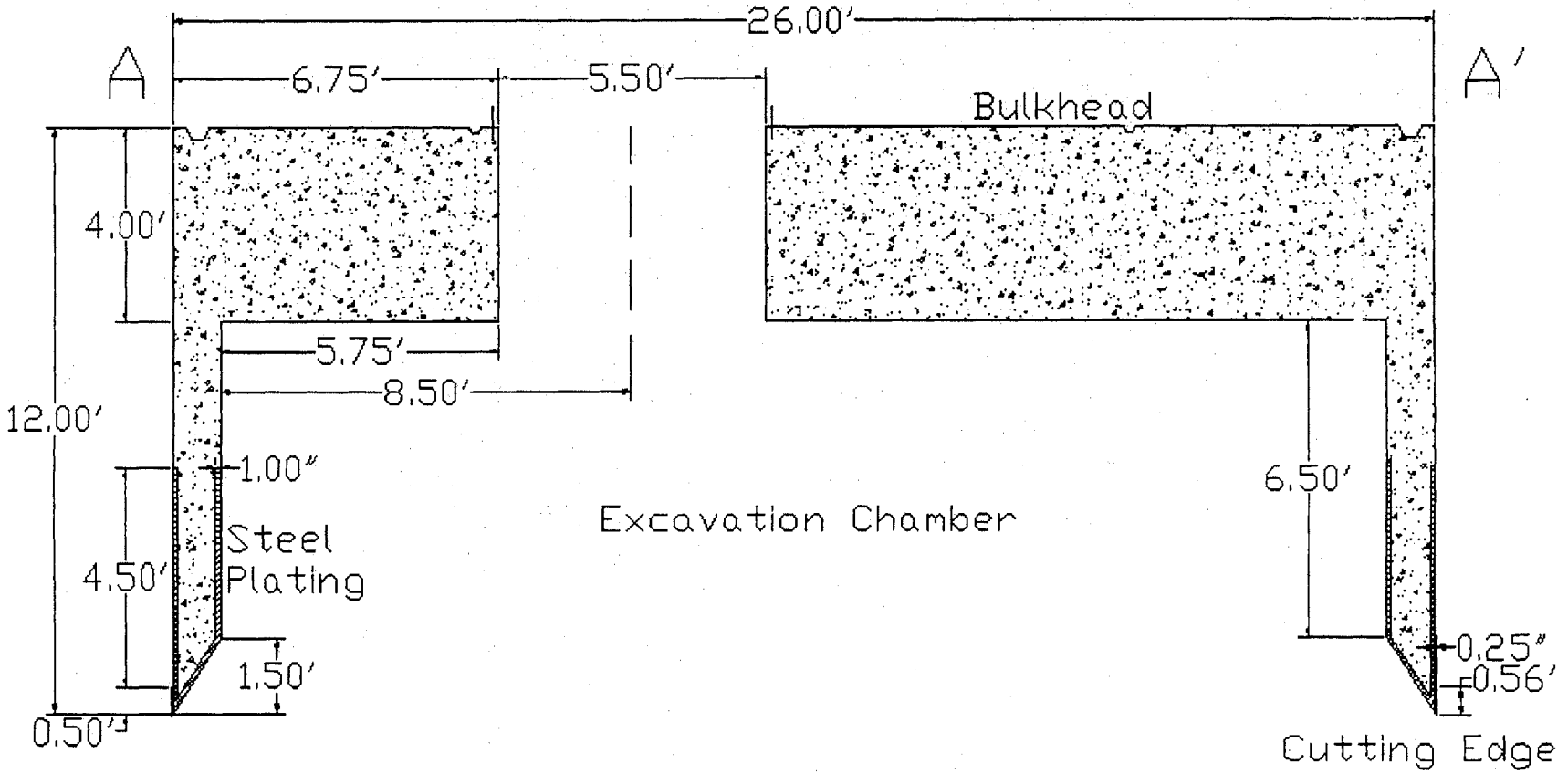

A
Section 1 Plan
2.75'
3.50'
26.00'
A'
Cutouts Spaced 120 Degrees
3.50' From Caisson Center
Joint Grooves Also Shown

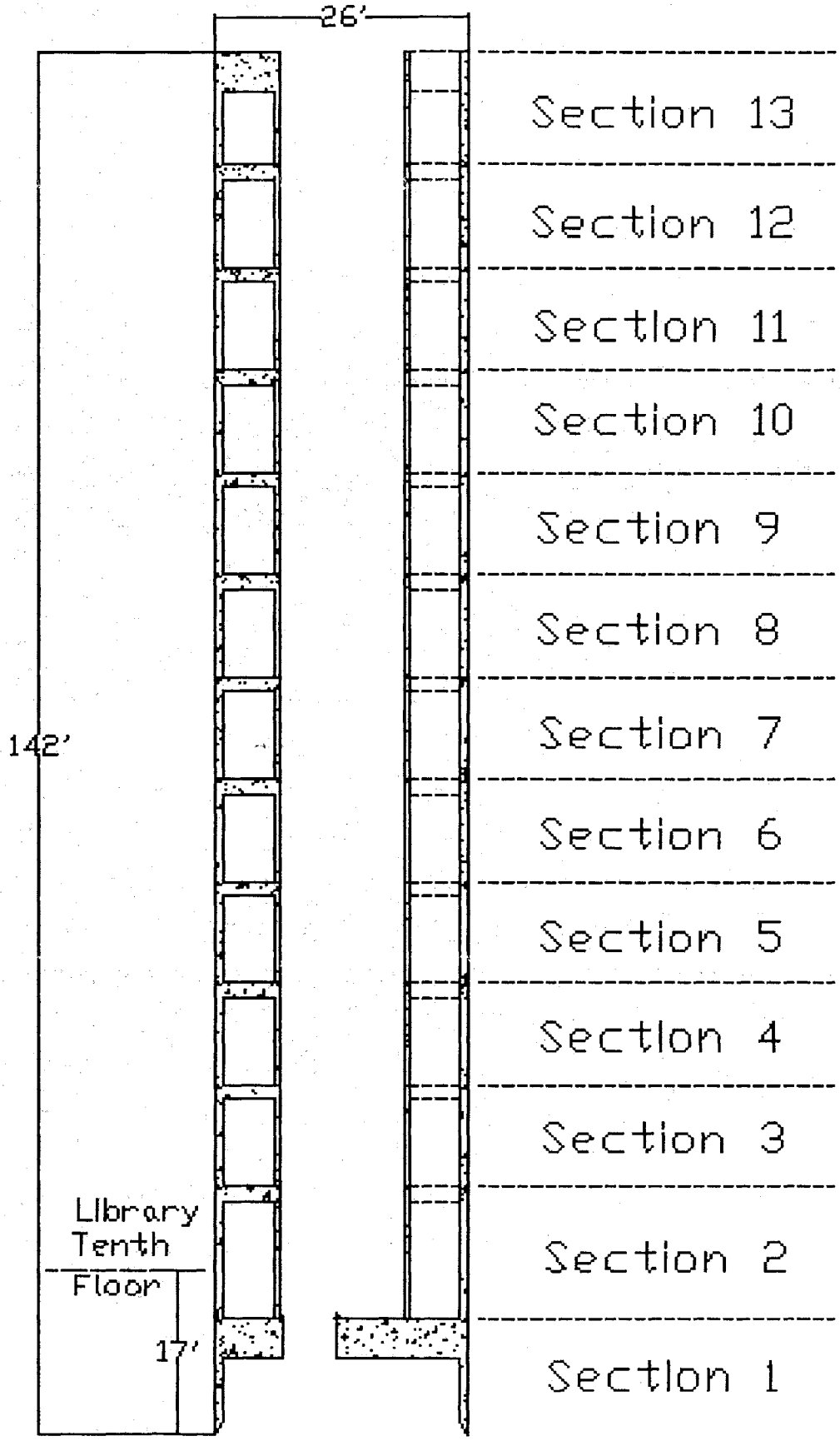
26'
142'
Section 13
Section 12
Section 11
Section 10
Section 9
Section 8
Section 7
Section 6
Section 5
Section 4
Section 3
Section 2
Section 1
Library
Tenth
Floor
17'

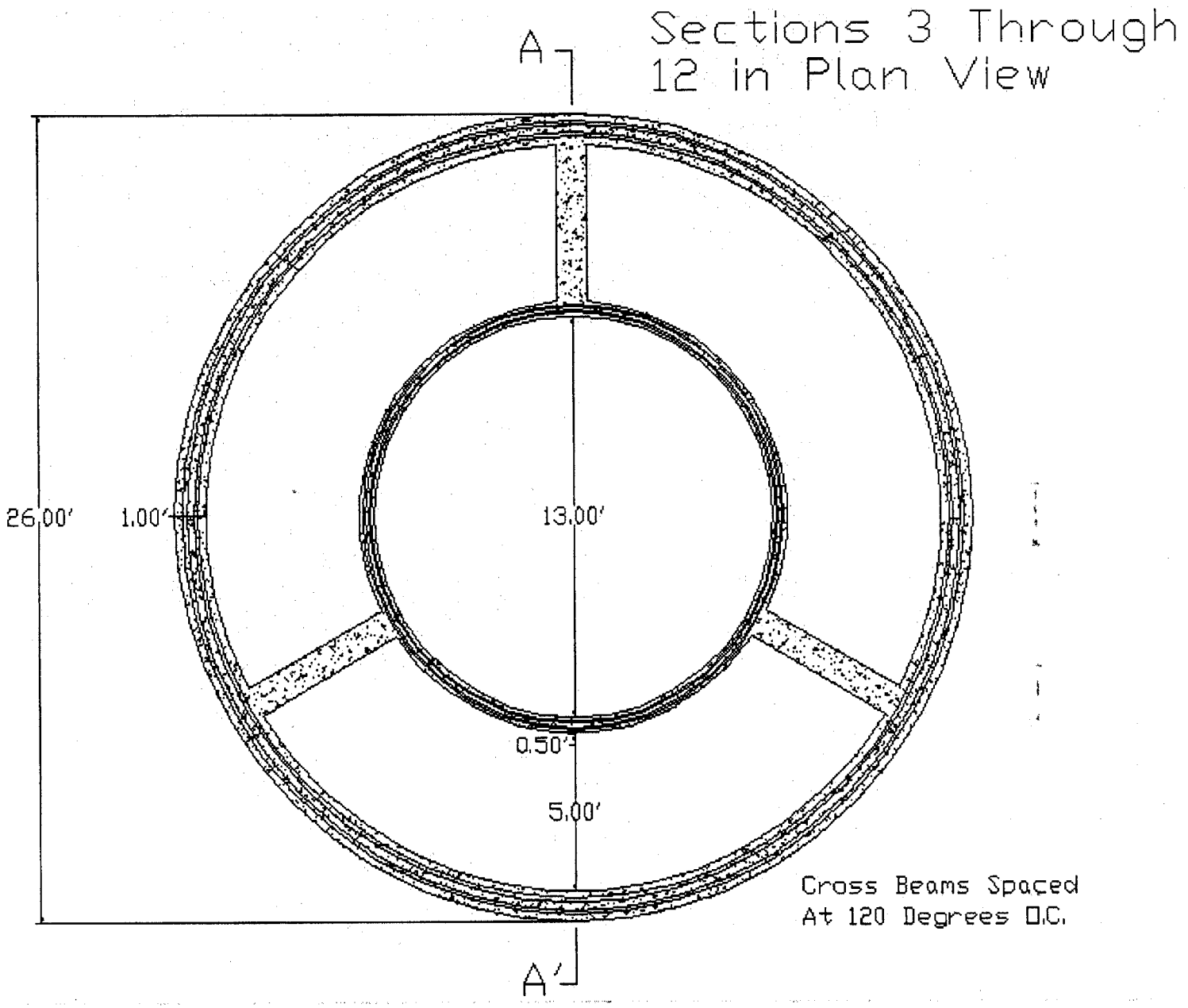
Sections 3 Through
12 in Plan View
A
A'
26.00'
1.00'
13.00'
0.50'
5.00'
Cross Beams Spaced
At 120 Degrees O.C.

Sections 3 through 12

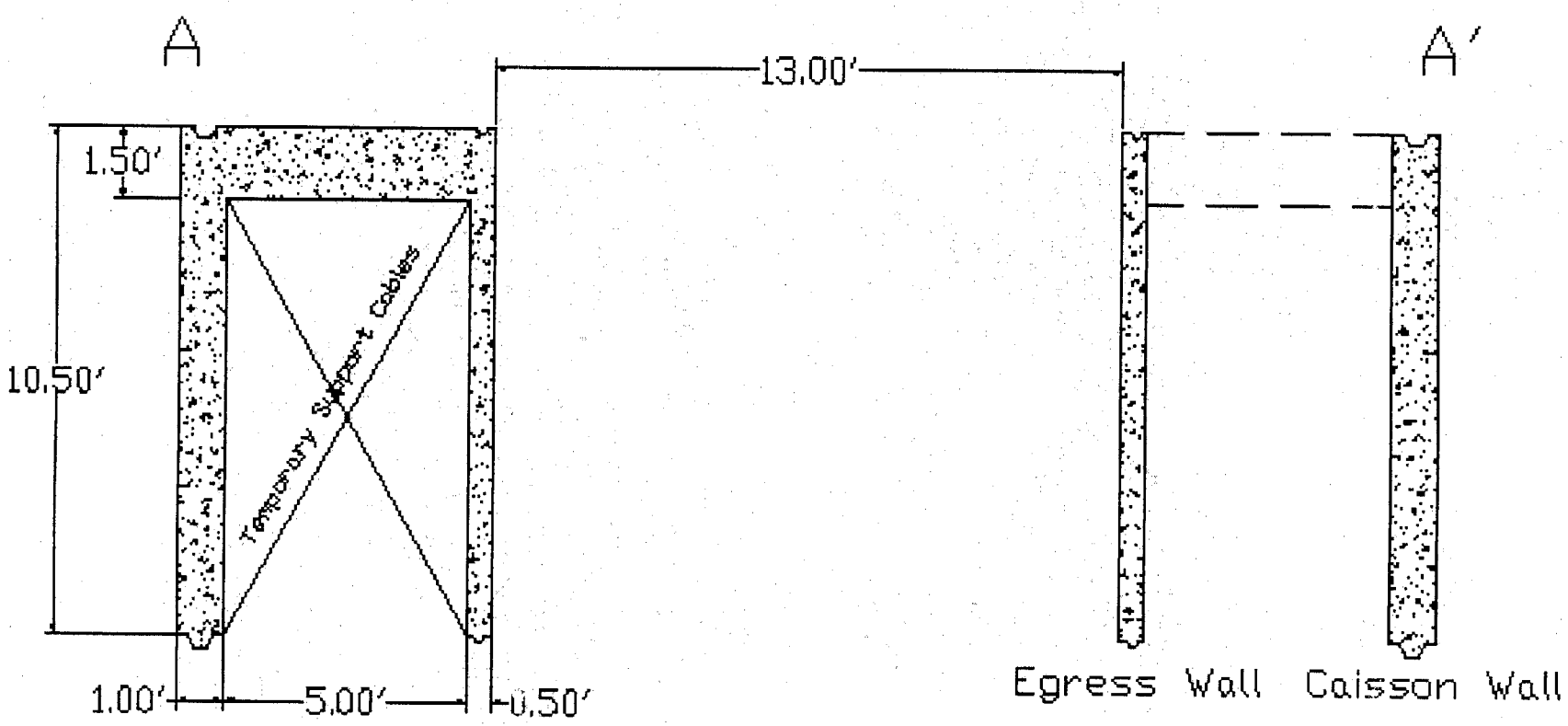

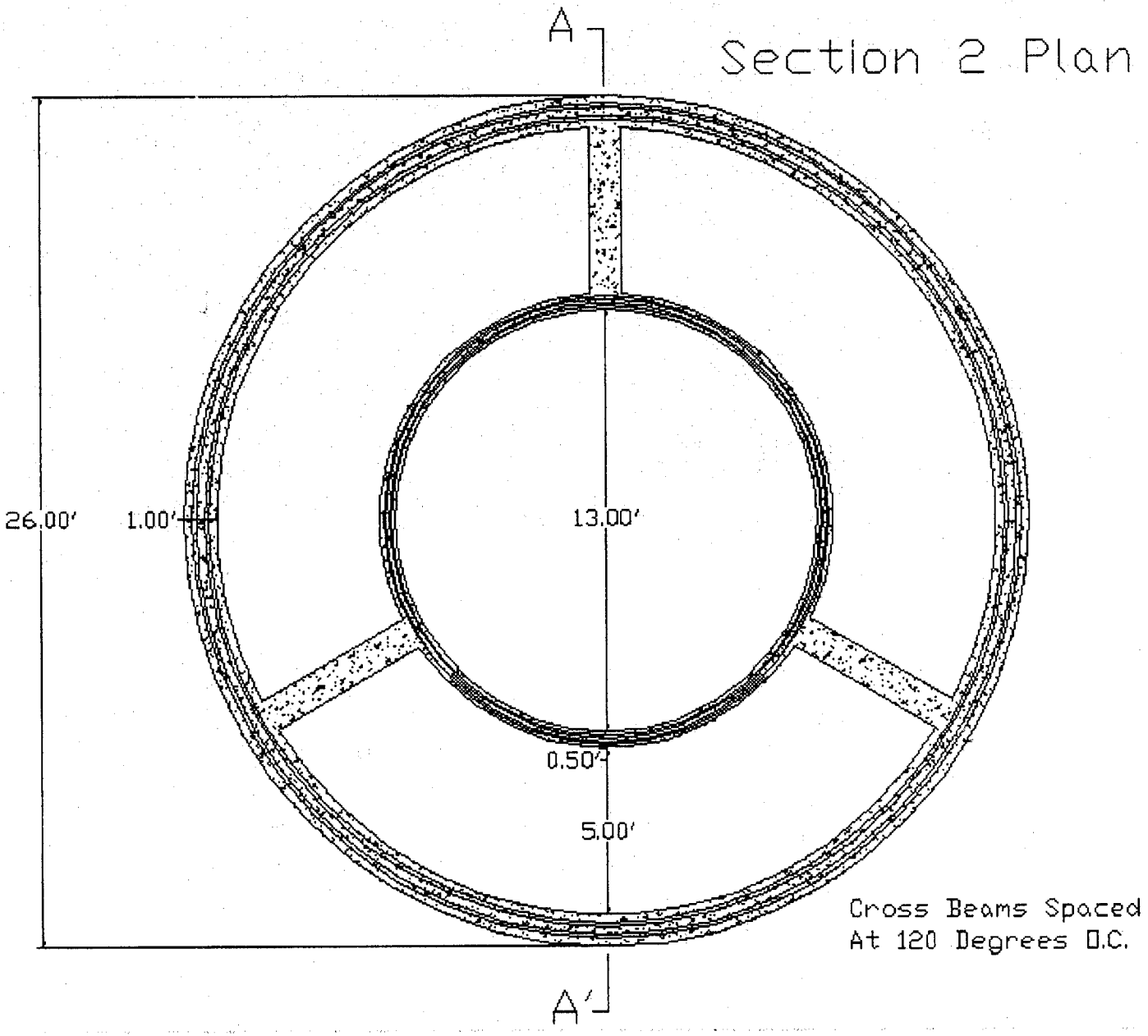
A
Section 2 Plan
26.00'
1.00'
13.00'
0.50'
5.00'
Cross Beams Spaced
At 120 Degrees O.C.
A'

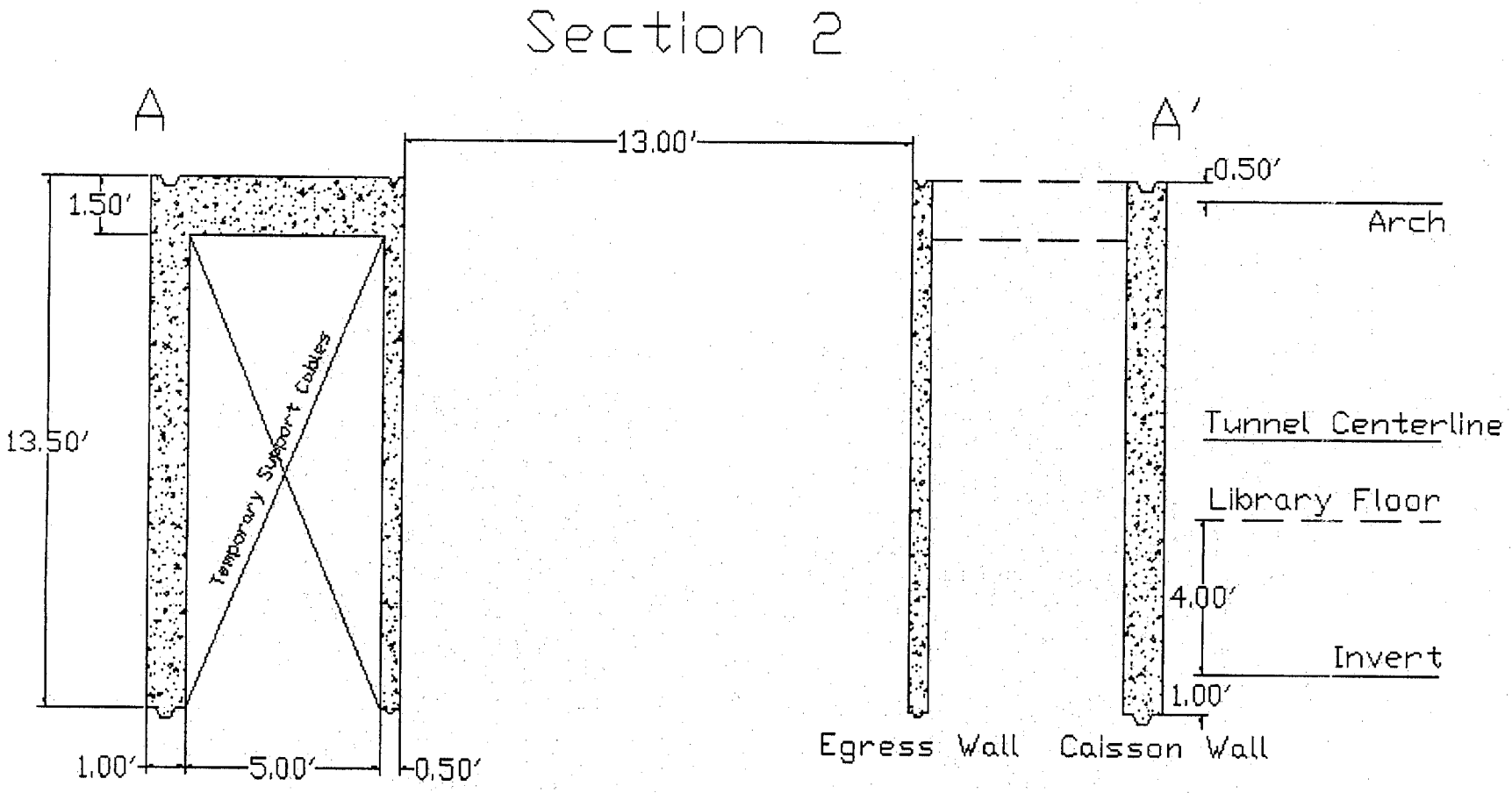
Section 2
A
A'
13.00'
0.50'
Arch
1.50'
13.50'
Temporary Support Cables
Tunnel Centerline
Library Floor
4.00'
Invert
1.00'
1.00'
5.00'
0.50'
Egress Wall
Caisson Wall

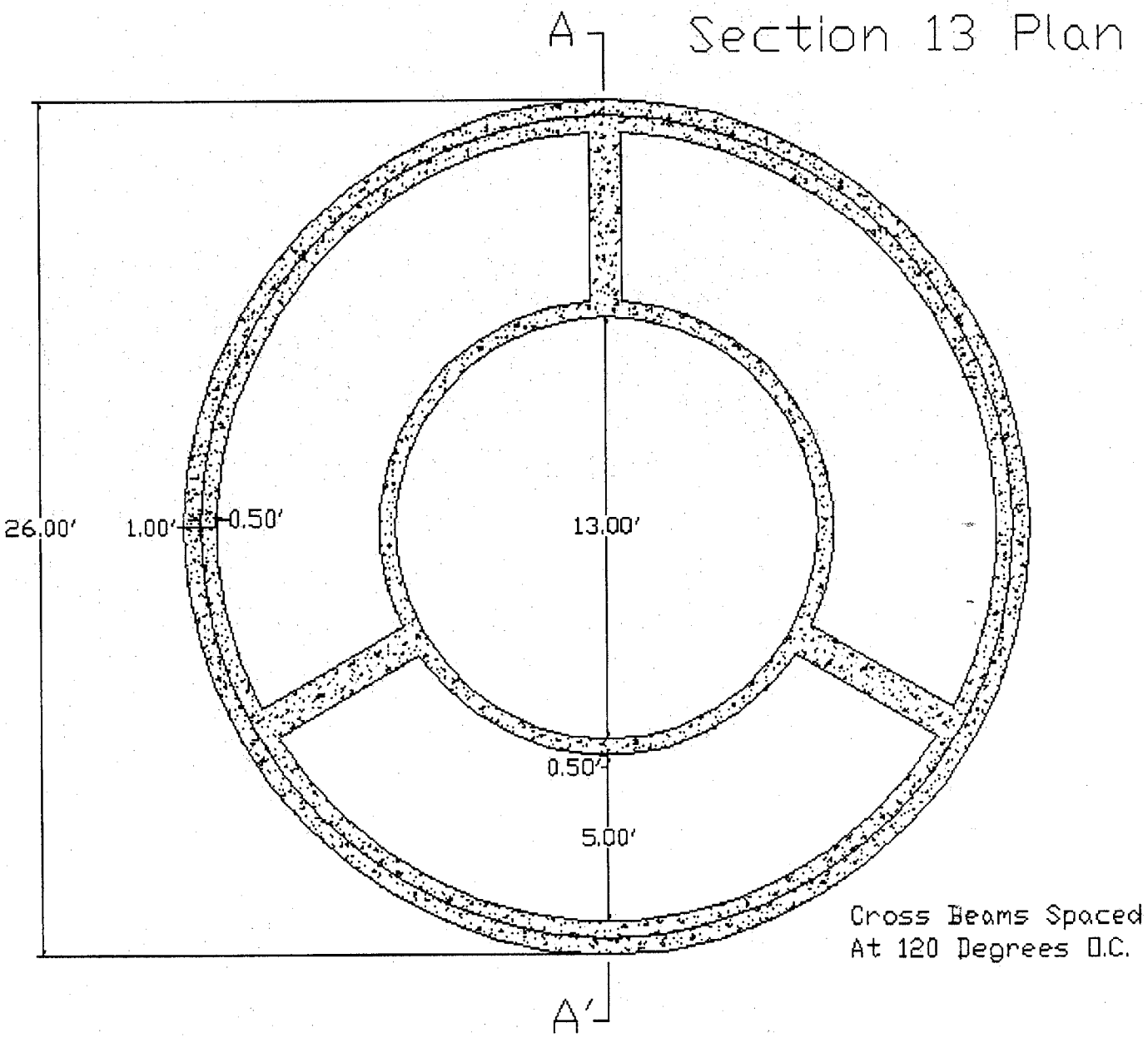
A
Section 13 Plan
26.00'
1.00'
0.50'
13.00'
0.50'
5.00'
Cross Beams Spaced
At 120 Degrees O.C.
A'

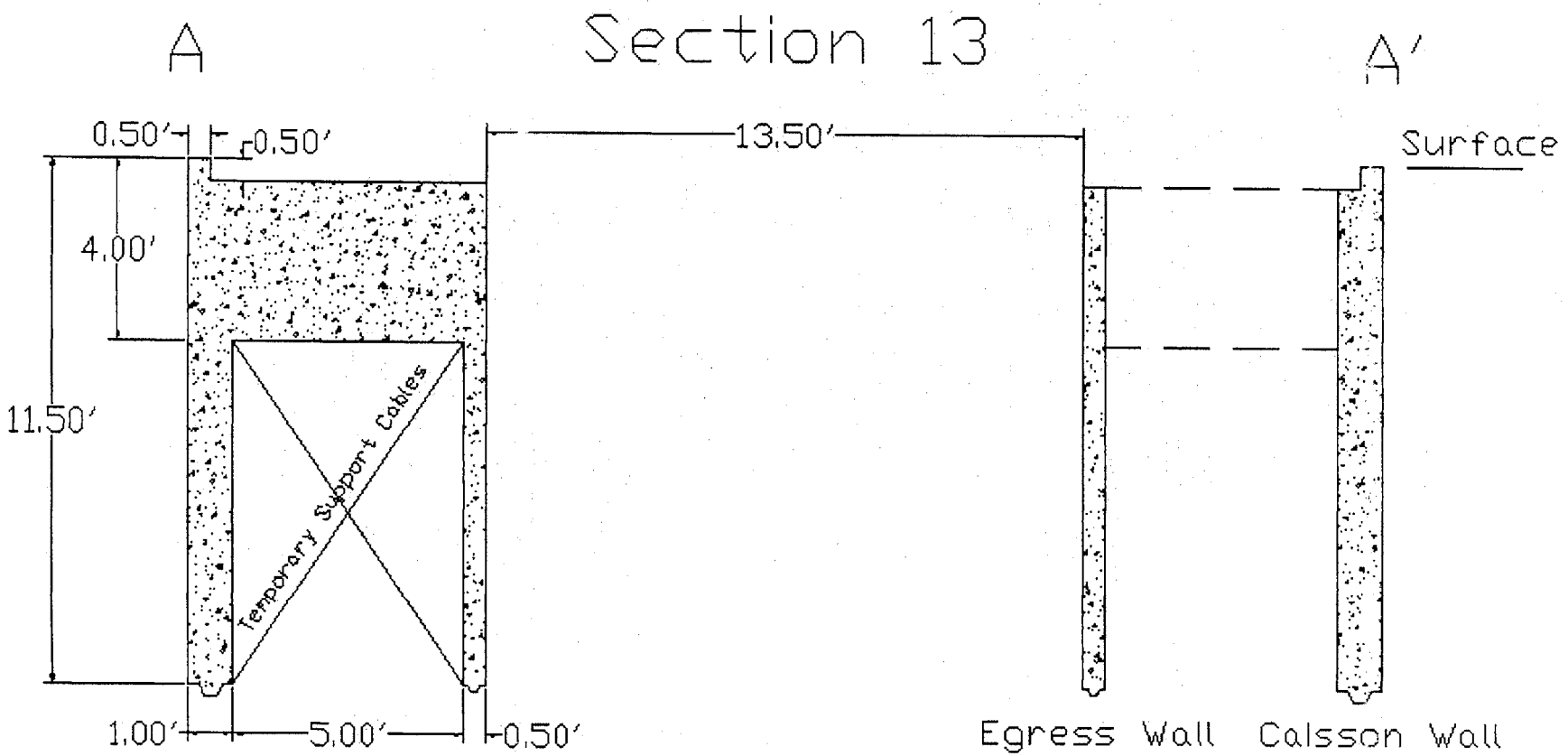
A
Section 13
A'
0.50'
0.50'
13.50'
Surface
4.00'
11.50'
Temporary Support Cables
1.00'
5.00'
0.50'
Egress Wall
Calsson Wall

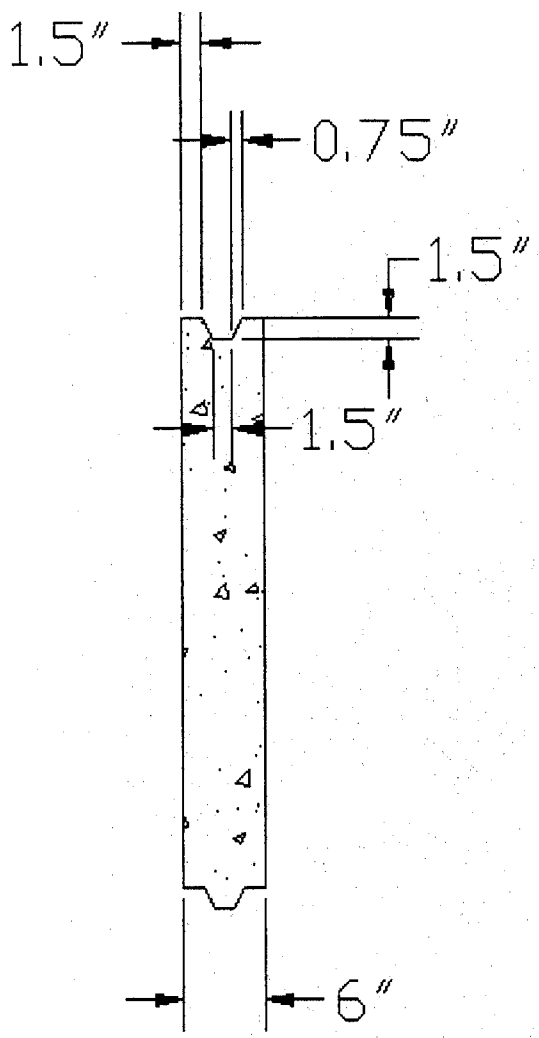

Egress Wall

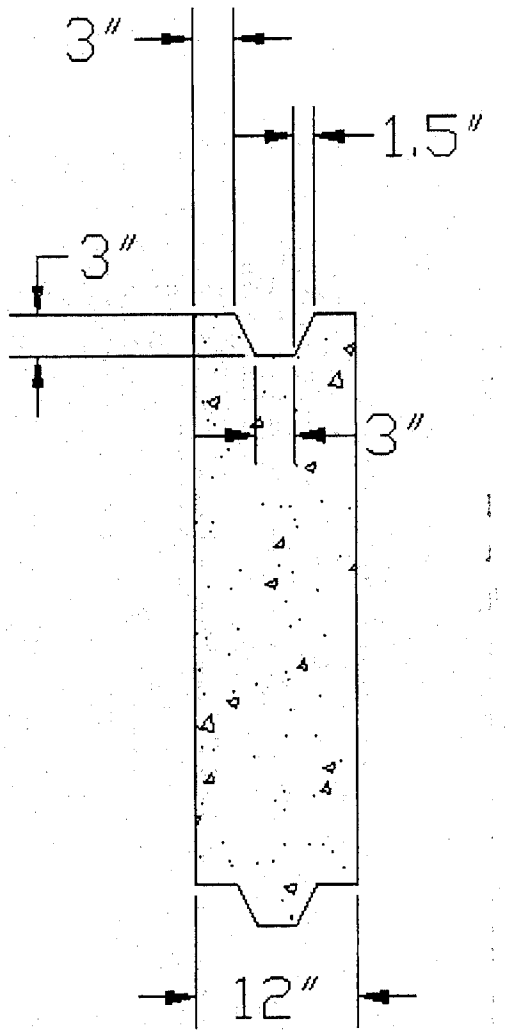

Caisson Wall

Detail of Caisson Joints

Caisson Launch Plan

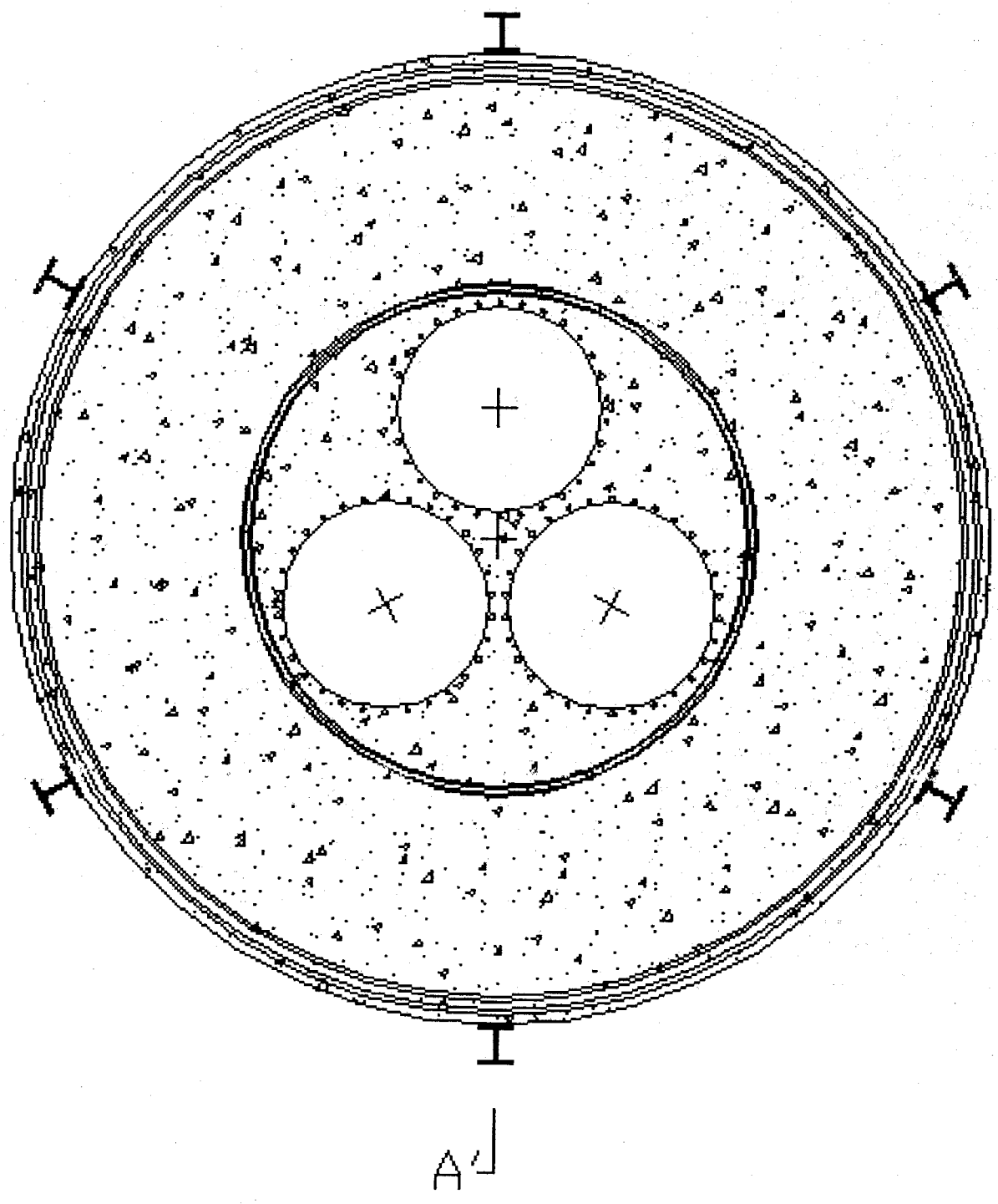

W12x120 Sections Spaced at 60 Degrees
At a Radius of 13' 0.25" from Caisson Center

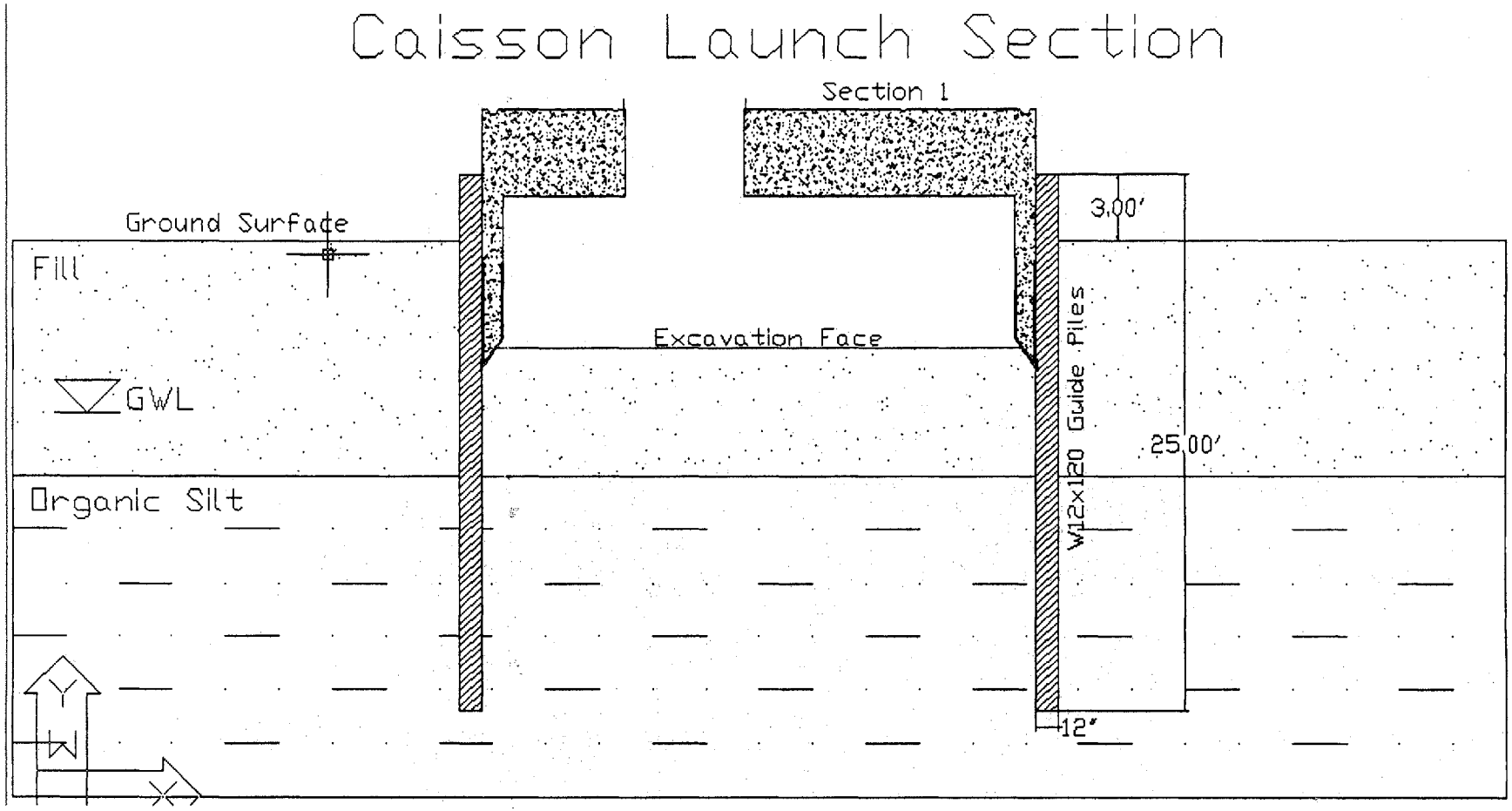
Caisson Launch Section
Section 1
Ground Surface
Fill
GWL
Excavation Face
3.00'
W12x120 Guide Piles
25.00'
Organic Silt
12"

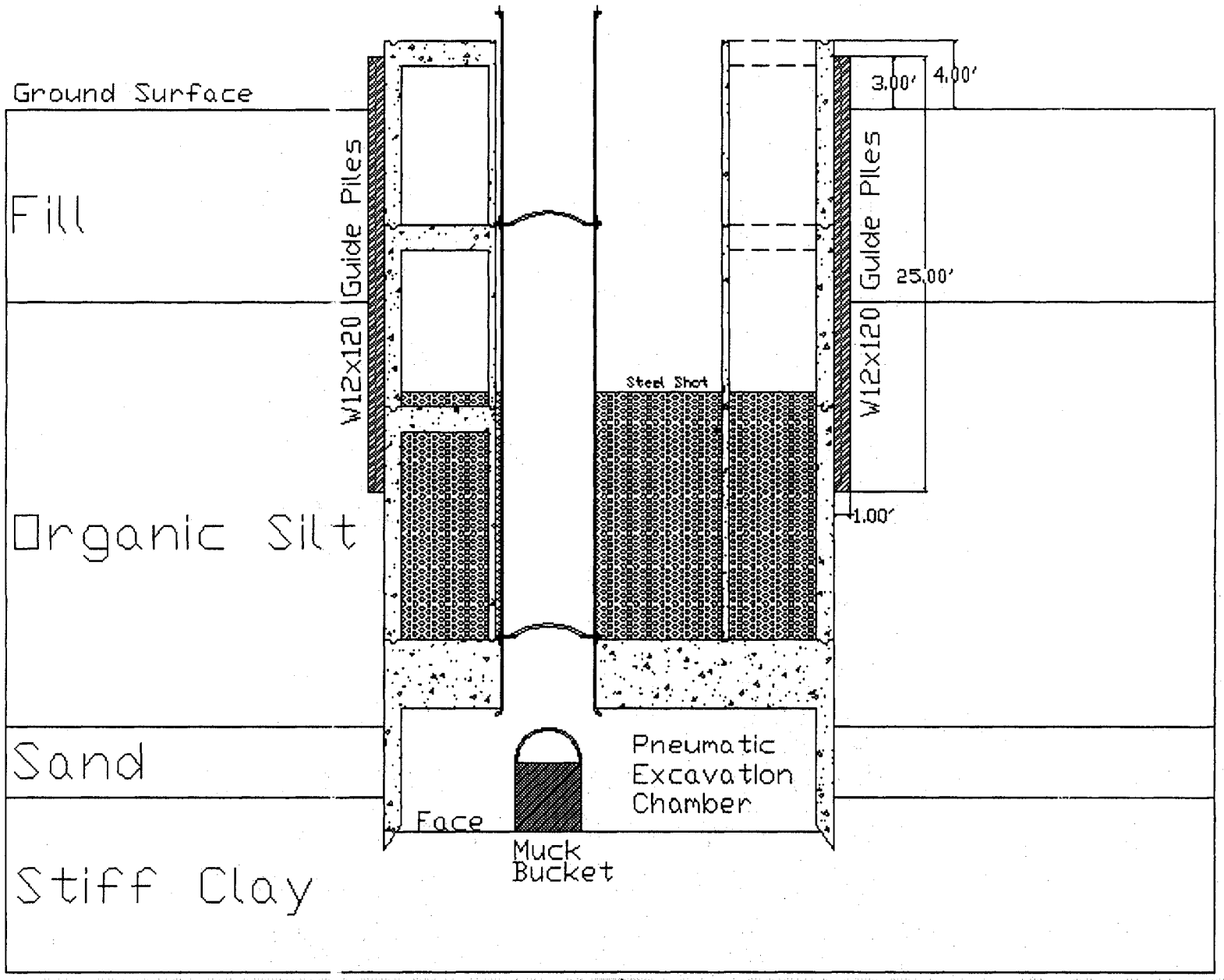
Ground Surface
Fill
Organic Silt
Sand
Stiff Clay
W12x120 Guide Piles
W12x120 Guide Piles
3.00'
4.00'
25.00'
1.00'
Steel Shot
Pneumatic
Excavation
Chamber
Face
Muck
Bucket

Ground Surface
Fill
Organic Silt
Sand
Stiff Clay
W12x120 Guide Piles
Lock Pipe
Air Lock
Steel Shot
Face
Pneumatic
Excavation
Chamber
3.00'
4.00'
25.00'
W12x120 Guide Piles
1.00'

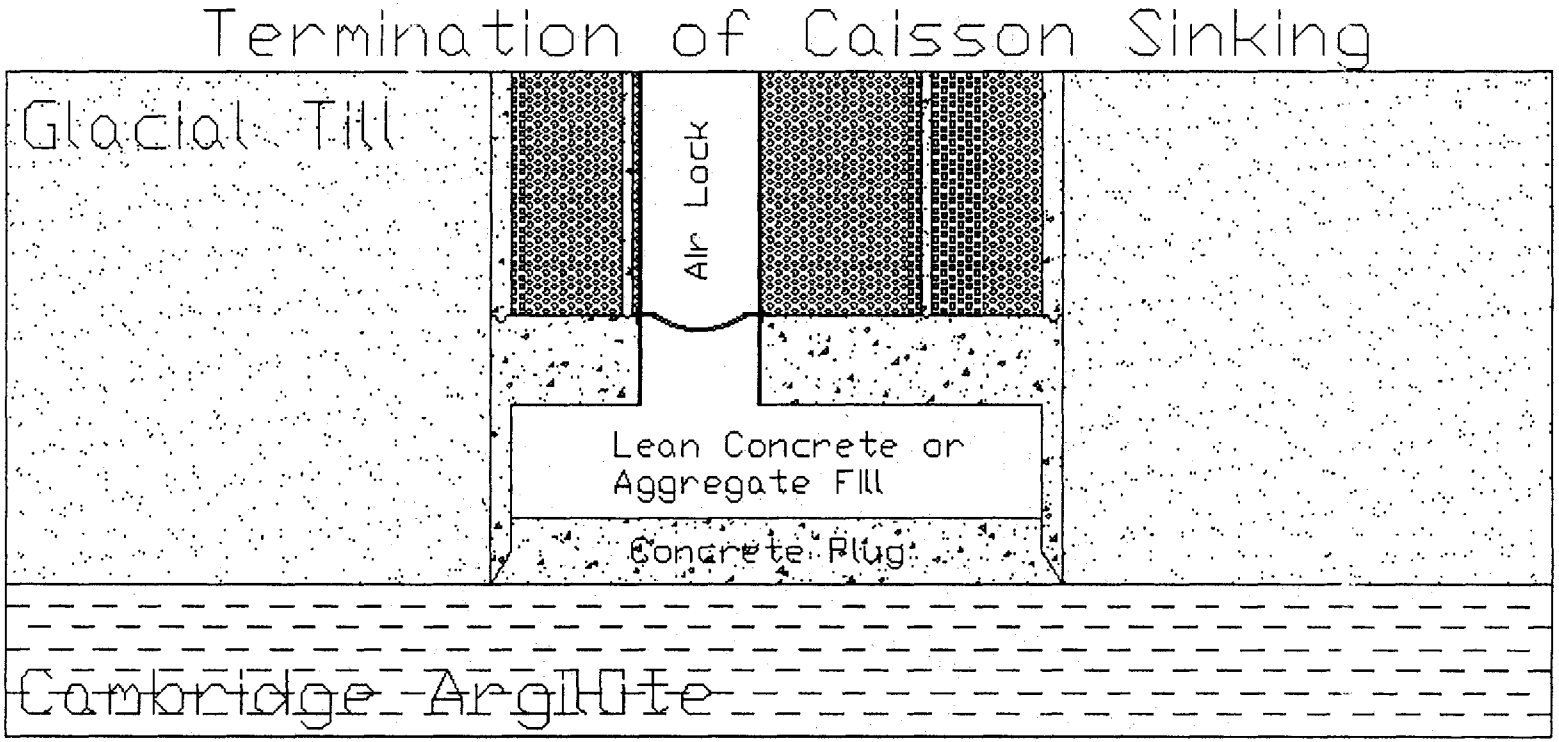
Termination of Caisson Sinking
Glacial Till
Air Lock
Lean Concrete or
Aggregate Fill
Concrete Plug
Cambridge Argillite

Bibliography

Bickel, J.O., T.R. Kuesel and E.H. King, *Tunnel Engineering Handbook*, 2nd Edition, Boston: Chapman and Hall, 1996, 544p.

Coller, J., Staheli, K., Bennet, D., and R. Post, A Review of Jacking Forces by both Theoretical and Empirical Methods as Compared with 20 Years of Practical Experience, 2001, http://www.trenchlessdataservice.com/microtnl/review.html

Bjerrum, L. and O. Eide, Stability of Strutted Excavations in Clay," Geotechnique, Vol. 6, No. 1, 1956, pp. 32-47.

Dennis, N. and R.E. Olson, Axial Capacity of Steel Pipe Piles in Clay, American Society of Civil Engineering Conference on Geotechnical Practice in Offshore Engineering, Austin, TX, 1983, pp. 370-389.

Industrial Supply, , http://www.aaa-industrialsupply.com/ and http://www.steel-ballast.com/ Steel Ballast, May 2, 2001.

Department of the Navy, Foundations and Earth Structures, Bureau of Yards and Docks, NAVDOCKS DM-7.2, Washington, DC: NAVFAC, 1982.

Jacky, J., The Coefficient of Earth Pressure at Rest, Journal of the Society of Hungarian Architects and Engineers, 1944, pp.355-358.

Ladd, C.C., personal communication regarding Shansep and Recompression soil strengths and parameters below MIT Campus, Professor of Soil Mechanics, Massachusetts Institute of Technology, 2001.

Massachusetts Institute of Technology, Boring 1 and 1A Logs, Sheet #MG 14 S 01 00, Archives of the Department of Facilities, MIT, 1948.

McCullough, D., The Great Bridge, New York: Simon and Schuster, 1972, pp. 173-178.

Megaw, T.M. and J.V. Bartlett, *Tunnels: Planning, Design, Construction*, Volume 2, New York: John Wiley and Sons, 1981, pp. 66-70.

Meyer, C., Design of Concrete Structures, New Jersey: Prentice Hall, 1996, pp.162-176.

Peck, R.B., Advantages and Limitations of the Observational Method, Geotechnique, Vol. 19, No. 2, 1969.

Proctor, R.V. and T.L. White, Earth Tunneling with Steel Supports, Youngstown Ohio: Commercial Shearing, Inc., 1977, pp. 229-234.

Rehkopf, J.C., J.B. Isaacson, C.M. Smith, A.I. Theophilou, N. Miller, and E.W. Craun, Subterranean Library at MIT: A Solution for the 21st Century, Masters of Engineering Project, Department of Civil and Environmental Engineering, Massachusetts Institute of Technology, 2001, 339p.

Richardson, H.W. and R.S. Mayo. *Practical Tunnel Driving*, New York: McGraw-Hill, 1941. pp. 85-89, 297.

Robinson, J.R., Piers, Abutments and Formwork for Bridges, London: Crosby Lockwood & Son, 1964, pp. 67-86.

RS Means, Heavy Construction Cost Data, 14th Edition, Kingston, Massachusetts: RS Means Company, Inc., 2000, p.56.

Shames, I.H. and J.M. Pitarresi, Introduction to Solid Mechanics, 3rd Edition, 2000, p.14.

Shapiro, M.J., A Picture History of the Brooklyn Bridge, New York: Dover Publications, 1983, p.27.

Skempton, A.W., Bearing Capacity of Clays, Proceedings of the Building Research Congress, England, 1951.

Summers, D., Mining 345: Strata Control, Rolla, Missouri: University of Missouri-Rolla, 2000, pp. 217-228.

Swatek, E.P. Jr., Foundation Engineering Handbook, H.F.Winterkorn and H. Fang editors, New York: Van Nostrand Reinhold, 1975, pp. 616-625.

Terzaghi, K., Theoretical Soil Mechanics, New York: John Wiley and Sons, 1943.

Timoshenko, S., Theory of Plates and Shells, 2nd Edition, New York: McGraw-Hill, 1959, pp.58-63.

Vesic, A.S., Analysis of Ultimate Loads on Shallow Foundations, American Society of Civil Engineers, Journal of the Soil Mechanics and Foundations Division, Vol. 99, No. SM2, pp. 45-73.

Whittle, A.J., personal communication regarding soil properties and strengths beneath MIT Campus and in Boston Area, Professor of Geotechnical Engineering, Massachusetts Institute of Technology, 2001.

Vita

Jon Brian Isaacson was in born Kansas City, Missouri on 24 November 1973. He grew up in Parkville, a northern suburb of Kansas City, and graduated from Park Hill High School in 1992. Later that same year, he went to Montana Tech in Butte, Montana to study Environmental Engineering. In the fall of 1994, Jon was accepted and transferred to the University of Missouri-Rolla's (UMR) Geological Engineering Department.

During his studies at UMR, he acquired a coop job with GeoSystems Engineering of Lenexa, Kansas, where he worked as a geotechnical field technician. He graduated cum laude, earning his Bachelor of Science in Geological Engineering from UMR in May of 1998. He obtained an internship with Haley and Aldrich of Boston, Massachusetts during the summer of 1998, working as an engineer. That fall, he returned to UMR to begin graduate study. During graduate school, Jon also actively pursued another undergraduate degree in Economics. His graduate studies involved the creation of three-dimensional digital geologic models as the basis for a geological investigation simulator designed by Dr. Paul M. Santi. In May of 2000, Jon graduated magna cum laude, earning a second Bachelor of Science in Economics. Later that summer he completed and defended his Master's thesis and graduated with a Masters of Science in Geological Engineering in July of 2000.

In the spring of 2000, Jon was accepted into the graduate program of the Civil and Environmental Engineering at the Massachusetts Institute of Technology. In the fall of 2000, Jon transferred to MIT where he entered the Masters of Engineering Program.

Jon B. Isaacson is an Engineer and Geologist Registrant in Training in Missouri. He is a member of many varied organizations, which include National Society of Professional Engineers, Association of Engineering Geologists, American Rock Mechanics Association, International Society of Rock Mechanics, American Underground-Construction Association, Society of Mining, Metallurgy, and Exploration, American Society of Civil Engineers, National Speleological Society, The Order of the Engineer, and Sigma Xi.

Unsurfaced Road Investigation and Management Plan, Fort Leonard Wood, Missouri, Reviews in Engineering Geology, Volume 14, Geological Society of America, J.B. Isaacson, A.E. Hurst, D. Miller, P.E. Albertson, 2001.

Construction of Digital Three-Dimensional Geologic Environments for a Subsurface Investigation Simulator, Masters Thesis 7804, University of Missouri-Rolla, Jon B. Isaacson, 2000, 125p.

How Our Investigation Strategy Influences Our Interpretations, Association of Engineering Geologists, 42nd Annual Program with Abstracts, Dr. Paul M. Santi and Jon B. Isaacson, 1999.

Geospatial Evaluation of Range Roads on Fort Leonard Wood, Missouri, Association of Engineering Geologists, 41st Annual Program with Abstracts, A.E. Hurst, B. Burton, J. Isaacson, C. Reiter, P. Albertson, 1998, p.99.